IMBALANCE OF CELLULAR REDOX-STATE IMPAIRS VASCULAR ENDOTHELIAL GROWTH FACTOR SURVIVAL AND ANGIOGENIC SIGNAL

by

MOHAMMED A. ABDELSAID

(Under the Direction of AZZA B. EL-REMESSY)

ABSTRACT

Achieving therapeutic angiogenesis remains an unrealized goal in cardiovascular diseases. We have previously shown that while low levels of peroxynitrite are required to transduce vascular endothelial growth factor (VEGF) signal, high levels of peroxynitrite can impair its signal, suggesting that changes in cellular redox-state can dictate the outcome for the VEGF signal. The overall goal of this project is to examine the impact and elucidate the molecular mechanisms by which shifting the cellular redox-state modulates the outcome of the VEGF angiogenic signal. Using an ischemic retinopathy mouse model, we demonstrated that excessive peroxynitrite formation impaired the VEGF survival signal via tyrosine nitration of the p85 regulatory subunit of the PI-3 kinase, which resulted in retinal endothelial cell death. Next, we assessed the impact of acute reductive stress by knocking down the expression of thioredoxin inhibiting protein (TXNIP), the endogenous inhibitor of the major antioxidant, thioredoxin. TXNIP deficient mice (TKO) experienced systemic and retinal reductive stress and expressed similar VEGF levels compared to wild type. However, retinal revascularization and VEGFR2 phosphorylation were significantly impaired in TKO mice. Low molecular weight protein tyrosine phosphatase (LMW-PTP), a redox-regulated phosphatase, regulates activation of

VEGFR2 and focal adhesion kinase (FAK), key mediators of VEGF-mediated cell migration. In vitro studies demonstrated that VEGF transiently oxidizes cellular glutathione (GSH) levels to facilitate S-glutathionylation and oxidative inhibition of LMW-PTP resulting in activation of FAK and cell migration. Mild shift of redox-state to oxidative stress augmented VEGF's angiogenic response while it was blunted by acute oxidative stress. Shifting redox-state to reductive stress using antioxidants or silencing TXNIP expression blunted S-glutathionylation of LMW-PTP, activation of VEGFR2 and angiogenic response. In summary, our results showed that while mild oxidative stress augments VEGF signal and angiogenic response, acute oxidative stress and acute reductive stress impair VEGF signal. Our findings identified S-glutathionylation of LMW-PTP as a novel therapeutic target to regulate VEGF angiogenic response.

INDEX WORDS: Angiogenesis, Peroxynitrite, Oxidative stress, Reductive stress, Vascular endothelial growth factor, Thioredoxin interacting protein, S-glutathionylation, Low molecular weight protein tyrosine phosphatases.

IMBALANCE OF CELLULAR REDOX-STATE IMPAIRS VASCULAR ENDOTHELIAL GROWTH FACTOR SURVIVAL AND ANGIOGENIC SIGNAL

by

MOHAMMED A. ABDELSAID

FORB, AIN SHAMS UNIVERSITY, EGYPT, 2001

MS, AL-AZHAR UNIVERSITY, EGYPT, 2006

A dissertation Submitted to the Graduate Faculty of The University of Georgia in Partial Fulfillment of the Requirements for the Degree

DOCTOR OF PHILOSOPHY

ATHENS, GEORGIA

2011

IMBALANCE OF CELLULAR REDOX-STATE IMPAIRS VASCULAR ENDOTHELIAL GROWTH FACTOR SURVIVAL AND ANGIOGENIC SIGNAL

by

MOHAMMED A. ABDELSAID

Major Professor:	Azza B. El-Remessy
Committee:	Susan C. Fagan
	Randall Tackett
	Adviye Ergul
	Somanath Shenoy

Electronic Version Approved:

Maureen Grasso
Dean of the Graduate School
The University of Georgia
December 2011

DEDICATION

To my father Soul, *Anwar Sherif Abdelsaid*, the man whom I owe everything I have and I could not pay him back.

To my mother, *Fatma Hassan*, my everlasting source of energy in life and back up plans.

To my small family, *Maha Coucha*, my beautiful faithful wife who always back me up and I dedicate my work to her to show my gratitude for her support and I want to tell her that she is the best thing that happened in my life. To *Ziyad Abdelsaid*, my son I hope it can inspire you one day in your life.

And finally to my mentor *Dr. Azza El-Remessy*, who had faith in me all these years and gave me her unconditional support, knowledge and time.

ACKNOWLEDGEMENTS

I would like to begin by thanking my advisor *Dr. Azza El-Remessy* for her insight, guidance, and encouragement. She has been a role-model for me in several aspects of life not just in science and research.

I also like to thank my doctoral committee – Drs. Susan C. Fagan, Adviye Ergul, Randall Tackett and Somanath Shenoy for their support through my doctoral work.

I would like to thank my laboratory team especially *Mrs. Su Matragon* and *Mrs. Bindu Pillia* for their technical support and help over the past 5 years, they were my second family.

My thanks for the CET faculty on their help during all these years and I wish the best of luck for my CET fellow students. Especial thanks for my true friend Dr. Mostafa El-gebaly for his valuable advice.

I greatly appreciate the support from AHA Southeast Affiliate Predoctoral-Fellowship: 2009-2011.

TABLE OF CONTENTS

Page

LIST OF FIGURES

Page

CHAPTER 1

INTRODUCTION AND LITERATURE REVIEW

Angiogenesis is the formation of new blood vessels from existing vessels. Angiogenesis is a multi-factorial process regulated by the balance between the pro- and anti-angiogenic factors [1, 2]. Although physiological angiogenesis is important for wound healing, recovery after stroke and myocardial infarction, pathological angiogenesis can be detrimental as in atherosclerosis, tumor growth and diabetic retinopathy [2-6]. Vascular endothelial growth factor (VEGF) is one of the potent angiogenic growth factors that regulates homeostasis of blood vessels and endothelial cells by modulating cell survival, permeability and cell migration [7, 8]. The VEGF family incorporates 5 structurally related ligands: A-D and PlGF (placenta growth factor). $VEGF_{165}$ (referred also as VEGF-A) is the most prominently expressed and heavily studied isoform in relation to the angiogenic process. VEGF-A binds two tyrosine kinase receptors, VEGFR-1 (Flt-1) and VEGFR-2 (Flk-1) [1]. Previous studies established the functional association between VEGFR-2 activation and angiogenesis [4, 7]. Therefore, regulation of VEGFR-2 activation controls VEGF-mediated angiogenic response.

Because of the critical and well-documented role of the VEGF in angiogenesis, targeting VEGF or its receptor VEGFR-2 has been an attractive therapeutic strategy [9-13]. Humanized monoclonal antibodies such as bevacizumab, ranibizumab and pegaptanib neutralize VEGF-A, resulting in prevention of tumor angiogenesis. Inhibitors of VEGFR tyrosine kinase such as sunitinib and sorafenib have been proven effective in anti-angiogenic tumor therapy. Although

successful, anti-VEGF treatments showed serious systemic side effects including hypertension, proteinuria, arterial thrombosis, modulating wound healing, bleeding and gastrointestinal perforation [14, 15]. Anti-VEGFs are also used in different proliferative eye diseases such as age macular degeneration (AMD), diabetic retinopathy, retinal vein occlusion and retinopathy of prematurity. Anti-VEGFs are only FDA approved for the AMD only and are used as off-label treatment in other ocular diseases. Nevertheless, the wide use of anti-VEGFs in proliferative retinopathy disease is limited by the debate regarding the safety of depriving other retinal cell types from intrinsic survival effects of the VEGF [16, 17]. On the other hand, exogenous delivery of VEGF, either using plasmid [18], adenovirus [19] or VEGF itself, to stimulate angiogenesis, in ischemic conditions, was successful only on the experimental level. Clinical practice failed to demonstrate a significant angiogenic response to VEGF gene therapy [1, 20, 21]. In summary, treatments that targeted delivery or removal of the VEGF have shown limited success suggesting the need to assess changes in the microenvironment to optimize the outcome of therapeutic angiogenesis.

Gap in knowledge

Oxidative stress is well-documented in ischemic cardiovascular disease such as stroke, atherosclerosis, thrombosis, plaque rapture and myocardial injury [22, 23]. The enthusiastic use of antioxidant in treatment and prevention of cardiovascular disease in experimental models initiated several randomized clinical trials. However, the results of clinical trials such as the Cardiovascular Disease, Hypertension and Hyperlipidemia, Adult-Onset Diabetes, Obesity, and Stroke (CHAOS) study, the Heart Outcomes Prevention Evaluation (HOPE) trial, the Secondary Prevention with and the Heart Protection Study (HPS) presented contradictory and disappointing results [24-26]. Retrospective studies for these major trials have shown striking limitations including the absence of a base-line biomarker for patient inclusion, the use of non-specific antioxidants lacking cell permeability and the rational for dose selection. In addition, it was not investigated whether antioxidant therapy managed to reverse the oxidative stress-induced protein post-translational modifications in these patients. These observations identified a gap in our knowledge about our understanding of oxidative stress-mediated protein modifications and how they can affect outcome in ischemic cardiovascular diseases. In present study, we examined the selective, cell permeable antioxidants including the specific peroxynitrite decomposition catalyst FeTPPS, the glutathione (GSH) precursor N-acetyl cysteine (NAC) and epicatechin, a flavenoid of the green tea extract that selectively blocks peroxynitrite-mediated tyrosine nitration.

Over the past decade, a great body of evidence has accumulated emphasizing the critical role of reactive oxygen species (ROS) and peroxynitrite, the reaction product of superoxide anion and nitric oxide, as signaling moieties for growth factor signaling [27-29]. Under physiological conditions, generation of ROS is counter-balanced by major antioxidant systems including glutathione and thioredoxin resulting in a balanced redox-state [30-32]. Nevertheless,

oxidative stress or high levels of ROS and peroxynitrite can impair VEGF signal resulting in apoptosis of endothelial cells [33-35]. These observations suggest that changes in ROS levels and redox-state can dictate the outcome of the VEGF signal. The limitations of previously tested antioxidant and targeting VEGF for regulating angiogenic response suggests the need to change our therapeutic strategies and target cellular micro-environment using selective and cell permeable antioxidant to improve the outcome of VEGF therapy in diseases characterized with aberrant angiogenesis.

The central hypothesis for this project is that shifting the balance of cellular redox-state to either oxidative stress or reductive stress will impair VEGF survival and angiogenic signal. Understanding the role of the redox-state and the molecular events that govern the VEGF signal will aid to devise more effective therapeutics to control angiogenic response.

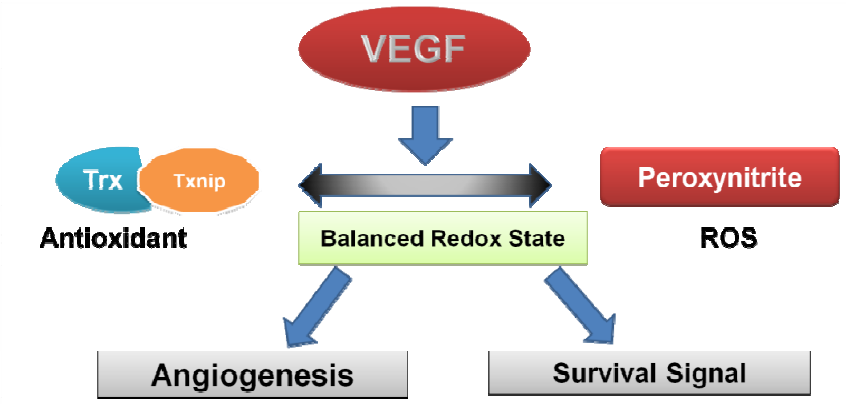

Fig. 1. Schematic diagram of the proposed hypothesis

The central hypothesis will be examined by the following specific aims:

Specific Aim 1: **To examine the detrimental effects of excessive oxidative stress on the VEGF's signal and function in a ischemic retinopathy mouse model.**

Rationale. Previous studies by our group have shown that exogenous high levels of peroxynitrite can inactivate VEGF survival signaling in retinal endothelial cells *in vitro* [34, 36]. We showed that tyrosine nitration-mediated dysfunction of PI 3-kinase caused impairment of the VEGF survival signal *in vitro*. Whether similar interplay between peroxynitrite-mediated nitration and VEGF can affect survival of retinal vascular endothelial cell *in vivo* remains unexplored.

The working hypothesis is that hyperoxia-induced high levels of peroxynitrite impair the VEGF signal by inhibiting PI-3 Kinase/Akt signaling.

We will use an ischemic retinopathy mouse model as it has two distinguished stages: an initial stage of hyperoxia-induced excessive peroxynitrite formation and retinal vaso-obliteration followed by a later stage of relative hypoxia, mild oxidative insult and retinal neovascularization. We will examine the mechanism by which early peroxynitrite-mediated tyrosine nitration can inhibit the p85 subunit of PI 3-kinase and trigger vascular cell death. We will also investigate the protective effects of the early intervention of tyrosine nitration on preventing retinal vaso-obliteration and later on preventing retinal neovascularization. We will compare the effects of inhibiting peroxynitrite formation using its specific decomposition catalyst FeTPPS, the glutathione (GSH) precursor N-acetyl cysteine (NAC) and epicatechin, a selective nitration inhibitor that does not modulate redox-state. The results are compiled and presented in chapter (2). The manuscript is published in the Journal of Pharmacology and Experimental Therapeutics; 2010 Jan, 332:125-134.

Specific Aim 2: To examine the effects of reductive stress on VEGF's signal and function in a hypoxia-induced neovascularization mouse model.

Rationale. So far, vascular research has focused on studying the sources of ROS in mediating VEGF's signal. However, little is known about the contribution of antioxidant systems. Endothelial cells have two main antioxidant systems, the glutaredoxin system and the thioredoxin system. The thioredoxin system is an ubiquitous thiol-reducing system that consists of thioredoxin (TRX), NADPH and homodimeric seleno-protein thioredoxin reductase [37] and the endogenous inhibitor thioredoxin-interacting protein (TXNIP) [31]. TXNIP expression is up-regulated under stress conditions, ischemia and hyperglycemia [38, 39]. Yet, the role of TXNIP in regulating the cellular redox-state and VEGF-induced angiogenesis has not been examined.

The working hypothesis is that knocking down the expression of TXNIP will shift the redox-state to reductive stress that can blunt VEGF-induced peroxynitrite formation and impair VEGFR2 phosphorylation and its downstream angiogenic signal. Since a pharmacological inhibitor of TXNIP is not available, molecular tools will be used to knock down TXNIP expression *in vivo* and *in vitro* in human retinal endothelial cells. These results are compiled and presented in chapter (3). The manuscript will be submitted to J. Angiogenesis.

Specific Aim 3: **To characterize the role of peroxynitrite-mediated S-glutathionylation of LMW-PTP in redox regulation of VEGF-angiogenic signal.**

Rationale. Our group has previously shown that low levels of peroxynitrite are required to transduce the VEGF angiogenic signal via thiol oxidation [27]. However, the impact of VEGF on modulating intracellular GSH levels and identifying a redox-sensitive molecular target to regulate angiogenesis remain unexplored. Low molecular weight protein tyrosine phosphatase (LMW-PTP) is a redox-sensitive target that plays a pivotal role in VEGF-mediated cell

migration and angiogenesis as it has been shown to regulate activation of VEGFR2 [40] as well as focal adhesion kinase (FAK) [41, 42]. However, the effects of VEGF-induced peroxynitrite on altering the redox-state of LMW-PTP and regulation of FAK remain unknown.

The working hypothesis is that VEGF-induced peroxynitrite can transiently alter cellular redox-state to transduce its signal through phosphorylation and activation of FAK by S-glutathionylation of its phosphatase the LMW-PTP. We will use human retinal endothelial cells to examine the effect of VEGF stimulation on cellular GSH levels and in particular, FAK through redox regulation of LMW-PTP. We will examine shifting the redox-state to oxidative stress by combining VEGF with escalating levels of peroxynitrite while reductive stress will be induced by antioxidants. The results are compiled and presented in chapter (4). Manuscript has been submitted to The Journal of Cell Science.

In summary, our studies demonstrate the critical role of achieving a balanced redox-state in mediating VEGF's survival and angiogenic signal. Our studies identified a novel molecular switch of LMW-PTP to regulate the VEGF signal at the VEGFR2 receptor level and downstream at the FAK level suggesting that targeting LMW-PTP expression and activity can modulate angiogenesis. In addition, better understanding of VEGF survival and angiogenic signal will improve diseases with aberrant angiogenesis such as stroke and myocardial infarction where reparative angiogenesis is required to decrease morbidity and other diseases where angiogenesis aggravates pathogenesis such as cancer and diabetic retinopathy.

References.

1. Testa, U., G. Pannitteri, and G.L. Condorelli, *Vascular endothelial growth factors in cardiovascular medicine.* J Cardiovasc Med (Hagerstown), 2008. **9**(12): p. 1190-221.
2. Folkman, J., *Angiogenesis.* Annu Rev Med, 2006. **57**: p. 1-18.
3. Carmeliet, P., *Angiogenesis in health and disease.* Nat Med, 2003. **9**(6): p. 653-60.
4. Munoz-Chapuli, R., A.R. Quesada, and M. Angel Medina, *Angiogenesis and signal transduction in endothelial cells.* Cell Mol Life Sci, 2004. **61**(17): p. 2224-43.
5. Abo-Auda, W. and R.L. Benza, *Therapeutic angiogenesis: review of current concepts and future directions.* J Heart Lung Transplant, 2003. **22**(4): p. 370-82.
6. Caldwell, R.B., et al., *Vascular endothelial growth factor and diabetic retinopathy: role of oxidative stress.* Curr Drug Targets, 2005. **6**(4): p. 511-24.
7. Ferrara, N., *Vascular endothelial growth factor.* Arterioscler Thromb Vasc Biol, 2009. **29**(6): p. 789-91.
8. Kajdaniuk, D., et al., *Vascular endothelial growth factor (VEGF) - part 1: in physiology and pathophysiology.* Endokrynol Pol. **62**(5): p. 444-55.
9. Takahashi, S., *Vascular endothelial growth factor (VEGF), VEGF receptors and their inhibitors for antiangiogenic tumor therapy.* Biol Pharm Bull. **34**(12): p. 1785-8.
10. Emmanouilides, C., et al., *Anti-VEGF antibody bevacizumab (Avastin) with 5FU/LV as third line treatment for colorectal cancer.* Tech Coloproctol, 2004. **8 Suppl 1**: p. s50-2.
11. Jorge, R., et al., *Intravitreal bevacizumab (Avastin) for persistent new vessels in diabetic retinopathy (IBEPE study).* Retina, 2006. **26**(9): p. 1006-13.
12. Ouhadj, O., et al., *[Intravitreal ranibizumab injections for the treatment of choroidal neovascularization complicating high myopia].* J Fr Ophtalmol. **33**(9): p. 649-54.

13. Dickler, M.N., et al., *A phase II trial of erlotinib in combination with bevacizumab in patients with metastatic breast cancer.* Clin Cancer Res, 2008. **14**(23): p. 7878-83.

14. Bellati, F., et al., *Current knowledge and open issues regarding Bevacizumab in gynaecological neoplasms.* Crit Rev Oncol Hematol.

15. des Guetz, G., et al., *Cardiovascular toxicity of anti-angiogenic drugs.* Target Oncol. **6**(4): p. 197-202.

16. van der Reis, M.I., et al., *A systematic review of the adverse events of intravitreal anti-vascular endothelial growth factor injections.* Retina. **31**(8): p. 1449-69.

17. Higashide, T., et al., *Adverse events associated with intraocular injections of bevacizumab in eyes with neovascular glaucoma.* Graefes Arch Clin Exp Ophthalmol.

18. Marshall, W.G., Jr., et al., *Electroporation-mediated delivery of a naked DNA plasmid expressing VEGF to the porcine heart enhances protein expression.* Gene Ther. **17**(3): p. 419-23.

19. Su, H., et al., *Additive effect of AAV-mediated angiopoietin-1 and VEGF expression on the therapy of infarcted heart.* Int J Cardiol, 2009. **133**(2): p. 191-7.

20. Rajagopalan, S., et al., *Regional angiogenesis with vascular endothelial growth factor in peripheral arterial disease: a phase II randomized, double-blind, controlled study of adenoviral delivery of vascular endothelial growth factor 121 in patients with disabling intermittent claudication.* Circulation, 2003. **108**(16): p. 1933-8.

21. Kastrup, J., et al., *Direct intramyocardial plasmid vascular endothelial growth factor-A165 gene therapy in patients with stable severe angina pectoris A randomized double-blind placebo-controlled study: the Euroinject One trial.* J Am Coll Cardiol, 2005. **45**(7): p. 982-8.

22. Whaley-Connell, A., P.A. McCullough, and J.R. Sowers, *The role of oxidative stress in the metabolic syndrome.* Rev Cardiovasc Med. **12**(1): p. 21-9.

23. Armstrong, A.W., et al., *Angiogenesis and oxidative stress: common mechanisms linking psoriasis with atherosclerosis.* J Dermatol Sci. **63**(1): p. 1-9.

24. Lonn, E., et al., *Effects of ramipril and vitamin E on atherosclerosis: the study to evaluate carotid ultrasound changes in patients treated with ramipril and vitamin E (SECURE).* Circulation, 2001. **103**(7): p. 919-25.

25. McQueen, M.J., et al., *The HOPE (Heart Outcomes Prevention Evaluation) Study and its consequences.* Scand J Clin Lab Invest Suppl, 2005. **240**: p. 143-56.

26. *Results of the low-dose (20 mg) pravastatin GISSI Prevenzione trial in 4271 patients with recent myocardial infarction: do stopped trials contribute to overall knowledge? GISSI Prevenzione Investigators (Gruppo Italiano per lo Studio della Sopravvivenza nell'Infarto Miocardico).* Ital Heart J, 2000. **1**(12): p. 810-20.

27. El-Remessy, A.B., et al., *Peroxynitrite mediates VEGF's angiogenic signal and function via a nitration-independent mechanism in endothelial cells.* Faseb J, 2007. **21**(10): p. 2528-39.

28. Colavitti, R., et al., *Reactive oxygen species as downstream mediators of angiogenic signaling by vascular endothelial growth factor receptor-2/KDR.* J Biol Chem, 2002. **277**(5): p. 3101-8.

29. Ushio-Fukai, M., *Redox signaling in angiogenesis: role of NADPH oxidase.* Cardiovasc Res, 2006. **71**(2): p. 226-35.

30. Casagrande, S., et al., *Glutathionylation of human thioredoxin: a possible crosstalk between the glutathione and thioredoxin systems.* Proc Natl Acad Sci U S A, 2002. **99**(15): p. 9745-9.

31. Patwari, P., et al., *The interaction of thioredoxin with Txnip. Evidence for formation of a mixed disulfide by disulfide exchange.* J Biol Chem, 2006. **281**(31): p. 21884-91.

32. Kanda, M., et al., *Glutaredoxin modulates platelet-derived growth factor-dependent cell signaling by regulating the redox status of low molecular weight protein-tyrosine phosphatase.* J Biol Chem, 2006. **281**(39): p. 28518-28.

33. Gu, W., et al., *Reactive oxygen species are critical mediators of coronary collateral development in a canine model.* Am J Physiol Heart Circ Physiol, 2003. **285**(4): p. H1582-9.

34. el-Remessy, A.B., et al., *Oxidative stress inactivates VEGF survival signaling in retinal endothelial cells via PI 3-kinase tyrosine nitration.* J Cell Sci, 2005. **118**(Pt 1): p. 243-52.

35. Yun, J., et al., *Redox-dependent mechanisms in coronary collateral growth: the "redox window" hypothesis.* Antioxid Redox Signal, 2009. **11**(8): p. 1961-74.

36. El-Remessy, A.B., et al., *High glucose-induced tyrosine nitration in endothelial cells: role of eNOS uncoupling and aldose reductase activation.* Invest Ophthalmol Vis Sci, 2003. **44**(7): p. 3135-43.

37. Meyer, Y., et al., *Thioredoxins and glutaredoxins: unifying elements in redox biology.* Annu Rev Genet, 2009. **43**: p. 335-67.

38. Perrone, L., et al., *Thioredoxin interacting protein (TXNIP) induces inflammation through chromatin modification in retinal capillary endothelial cells under diabetic conditions.* J Cell Physiol, 2009. **221**(1): p. 262-72.

39. Cha-Molstad, H., et al., *Glucose-stimulated expression of Txnip is mediated by carbohydrate response element-binding protein, p300, and histone H4 acetylation in pancreatic beta cells.* J Biol Chem, 2009. **284**(25): p. 16898-905.

40. Huang, L., et al., *HCPTPA, a protein tyrosine phosphatase that regulates vascular endothelial growth factor receptor-mediated signal transduction and biological activity.* J Biol Chem, 1999. **274**(53): p. 38183-8.

41. Chiarugi, P., *The redox regulation of LMW-PTP during cell proliferation or growth inhibition.* IUBMB Life, 2001. **52**(1-2): p. 55-9.

42. Chiarugi, P., et al., *Two vicinal cysteines confer a peculiar redox regulation to low molecular weight protein tyrosine phosphatase in response to platelet-derived growth factor receptor stimulation.* J Biol Chem, 2001. **276**(36): p. 33478-87.

CHAPTER 2

EARLY INTERVENTION OF TYROSINE NITRATION PREVENTS VASO-OBLITERATION AND NEOVASCULARIZATION IN ISCHEMIC RETINOPATHY [1]

---

[1] Mohammed A. Abdelsaid, Bindu A. Pillai, Suraporn Matragoon, Roshini Prakash, Mohamed Al-Shabrawey, Azza B. El-Remessy.

Abstract

Diabetic retinopathy and retinopathy of prematurity are blinding disorders that follow a pathological pattern of ischemic retinopathy and affect premature infants and working-age adults. Yet, the treatment options are limited to laser photocoagulation. The goal of this study is to elucidate the molecular mechanism and examine the therapeutic effects of inhibiting tyrosine nitration on protecting early retinal vascular cell death and late neovascularization in the ischemic retinopathy model. Ischemic retinopathy was developed by exposing neonatal mice to 75% oxygen [postnatal day (p) 7–p12] followed by normoxia (21% oxygen) (p12–p17). Peroxynitrite decomposition catalyst 5,10,15,20-tetrakis(4-sulfonatophenyl)porphyrinato iron III chloride (FeTPPS) (1 mg/kg), the nitration inhibitor epicatechin (10 mg/kg) or the thiol donor *N*-acetylcysteine (NAC, 150 mg/kg) were administered (p7–p12) or (p7–p17). Vascular endothelial cells were incubated at hyperoxia (40% oxygen) or normoxia (21% oxygen) for 48 h.

Vascular density was determined in retinal flat mounts labeled with isolectin B4. Expression of vascular endothelial growth factor, caspase-3, and poly (ADP ribose) polymerase (PARP), activation of Akt and p38 mitogen-activated protein kinase (MAPK), and tyrosine nitration of the phosphatidylinositol (PI) 3-kinase p85 subunit were analyzed by Western blot. Hyperoxia-induced peroxynitrite caused endothelial cell apoptosis as indicated by expression of cleaved caspase-3 and PARP leading to vaso-obliteration. These effects were associated with significant tyrosine nitration of the p85 subunit of PI 3-kinase, decreased Akt activation, and enhanced p38 MAPK activation. Blocking tyrosine nitration of PI 3-kinase with epicatechin or NAC restored Akt phosphorylation, and inhibited vaso-obliteration at p12 and neovascularization at p17 comparable with FeTPPS. Early inhibition of tyrosine nitration with use of epicatechin or NAC can represent safe and effective vascular-protective agents in ischemic retinopathy.

Introduction

Retinopathy of prematurity (ROP) and diabetic retinopathy (DR) are potentially blinding disorders that affect premature infants and working-age adults, respectively, in the United States (Aiello et al., 1998; Chen and Smith, 2007). ROP and DR follow a pathological progression pattern characteristic of ischemic retinopathy, where the loss of retinal capillary is an early initiating event, leading to a poorly controlled process of retinal neovascularization and the development of proliferative retinopathy (for review see, Caldwell et al., 2003). So far, the standard treatment for retinal neovascularization is limited to laser photocoagulation. Although successful, this treatment is invasive and results in loss of peripheral vision (for review see, Ali and El-Remessy, 2009). The lack of approved pharmacological treatment for DR and ROP creates a great need for finding new effective therapeutic modalities to treat these devastating diseases. The mechanisms that control the process of retinal neovascularization are therefore of major clinical importance.

Peroxynitrite formed by reaction of nitric oxide and superoxide anion mediates a variety of biological processes including inhibition of key metabolic enzymes, lipid peroxidation, nitration of the protein tyrosine residue, and reduction of cellular antioxidant defenses by oxidation of thiol pools (Pacher et al., 2007). A critical role of increased oxidative stress and, in particular, the peroxynitrite is supported by previous studies showing that increases in peroxynitrite formation cause capillary endothelial cell apoptosis leading to vascular cell loss in DR and ROP models (Brooks et al., 2001; Gu et al., 2002; Sennlaub et al., 2002; Beauchamp et al., 2004; Kowluru and Odenbach, 2004; Kowluru et al., 2007). Moreover, clinical studies showed that infants with active ROP have low serum levels of reduced glutathione (GSH), suggesting compromised antioxidant defense (Papp et al., 1999; Wright et al., 2006). We and others have shown that increased peroxynitrite formation correlates with capillary endothelial

cell apoptosis (Du et al., 2002; Sennlaub et al., 2002; Zou et al., 2002; Gu et al., 2003; el-Remessy et al., 2005; Drel et al., 2008). However, the molecular mechanism for peroxynitrite-induced vascular cell death and the therapeutic role of blocking tyrosine nitration were not investigated in models of ischemic retinopathy.

In the present study, we took advantage of using the ischemic retinopathy mouse model because it has two distinguished stages: initial stage of hyperoxia (75% oxygen) characterized with excessive peroxynitrite formation and capillary dropout, followed by a later stage of hypoxia (21% oxygen) characterized with mild oxidative insult and retinal neovascularization (Al-Shabrawey et al., 2005; El- Remessy et al., 2007). We compared the effects of selectively blocking the tyrosine nitration by use of epicatechin, one of the green tea extracts that has no antioxidant properties but selectively inhibits tyrosine nitration process, versus 5,10,15,20-tetrakis(4-sulfonatophenyl)porphyrinato iron III chloride (FeTPPS) the specific peroxynitrite decomposition catalyst or N-acetylcysteine (NAC), which is a dietary supplement, general antioxidant, and a thiol donor. Although we showed previously that blocking tyrosine nitration by use of the selective nitration inhibitor epicatechin can restore VEGF survival signal (El-Remessy et al., 2005), it enhances VEGF's angiogenic signal in vitro and retinal neovascularization in vivo (El-Remessy et al., 2007).

Our previous studies showed that high levels of peroxynitrite inhibit the pro-survival signal of VEGF and basic fibroblast growth factor and cause endothelial cell death in culture models of diabetic retinopathy and retinopathy of prematurity (Gu et al., 2003; el-Remessy et al., 2005). Here, we elucidate the molecular mechanism by which peroxynitrite-mediated tyrosine nitration can inhibit p85 subunit of PI 3-kinase and trigger vascular cell death in vivo. We also investigate the effects of the early intervention of tyrosine nitration on preventing retinal vascular

cell death and vaso-obliteration during hyperoxic stage [postnatal day (p) 7 to p12] and the continuous intervention (p7–p17) on preventing retinal neovascularization. Our results suggest that early blocking tyrosine nitration and peroxynitrite formation could be considered as a new effective therapeutic target for a possible control of common ischemic proliferative retinopathy diseases.

Materials and Methods

Cell Culture.

Primary cultures of bovine retinal endothelial (BRE) cells were prepared as described previously (El-Remessy et al., 2007). Cells from passages 4 to 8 were used in all experiments. Cells were maintained in M199 supplemented with 10% fetal bovine serum, 10% CS-C complete medium, 2 mM glutamine, 100 U/ml penicillin, and 100 μg/ml streptomycin at 37°C in a humidified CO_2 incubator.

Treatment during Hyperoxia and Normoxia.

BRE cells were grown to 80% confluence and then switched to serum-free medium and placed in a hyperoxic (40% O_2, 5%CO_2) or normoxic (21% O_2, 5% CO_2) environment for 48 h unless otherwise indicated. The 40% O_2 level was chosen for hyperoxia (40% oxygen) exposure based on previous research showing that 40% O_2 generates significant peroxynitrite without inducing toxicity in retinal cells (Gu et al., 2003). The hyperoxia (40% oxygen) exposure was performed in a humidified incubator modified by installing the PROOX model 110 oxygen regulator (Biospherix, Redfield, NY). The oxygen level was monitored continuously by use of the PROOX oxygen sensor.

Animals.

All experiments were performed with use of C57Bl/6 mice and were approved by the institutional Committee for Animal Use in Research and Education at the Veterans Affairs Medical Center and conformed to the Statement for the Use of Animals in Ophthalmic and Vision Research of The Association for Research in Vision and Ophthalmology.

Ischemic Retinopathy Mouse Model.

Following the protocol of Smith et al. (1994), on p7 newborn mice were placed along with their dams into a custom-built chamber in which the partial pressure of oxygen was maintained at 75% (Biospherix). Mice were maintained in 75% oxygen for up to 5 days (p12), after which they were transferred back to room air (relative hypoxia 21% oxygen). Room temperature was maintained at 20°C, and rooms were illuminated with standard fluorescent lighting on a 12-h light/dark cycle. Newborn mice were nursed by the dams that were given food (standard mouse chow) and water.

Treatment during Hyperoxia and Hypoxia Periods.

Animals were treated by daily intraperitoneal injections with the following inhibitors: peroxynitrite decomposition catalyst FeTPPS (1 mg/kg; Calbiochem, San Diego, CA); the nitration inhibitor, (-)-*cis*- 3,3`,4`,5,7-pentahydroxyflavane, (2*R*,3*R*)-2-(3,4-dihydroxyphenyl)-3,4-dihydro-1(2*H*)-benzopyran-3,5,7-triol (epicatechin, 10 mg/ kg; Sigma-Aldrich, St. Louis, MO); or the general antioxidant, NAC (150 mg/kg; Sigma-Aldrich). Animals were treated either during hyperoxia stage (75% oxygen) only (p7–p12) or during hyperoxia (75% oxygen) and hypoxia stage (21% oxygen) (p7–p17). Control animals were injected with the vehicle. The treatment regimen was optimized and described previously (El-Remessy et al., 2007).

Dissecting Retinal Tissue.

Pups were deeply anesthetized by an intraperitoneal injection of 40 mg/kg Avertin 2. One eye was enucleated and fixed in 2% paraformaldehyde overnight to be flat-mounted. For the other eye, retinas were isolated and snap frozen for biochemical assays.

Analysis of Vaso-Obliteration and Neovascularization.

Retinal vascular distribution was analyzed by use of retinal flat mounts labeled with biotinylated *Griffonia simplicifolia* lectin B4 and Texas Red-conjugated Avidin D (Vector Laboratories, Burlingame, CA). Retinas were viewed and imaged with fluorescence AxioObserver Zeiss Microscope (Carl Zeiss GmbH, Jena, Germany). Vaso-obliteration was assessed on p12 and p17 as described previously (Al- Shabrawey et al., 2005). The areas of retinal neovascularization were assessed on p17 as described previously (El-Remessy et al., 2007).

Oxidized and Reduced Glutathione Ratio.

Total glutathione including GSH and oxidized glutathione (GSSG) were measured by use of a kit (Northwest Life Science, Vancouver, WA) according to manufacturer's protocol. For total glutathione, retinas were lysed in phosphate buffer (100 mM potassium phosphate and 1 mM EDTA) and were mixed with an equal amount of 10 mM 5,5`-dithiobis (2-nitrobenzoic acid) in the presence of glutathione reductase and NADPH producing a measurable yellow color. The color was measured at a wavelength of 412 nm. To detect GSSG, samples were treated with 10 mM 2-vinylpyridine (Sigma-Aldrich) in ethanol to sequester all the reduced GSH then measured using the same protocol of the glutathione. GSH was calculated as the difference between total glutathione and GSSG.

Determination of Retinal Lipid Peroxides.

The assay was performed on retinal lysates as described previously (Ali et al., 2008). In brief, retinal lysate is reacted with 20% acetic acid, 8% SDS, and thiobarbituric acid at 95°C for 60 min, and the reaction was cooled down on ice. The samples were centrifuged and the supernatant was extracted with *n*-butanol and pyridine (15:1, respectively) and the absorbance of the organic solvent layer measured at 532 nm. The results were compared with an external standard (tetramethoxypropane). The Bradford assay (Bio-Rad Laboratories, Hercules, CA) was performed to determine the protein concentration of the retinal lysate. Lipid peroxide level was expressed in nanomoles of malondialdehyde per milligram of total protein.

Western Blotting Analysis.

Retinas and BRE cells were harvested after various treatments and lysed in modified radioimmunoprecipitation assay buffer (Millipore Corporation, Billerica, MA) 30 min on ice. Insoluble material was removed by centrifugation at 14,000*g* at 4°C for 30 min. Fifty micrograms of total protein was boiled in 6X Laemmli sample buffer, separated on a 10 to 12% SDS-polyacrylamide gel by electrophoresis, transferred to nitrocellulose, and reacted with specific antibody. The primary antibodies for cleaved caspase-3, phospho-p38, p38, phospho-Akt, or Akt were obtained from (Cell Signaling Technology Inc., Danvers, MA) and were detected by use of a horseradish peroxidase conjugated antibody and enhanced chemiluminescence (GE Healthcare, Piscataway, NJ). The films were subsequently scanned, and band intensity was quantified by use densitometry software (α Innotech, San Leandro, CA). For PI 3-kinase tyrosine nitration, retinal lysates were incubated with p85 antibody and A/G agarose beads overnight. The precipitated proteins were analyzed by SDS-polyacrylamide gel electrophoresis and blotted with nitrotyrosine antibody or p85 for equal loading as described

above. Antibodies for p85 subunit of the PI 3-kinase and nitrotyrosine were obtained from (Millipore Corporation). For VEGF, retinal lysates were subjected to heparin beads (Sigma-Aldrich) as described previously (Platt et al., 2005). In brief, the beads were pelleted at 5000*g* for 1 min, washed in 400 mM NaCl and 20 mM Tris, and loaded onto a 4 to 20% gradient Tris glycine precast gel (Bio-Rad Laboratories). After blocking, the membrane was incubated with VEGF primary antibody (Calbiocam, Gibbstown, NJ). The band was visualized and quantified as described above.

Detection of Nitrotyrosine.

Relative amounts of proteins nitrated on tyrosine were measured by use of slot-blot techniques as described previously (El-Remessy et al., 2003). In brief, radioimmunoprecipitation assay lysate was immobilized onto nitrocellulose membrane by use of a slot-blot microfiltration unit (Bio-Rad Laboratories). A dilution series of peroxynitrite-modified bovine serum albumin (Cayman Chemical, Ann Harper, MI) was loaded to generate a standard curve, and nitrotyrosine was detected by use of a polyclonal anti-nitrotyrosine antibody (Millipore Corporation) followed by peroxidase-labeled goat anti-mouse IgG and enhanced chemiluminescence. Relative levels of nitrotyrosine immunoreactivity were determined by densitometry software (Alpa Innotech).

Data Analysis.

The results were expressed as mean ± S.E. Differences among experimental groups were evaluated by analysis of variance, and the significance of difference between groups was assessed by the post hoc test (Fisher's protected least significant difference) when indicated. Significance was defined as $P < 0.05$.

Results

Blocking tyrosine nitration decreases retinal vaso- obliteration.

Previous studies showed a positive correlation between retinal vascular cell death, increases in peroxynitrite formation, and tyrosine nitration. Therefore, we screened the protective effects of selective inhibition of tyrosine nitration by use of epicatechin or the general antioxidant and the thiol donor NAC versus decomposing peroxynitrite using FeTPPS, a selective peroxynitrite decomposition catalyst. As shown in Fig. 1, A–D, exposing the developing retina of pups (p7–p12) to high oxygen concentration caused retinal vaso-obliteration as indicated by the capillary dropout area in the central retina. Treatment of pups with FeTPPS (1 mg/kg), epicatechin (10 mg/kg), or NAC (150 mg/kg) significantly reduced central capillary dropout by 34.2%, 25%, and 42%, respectively (Fig. 1E). NAC showed superior effect over epicatechin in protecting the retina from vascular cell death as shown (Fig. 1E). Treatment of control pups with FeTPPS, epicatechin, or NAC did not alter physiological retinal vascular density (data not shown). These results suggest that selective blocking of tyrosine nitration has a protective effect comparable with decomposing peroxynitrite or preventing thiol oxidation on retinal vascular cell death.

Blocking tyrosine nitration prevents retinal apoptosis.

Apoptosis has been postulated as the mechanism by which vascular cell death occurs in ischemic retinopathy. Therefore, we investigated the expression of apoptotic markers before p12. Exposing the retina (p7–p9) to high oxygen resulted in increases in cleaved caspase-3 (Fig. 2A). Treatment with FeTPPS, epicatechin, or NAC significantly reduced cleaved caspase-3 by 46.5%, 51%, and 43.5% respectively (Fig. 2A). Apoptosis was further confirmed by detecting poly (ADP ribose) polymerase (PARP), a cleavage target of caspase-3 (Fig. 2B). Retinas exposed to

hyperoxia (75% oxygen) showed an increase in PARP activation. Treatment with FeTPPS, epicatechin, or NAC reduced PARP activation by 50%, 64%, and 71.5%, respectively.

Effect of inhibition of tyrosine nitration on VEGF.

Down-regulation of VEGF expression has been postulated to cause vaso-obliteration of the newly formed capillaries (Alon et al., 1995). Therefore, we tested whether the protective effects of blocking tyrosine nitration on preventing retinal vaso-obliteration involve alteration of VEGF expression. As shown in Fig. 3, exposing the retina (p7–p12) to high oxygen resulted in modest but significant decreases in VEGF expression compared with retinas developed at normal oxygen. It is interesting that treatment with FeTPPS, epicatechin, or NAC did not affect VEGF expression compared with PBS treated pups (Fig. 3).

Blocking tyrosine nitration selectively decreases nitrative stress.

The retina is believed to be vulnerable to nitrative and oxidative damage because of the abundance of polyunsaturated fatty acids. Hyperoxia (75% oxygen) showed a significant increase in the nitrotyrosine formation compared with normoxia (21% oxygen) (Fig. 4A). Treatment of pups with FeTPPS, epicatechin, or NAC significantly decreased nitrotyrosine formation (50%, 58%, and 60% respectively). In addition to tyrosine nitration, peroxynitrite can cause thiol oxidation, which compromises antioxidant defense. Measuring the ratio between the cellular oxidized to reduced glutathione is used as a marker for the retinal antioxidant defense. Normal tissue has a balanced ratio between oxidized and reduced glutathione. As shown in Fig. 4B, retinas from p12 pups exposed to high oxygen showed (4-fold) increases in the tissue GSSG/GSH ratio. Treatment with either FeTPPS or NAC significantly restored the GSSG/GSH ratio and increased the retinal antioxidant defense. In contrast, treatment with epicatechin has a modest but not significant effect on the GSSG/GSH ratio.

Hyperoxia causes tyrosine nitration of p85 subunit of PI 3-Kinase.

Our previous work has shown that the p85 regulatory subunit of PI 3-kinase is a susceptible target for peroxynitrite-induced tyrosine nitration in endothelial cells (el-Remessy et al., 2005). As shown in Fig. 5A, retinas from p12 that were exposed to high oxygen showed a (4-fold) increase in tyrosine nitration of p85 compared with normoxia (21% oxygen). Treatment (p7–p12) with epicatechin or NAC significantly reduced the nitrating effect of peroxynitrite on tyrosine residues similar to decomposing peroxynitrite with FeTPPS.

Hyperoxia-induced nitration inhibits Akt survival and activates p38 MAPK.

Because the retina is composed of several cell types, we further examined the role of tyrosine nitration in hyperoxia-induced vascular cell death. BRE cells were cultured in high oxygen conditions (40%) and compared with normoxia (21%). BRE cells showed 2.3-fold increase in tyrosine nitration of the p85 subunit compared with normoxia (21% oxygen) (Fig. 5B). Treatment with FeTPPS (2.5 μM), epicatechin (100 μM), or NAC (1 mM) for 48 h significantly reduced hyperoxia-induced p85 tyrosine nitration (Fig. 5B). To confirm the inhibitory effect of tyrosine nitration on PI 3-kinase, we tested the effects of inhibitors on Akt phosphorylation. Akt, a downstream target of PI 3-kinase, mediates cell survival by inhibiting apoptotic processes. Hyperoxia (40% oxygen) significantly decreased Akt phosphorylation compared with normoxia (21% oxygen) by 40% (Fig. 6A). Treating cells with FeTPPS, epicatechin, or NAC for 48 h restored Akt activation. PI 3-kinase/ Akt signaling promotes endothelial cell survival by inhibiting p38 MAPK-dependent apoptosis (Gratton et al., 2001). Therefore, blockade of PI 3-kinase/Akt via tyrosine nitration of p85 subunit can lead to enhanced activation of p38 MAPK and endothelial apoptosis. As shown in Fig. 6B, cells cultured in hyperoxia (40% oxygen) showed a 2-fold increase in p38 MAPK phosphorylation that was decreased by treatment with

FeTPPS, epicatechin, or NAC. Increases in p38 MAPK phosphorylation were also observed in p12 retinas subjected to high oxygen compared with controls (Fig. 6C). Retinas from PBS-treated pups showed a 2-fold increase in p38 MAPK phosphorylation compared with normoxia (21% oxygen). Treatments with FeTPPS, epicatechin, or NAC reduced p38 MAPK phosphorylation by 34.6%, 36.6%, and 49.1% respectively. Next, we evaluated the effects of hyperoxia (40% oxygen) to induce endothelial cell apoptosis. As shown in Fig. 6D, hyperoxia (40% oxygen) induced endothelial cell apoptosis as indicated by increased expression of cleaved caspase-3. Blocking tyrosine nitration with FeTPPS, epicatechin, or NAC protected the cells against apoptosis by decreasing the level of cleaved caspase-3 by 50%, 43%, and 46% respectively.

Early intervention of tyrosine nitration prevents retinal oxidative injury.

Lipid peroxidation has been established as a general marker of oxidative stress and cellular injury. As shown in Fig. 7A, retinas from pups that underwent hyperoxia (75% oxygen) and hypoxia (21% oxygen) (p7–p17) showed high levels of lipid peroxides compared with the pups in normal air. Early intervention with FeTPPS, epicatechin, or the thiol donor NAC decreased lipid peroxidation, hence, the cellular injury. It is interesting that treatment with FeTPPS or the thiol donor NAC, but not epicatechin, restored the antioxidant defense as indicated by the ratio of GSSG to GSH (Fig. 7B). These results confirm the effect of epicatechin in selectively blocking tyrosine nitration without exerting antioxidant effect.

Early intervention of tyrosine nitration prevents retinal neovascularization.

Our previous studies showed that blocking nitration after vaso-obliteration (p12–p17) did not prevent retinal neovascularization (El-Remessy et al., 2007). Here, we tested the long-term protective effects of blocking tyrosine nitration during both hyperoxia (75% oxygen) and

hypoxia (21% oxygen) (p7–p17). Compared with PBS-treated pups, treatment with epicatechin significantly reduced (by 62.1%) retinal neovascularization. This effect was comparable with, but to a lesser extent, pups treated with FeTPPS or NAC that had a 76.8% and 71.5% reduction in neovascularization, respectively (Fig. 8, A–E). Next, we measured the capillary dropout areas at the end of hypoxia (21% oxygen) (p17) to test the effect of treatment on the physiological revascularization in the central retina. As expected in this model, PBS-treated controls showed a 29% reduction in capillary dropout areas compared with the reduction at the end of hyperoxia (75% oxygen) (p12). Treatment with FeTPPS, epicatechin, or NAC further reduced capillary dropout areas by 55%, 50%, and 60%, respectively, compared with p17 PBS-treated animals; suggesting that blocking peroxynitrite did not alter physiological revascularization; instead, it enhanced vascular regrowth and continued protection from vaso-obliteration (Fig. 8F).

Discussion

The present study documents novel data suggesting that 1) Peroxynitrite mediates retinal vaso-obliteration via tyrosine nitration of p85 kinase and inhibition of PI 3kinase/Akt survival pathway; 2) Blocking tyrosine nitration restores survival signal and prevents endothelial cell apoptosis and retinal ischemia and 3) early intervention with treatments that target peroxynitrite and tyrosine nitration prevents retinal neovascularization. To our knowledge this is the first *in vivo* study to elucidate the mechanism by which peroxynitrite-mediated tyrosine nitration and inhibition of PI 3-kinase survival pathway trigger vascular cell death in ischemic retinopathy model. Our results also demonstrate that targeting tyrosine nitration with dietary supplements such as epicatechin and NAC represent potentially safe and effective therapeutic strategy that could be translated to patients with ischemic-proliferative diseases.

The focus of the current study is to test the protective effects of blocking peroxynitrite and tyrosine nitration on retinal cell death *in vitro* and on preventing vaso-obliteration and neovascularization *in vivo*. Therefore, we took the advantage of using ischemic retinopathy mouse model as it has two distinguished stages: initial vascular cell death and vaso-obliteration, which are associated with excessive peroxynitrite formation followed by retinal neovascularization which is associated with mild oxidative insult (Al-Shabrawey et al., 2005; El-Remessy et al., 2007). We used epicatechin, a flavonoid and one of the green tea extract that selectively block peroxynitrite-mediated tyrosine nitration but not thiol oxidation (Schroeder et al., 2001; El-Remessy et al., 2005; El-Remessy et al., 2007) and compared its effects to blocking peroxynitrite using FeTPPs, the peroxynitrite decomposition catalyst or blocking thiol oxidation using the dietary supplement and the thiol donor NAC (El-Remessy et al., 2005; El-Remessy et al., 2007). Our results showed that exposing the developing retina to high oxygen induces

significant capillary drop out areas that was accompanied with nitrotyrosine formation and apoptosis as indicated by increased expression of cleaved caspase-3 expression and poly (ADP-ribose) polymerase (PARP). These results are in agreement with previous experimental and clinical studies showing that ischemic retinopathy is associated with increases in retinal oxidative damage and decreases in antioxidant defense (Papp et al., 1999; Brooks et al., 2001; Gu et al., 2002; Beauchamp et al., 2004; Wright et al., 2006; Bartoli et al., 2008). Our results showing that hyperoxia caused significant increases in cleaved PARP, the caspase-3 substrate *in vitro* and *in vivo* lend further support to the previous reports of the critical role of caspase-3 in executing peroxynitrite-induced apoptosis in endothelial cells (Kotamraju et al., 2001; Gu et al., 2003; Zhu et al., 2004; El-Remessy et al., 2005). Treatment with epicatechin blocked tyrosine nitration and significantly reduced capillary dropout areas and the expression of cleaved caspase-3 and PARP. However, epicatechin did not alter GSSG/GSH ratio confirming its selective properties in blocking tyrosine nitration but not thiol oxidation. On the other hand, treatment with FeTPPs or NAC not only blocked tyrosine nitration but also improved GSSG/GSH ratio indicating restoration of retinal antioxidant defense which explain the superior effects of NAC and FeTPPs in reducing vaso-obliteration over epicatechin. In contrast, NAC failed to show protective effects on reducing retinal avascularity and apoptosis in a rat model of ROP that could be attributed to the different nature of model and shorter duration of treatment (Saito et al., 2007). Our results establish a unique role of selective blocking tyrosine nitration, apart from the anti-oxidant effect, in preventing retinal vaso-obliteration and support the notion of its therapeutic intervention for ischemic retinal diseases.

To elucidate the molecular mechanisms by which blocking tyrosine nitration protect the retina from apoptosis, we determined the expression of VEGF as its down-regulation has been postulated to cause vaso-obliteration of the newly formed capillaries (Alon et al., 1995). In agreement, our results showed modest but significant decrease in VEGF expression in hyperoxic retinas. However, treatment with FeTPPs, epicatechin or NAC did not alter VEGF expression compared to PBS-treated ones. These results suggest that the protective effects of blocking peroxynitrite and tyrosine nitration in preventing retinal apoptosis and vaso-obliteration are not mediated by altering VEGF expression level, instead by modulating VEGF signal.

VEGF's function as a survival factor for endothelial cells is well established (Duh and Aiello, 1999). VEGF activation of VEGFR2 transduces anti-apoptic signal via PI 3-kinase/Akt signaling pathway (Gerber et al., 1998; Fujio and Walsh, 1999). Tyrosine nitration and subsequent inhibition of the p85 regulatory subunit of PI 3-kinase have been documented in response to peroxynitrite (Hellberg et al., 1998; El-Remessy et al., 2005). Here, we show that retinas from pups exposed to hyperoxia (75% oxygen) showed significant increases (4-fold) in tyrosine nitration of p85 subunit compared to pups in normoxia (21% oxygen). Similar pattern was observed in retinal endothelial cultures maintained at hyperoxia (75% oxygen) compared to the one maintained at normal oxygen. These effects were associated with impaired Akt phosphorylation, increased p38 MAPK phosphorylation and increased expression of the apoptotic marker caspase-3. Treatment with epicatechin or NAC had comparable effects to FeTPPs, and prevented tyrosine nitration of p85, restored Akt survival pathway and reduced the activation of p38 MAPK apoptotic pathway. These results confirm the relationship between nitration of p85, decreases in Akt activity and the pro-apoptotic effects of hyperoxia-induced peroxynitrite. Our findings lend further support to previous reports of significant increases in

oxidative and nitrative stress in ischemic retinopathy model (Papp et al., 1999; Brooks et al., 2001; Gu et al., 2002; Gu et al., 2003; Beauchamp et al., 2004; Saito et al., 2007; Medina et al., 2008). Understanding of the molecular pathogenesis of ischemic retinopathy provides the basis for identifying novel therapeutic targets. The role of the hypoxia-induced factors VEGF and erythropoietin as well as the maternally derived factors insulin-like growth factor-1 have begun to be elucidated (see review (Heidary et al., 2009)). However, our study is the first we know of that elucidates the molecular mechanism of the tyrosine nitration of p85 leading to inactivation of the PI 3-kinase/Akt survival signal and activation of the pro-apoptotic p38 MAPK signal in the ischemic retinopathy model. A scheme of the proposed mechanism is depicted in Fig. 9. These findings explain the protective effects of epicatechin in preventing vaso-obliteration even though it did not completely restore retinal anti-oxidant defense.

Retinal neovascularization takes place as a result of an initial stage of capillary loss leading to inner retinal ischemia that drives up-regulation of angiogenic growth factors (Mizutani et al., 1996). The combined vascular protection of reducing pathological neovascularization while allowing physiological revascularization of the retina is the ideal therapeutic modality for ischemic retinopathy diseases. Therefore, it is critical to evaluate the effects of early blocking of tyrosine nitration and capillary drop out on preventing the subsequent neovascularization. Continuous intervention of tyrosine nitration during both hyperoxia (75% oxygen) and hypoxia 21% oxygen (p7-p17) with epicatechin, FeTPPs or NAC significantly reduced lipid peroxidation, retinal neovascularization and further reduced central capillary drop out compared to PBS-controls. The vascular protective effects of epicatechin in the current study are mainly due its effects in preventing earlier vaso-obliteration and hence the stimulus to neovascularization. This concept is further supported by our previous findings that late intervention with epicatechin after

vaso-obliteration (p12-p17) did not prevent retinal neovascularization (El-Remessy et al., 2005; El-Remessy et al., 2007). The vascular protective effects of NAC and FeTPPs were associated with restoration of anti-oxidant defense as indicated by GSSG/GSH ratio, but not of epicatechin confirming its selective effect of inhibiting tyrosine nitration apart from thiol oxidation. While the vascular protective effects of FeTPPs are significant, the fact that it contains iron will limit its therapeutic use for chronic administration. The vascular effects of NAC were superior to epicatechin but did not reach significance and this could be attributed to the antioxidant of NAC over epicatechin. New studies showed that NAC also may have other mechanism that can interfere with cell proliferation by regulating the cell cycle regulatory protein (Menon et al., 2007). However, both epicatechin and NAC prove effective and the fact that they are already available as dietary supplements open the door for therapeutic utility. Together, these results point out the importance of the timing and the molecular target of intervention. In support, studies using the same ischemic retinopathy model showed that early intervention with omega-3 polyunsaturated fatty acid failed to rescue oxygen-induced vessel loss during hyperoxia (75% oxygen) but prevented late retinal neovascularization (Connor et al., 2007). On the other hand, intervention with statins effectively reduced retinal oxidative stress, capillary drop out and prevented neovascularization (Bartoli et al., 2008; Medina et al., 2008).

In conclusion, our study is the first to elucidate the mechanism by which tyrosine nitration of p85 kinase and inhibition of PI 3-kinase/Akt survival pathway causes vascular cell death *in vivo* and to demonstrate the vascular protective effects of the early and continuous intervention of peroxynitrite and tyrosine nitration on retinal vessel loss and neovascularization. Furthermore, our results provide compelling evidence that targeting tyrosine nitration with safe dietary supplements such as epicatechin and NAC in animal models should provide the rationale for testing these agents as a possible control of common ischemic proliferative retinopathy such as DR and ROP.

References

Aiello LP, Gardner TW, King GL, Blankenship G, Cavallerano JD, Ferris FL, 3rd and Klein R (1998) Diabetic retinopathy. *Diabetes Care* 21:143-156.

Al-Shabrawey M, Bartoli M, El-Remessy AB, Platt DH, Matragoon S, Behzadian MA, Caldwell RW and Caldwell RB (2005) Inhibition of NAD(P)H oxidase activity blocks vascular endothelial growth factor overexpression and neovascularization during ischemic retinopathy. *Am J Pathol* 167:599-607.

Ali TK and El-Remessy AB (2009) Diabetic retinopathy: current management and experimental therapeutic targets. *Pharmacotherapy* 29:182-192.

Ali TK, Matragoon S, Pillai BA, Liou GI and El-Remessy AB (2008) Peroxynitrite mediates retinal neurodegeneration by inhibiting nerve growth factor survival signaling in experimental and human diabetes. *Diabetes* 57:889-898.

Alon T, Hemo I, Itin A, Pe'er J, Stone J and Keshet E (1995) Vascular endothelial growth factor acts as a survival factor for newly formed retinal vessels and has implications for retinopathy of prematurity. *Nat Med* 1:1024-1028.

Bartoli M, Al-Shabrawey M, Labazi M, Behzadian AM, Istanboli M, El-Remessy A, Caldwell RW, Marcus DM and Caldwell RB (2008) HMG-CoA reductase inhibitors (statins) prevents retinal neovascularization in a model of oxygen-induced retinopathy. *Invest Ophthalmol Vis Sci*.

Beauchamp MH, Sennlaub F, Speranza G, Gobeil J, Fernand, Checchin D, Kermorvant-Duchemin E, Abran D, Hardy P and Lachapelle P (2004) Redox-dependent effects of

nitric oxide on microvascular integrity in oxygen-induced retinopathy. *Free Radical Biology and Medicine* 37:1885-1894.

Brooks SE, Gu X, Samuel S, Marcus DM, Bartoli M, Huang PL and Caldwell RB (2001) Reduced severity of oxygen-induced retinopathy in eNOS-deficient mice. *Invest Ophthalmol Vis Sci* 42:222-228.

Caldwell RB, Bartoli M, Behzadian MA, El-Remessy AE, Al-Shabrawey M, Platt DH and Caldwell RW (2003) Vascular endothelial growth factor and diabetic retinopathy: pathophysiological mechanisms and treatment perspectives. *Diabetes Metab Res Rev* 19:442-455.

Chen J and Smith LE (2007) Retinopathy of prematurity. *Angiogenesis* 10:133-140.

Connor KM, SanGiovanni JP, Lofqvist C, Aderman CM, Chen J, Higuchi A, Hong S, Pravda EA, Majchrzak S, Carper D, Hellstrom A, Kang JX, Chew EY, Salem N, Jr., Serhan CN and Smith LE (2007) Increased dietary intake of omega-3-polyunsaturated fatty acids reduces pathological retinal angiogenesis. *Nat Med* 13:868-873.

Drel VR, Pacher P, Ali TK, Shin J, Julius U, El-Remessy AB and Obrosova IG (2008) Aldose reductase inhibitor fidarestat counteracts diabetes-associated cataract formation, retinal oxidative-nitrosative stress, glial activation, and apoptosis. *Int J Mol Med* 21:667-676.

Du Y, Smith MA, Miller CM and Kern TS (2002) Diabetes-induced nitrative stress in the retina, and correction by aminoguanidine. *J Neurochem* 80:771-779.

Duh E and Aiello LP (1999) Vascular endothelial growth factor and diabetes: the agonist versus antagonist paradox. *Diabetes* 48:1899-1906.

El-Remessy AB, Abou-Mohamed G, Caldwell RW and Caldwell RB (2003) High glucose-induced tyrosine nitration in endothelial cells: role of eNOS uncoupling and aldose reductase activation. *Invest Ophthalmol Vis Sci* 44:3135-3143.

El-Remessy AB, Al-Shabrawey M, Platt DH, Behzadian MA, Bartoli M, Ghaly N, Tsai N-T, Motamed K and Caldwell RB (2007) Peroxynitrite mediates VEGF's angiogenic signal and function via nitration independent mechanism in endothelial cells. *FASEB J.* 21:2528-2539.

El-Remessy AB, Bartoli M, Platt DH, Fulton D and Caldwell RB (2005) Oxidative stress inactivates VEGF survival signaling in retinal endothelial cells via PI 3-kinase tyrosine nitration. *J Cell Sci* 118:243-252.

Fujio Y and Walsh K (1999) Akt mediates cytoprotection of endothelial cells by vascular endothelial growth factor in an anchorage-dependent manner. *J Biol Chem* 274:16349-16354.

Gerber HP, McMurtrey A, Kowalski J, Yan M, Keyt BA, Dixit V and Ferrara N (1998) Vascular endothelial growth factor regulates endothelial cell survival through the phosphatidylinositol 3'-kinase/Akt signal transduction pathway. Requirement for Flk-1/KDR activation. *J Biol Chem* 273:30336-30343.

Gratton JP, Morales-Ruiz M, Kureishi Y, Fulton D, Walsh K and Sessa WC (2001) Akt down-regulation of p38 signaling provides a novel mechanism of vascular endothelial growth factor-mediated cytoprotection in endothelial cells. *J Biol Chem* 276:30359-30365.

Gu X, El-Remessy A, Brooks SE, Al-Shabrawey M, Tsai NT and Caldwell RB (2003) Hyperoxia Induces Retinal Vascular Endothelial Cell Apoptosis through Formation of Peroxynitrite. *Am J Physiol Cell Physiol*.

Gu X, Samuel S, El-Shabrawey M, Caldwell RB, Bartoli M, Marcus DM and Brooks SE (2002) Effects of sustained hyperoxia on revascularization in experimental retinopathy of prematurity. *Invest Ophthalmol Vis Sci* 43:496-502.

Heidary G, Vanderveen D and Smith LE (2009) Retinopathy of prematurity: current concepts in molecular pathogenesis. *Semin Ophthalmol* 24:77-81.

Hellberg CB, Boggs SE and Lapetina EG (1998) Phosphatidylinositol 3-kinase is a target for protein tyrosine nitration. *Biochem Biophys Res Commun* 252:313-317.

Kotamraju S, Hogg N, Joseph J, Keefer LK and Kalyanaraman B (2001) Inhibition of oxidized low-density lipoprotein-induced apoptosis in endothelial cells by nitric oxide. Peroxyl radical scavenging as an antiapoptotic mechanism. *J Biol Chem* 276:17316-17323.

Kowluru RA, Kanwar M and Kennedy A (2007) Metabolic memory phenomenon and accumulation of peroxynitrite in retinal capillaries. *Exp Diabetes Res* 2007:21976.

Kowluru RA and Odenbach S (2004) Effect of long-term administration of alpha-lipoic acid on retinal capillary cell death and the development of retinopathy in diabetic rats. *Diabetes* 53:3233-3238.

Medina RJ, O'Neill CL, Devine AB, Gardiner TA and Stitt AW (2008) The pleiotropic effects of simvastatin on retinal microvascular endothelium has important implications for ischaemic retinopathies. *PLoS ONE* 3:e2584.

Menon SG, Sarsour EH, Kalen AL, Venkataraman S, Hitchler MJ, Domann FE, Oberley LW and Goswami PC (2007) Superoxide signaling mediates N-acetyl-L-cysteine-induced G1 arrest: regulatory role of cyclin D1 and manganese superoxide dismutase. *Cancer Res* 67:6392-6399.

Mizutani M, Kern TS and Lorenzi M (1996) Accelerated death of retinal microvascular cells in human and experimental diabetic retinopathy. *J Clin Invest* 97:2883-2890.

Pacher P, Beckman JS and Liaudet L (2007) Nitric oxide and peroxynitrite in health and disease. *Physiol Rev* 87:315-424.

Papp A, Nemeth I, Karg E and Papp E (1999) Glutathione status in retinopathy of prematurity. *Free Radic Biol Med* 27:738-743.

Platt DH, Bartoli M, El-Remessy AB, Al-Shabrawey M, Lemtalsi T, Fulton D and Caldwell RB (2005) Peroxynitrite increases VEGF expression in vascular endothelial cells via STAT3. *Free Radic Biol Med* 39:1353-1361.

Saito Y, Geisen P, Uppal A and Hartnett ME (2007) Inhibition of NAD(P)H oxidase reduces apoptosis and avascular retina in an animal model of retinopathy of prematurity. *Mol Vis* 13:840-853.

Schroeder P, Klotz LO, Buchczyk DP, Sadik CD, Schewe T and Sies H (2001) Epicatechin selectively prevents nitration but not oxidation reactions of peroxynitrite. *Biochem Biophys Res Commun* 285:782-787.

Sennlaub F, Courtois Y and Goureau O (2002) Inducible nitric oxide synthase mediates retinal apoptosis in ischemic proliferative retinopathy. *J Neurosci* 22:3987-3993.

Smith LE, Wesolowski E, McLellan A, Kostyk SK, D'Amato R, Sullivan R and D'Amore PA (1994) Oxygen-induced retinopathy in the mouse. *Invest Ophthalmol Vis Sci* 35:101-111.

Wright KW, Sami D, Thompson L, Ramanathan R, Joseph R and Farzavandi S (2006) A physiologic reduced oxygen protocol decreases the incidence of threshold retinopathy of prematurity. *Trans Am Ophthalmol Soc* 104:78-84.

Zhu C, Wang X, Qiu L, Peeters-Scholte C, Hagberg H and Blomgren K (2004) Nitrosylation precedes caspase-3 activation and translocation of apoptosis-inducing factor in neonatal rat cerebral hypoxia-ischaemia. *J Neurochem* 90:462-471.

Zou MH, Shi C and Cohen RA (2002) High glucose via peroxynitrite causes tyrosine nitration and inactivation of prostacyclin synthase that is associated with thromboxane/prostaglandin H(2) receptor-mediated apoptosis and adhesion molecule expression in cultured human aortic endothelial cells. *Diabetes* 51:198-203.

Fig. 2.1.A-D

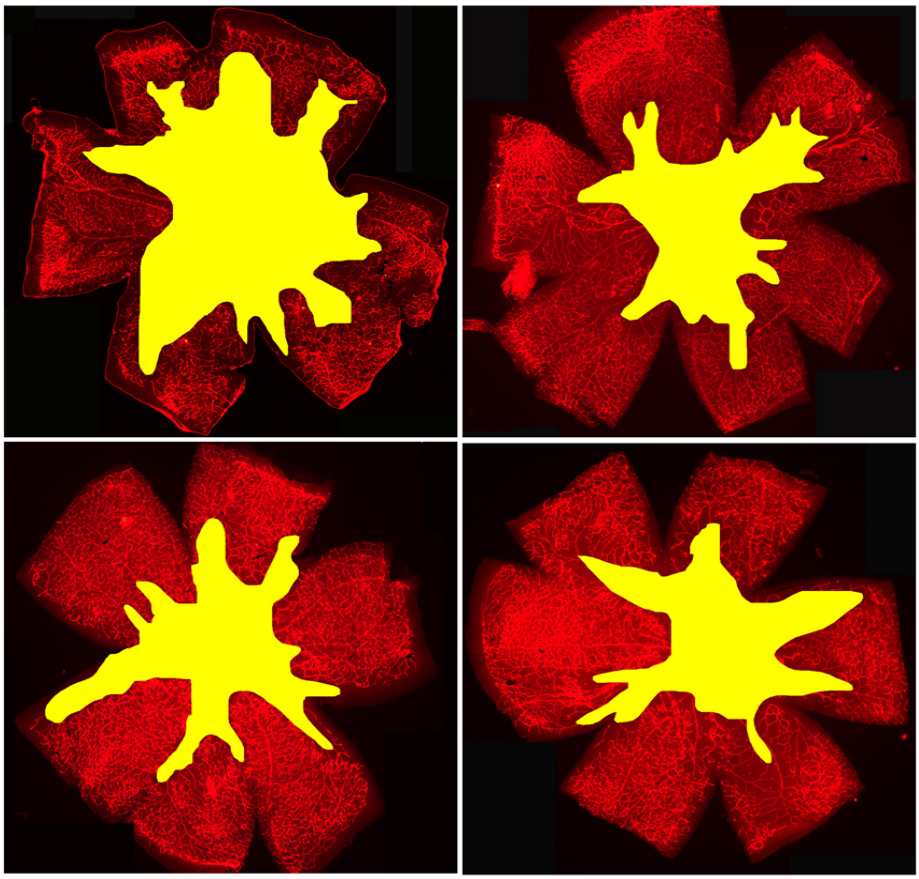

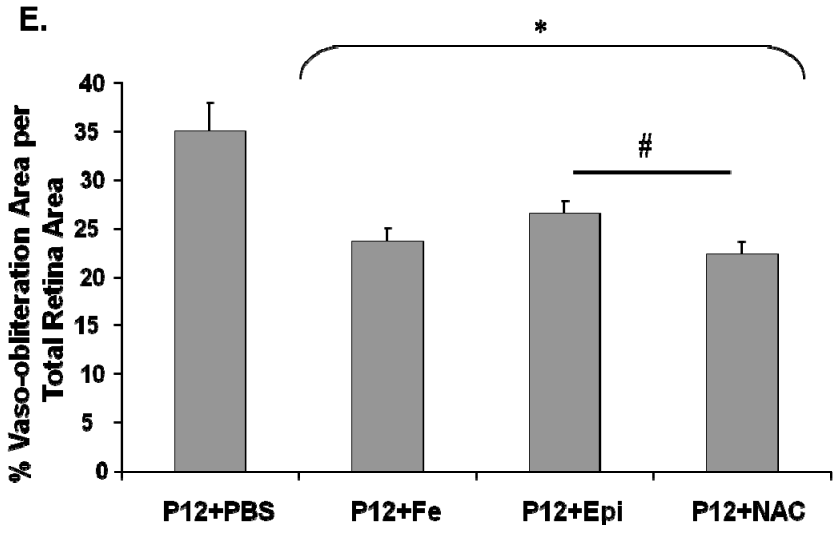
E.
*
#
% Vaso-obliteration Area per Total Retina Area
40
35
30
25
20
15
10
5
0
P12+PBS
P12+Fe
P12+Epi
P12+NAC

Fig. 2.1. Blocking peroxynitrite formation or tyrosine nitration decreases retinal vaso-obliteration.

(A-D) Flat-mounted retinas reacted with GSI lectin to localize capillary obliteration. Mice pups were maintained in hyperoxia (p7-p12) and treated with FeTPPs (1 mg/kg/day, i.p.), epicatechin (10 mg/kg/day, i.p) or NAC (150 mg/kg/day, i.p.). Exposing the developing retina to high oxygen resulted in 35% central capillary dropout area (Shaded yellow areas). Treatment with FeTPPs, epicatechin or NAC significantly reduced the capillary dropout areas.

(E) Statistical analysis of the ratio of central capillary dropout areas to total retinal area in PBS treated and other treated retinas showing the protective effects of blocking peroxynitrite formation and tyrosine nitration on retinal vaso-obliteration. (*$P<0.05$, n=10-12 inhibitors compared to vehicle). (#$P<0.05$, n=10-12 NAC compared to epicatechin).

Fig. 2.2.

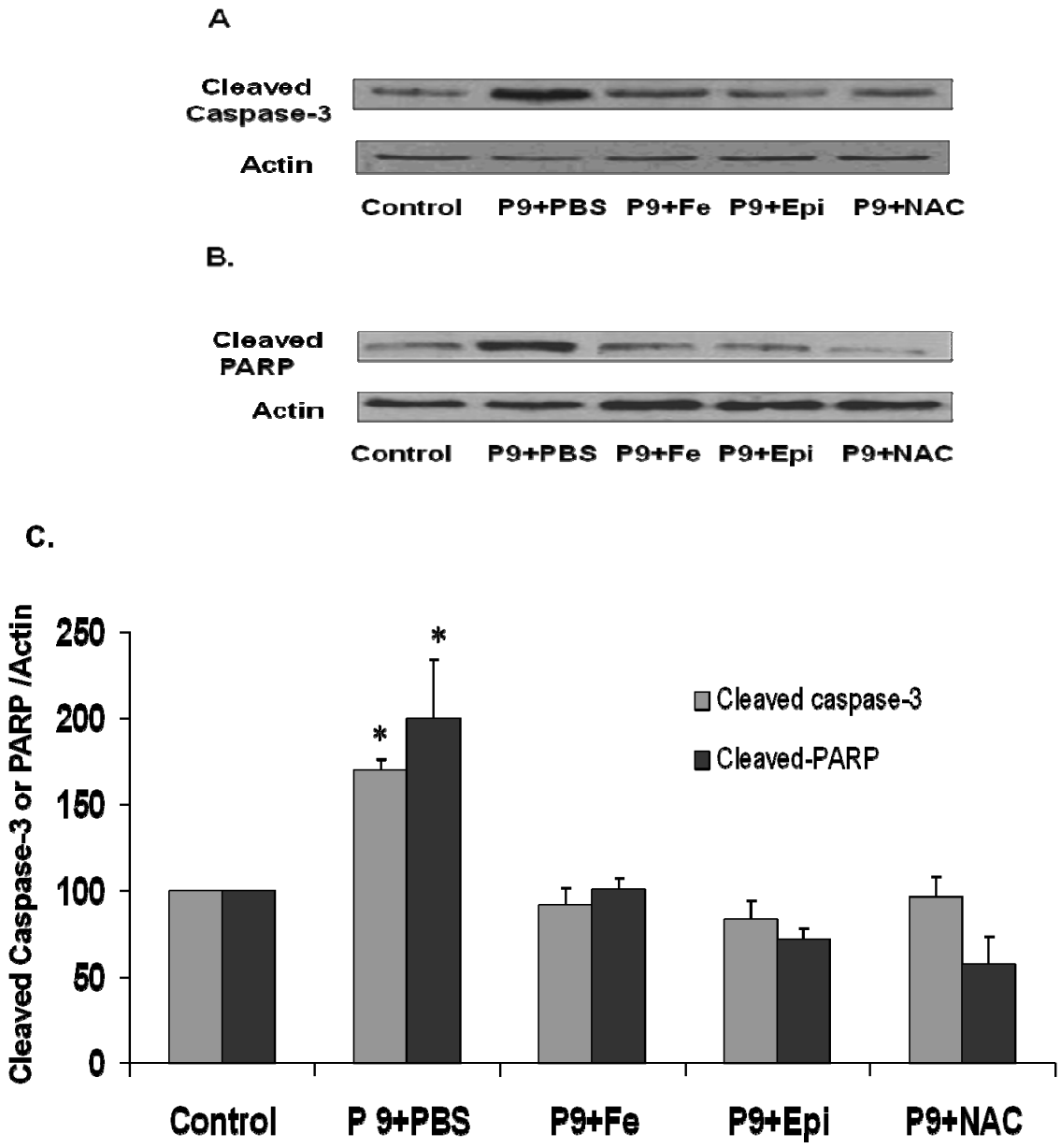
A
Cleaved Caspase-3
Actin
Control
P9+PBS
P9+Fe
P9+Epi
P9+NAC
B.
Cleaved PARP
Actin
Control
P9+PBS
P9+Fe
P9+Epi
P9+NAC
C.
Cleaved Caspase-3 or PARP /Actin
250
200
150
100
50
0
*
*
Cleaved caspase-3
Cleaved-PARP
Control
P 9+PBS
P9+Fe
P9+Epi
P9+NAC

Fig. 2.2. Blocking peroxynitrite formation or tyrosine nitration prevents retinal apoptosis markers.

(A) Western Blot analysis of retinal lysates (50 μg) show that exposing retina to hyperoxia (p7-p9) resulted in significant increases in apoptosis as indicated by 2 fold increase in cleaved Caspase-3 expression compared to normoxic control. Treatment with FeTPPs (1 mg/kg/day, i.p.), epicatechin (10 mg/kg/day, i.p) or NAC (150 mg/kg/day, i.p.) reduced cleaved caspase-3 expression to normal levels (**P*<0.05, *n*=4 vehicle treated hyperoxia compared to normal oxygen and inhibitors). **(B)** Western Blot analysis of retinal lysates (50 μg) show that exposing retina to hyperoxia (p7-p9) resulted in significant increases in apoptosis as indicated by 2 fold increase in cleaved PARP expression compared to normoxic control. Treatment with FeTPPs (1 mg/kg/day, i.p.), epicatechin (10 mg/kg/day, i.p) or NAC (150 mg/kg/day, i.p.) normalized cleaved PARP expression (**P*<0.05, *n*=4 vehicle treated hyperoxia compared to normal oxygen and inhibitors).

Fig. 2.3.

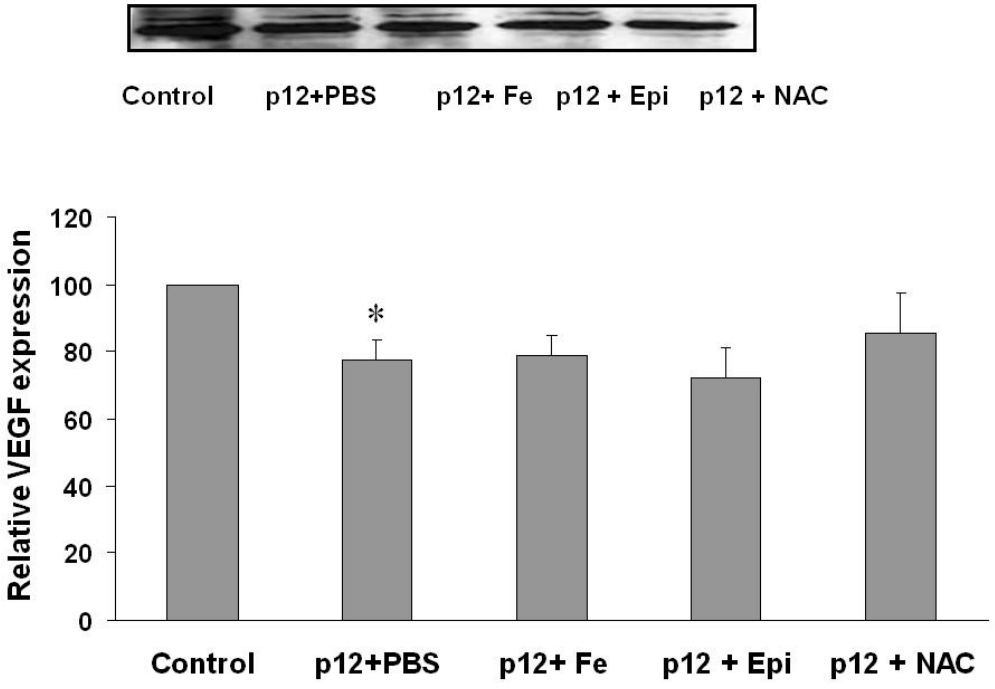
Control
p12+PBS
p12+ Fe
p12 + Epi
p12 + NAC
Relative VEGF expression
120
100
80
60
40
20
0
*
Control
p12+PBS
p12+ Fe
p12 + Epi
p12 + NAC

Fig. 2.3. Effect of inhibition of tyrosine nitration on VEGF

A representative image for western blot analysis of retinal lysates (100 μg) shows that exposing retina to hyperoxia (p7-p12) resulted in significant decreases in retinal VEGF expression. Treatment with FeTPPs (1 mg/kg/day, i.p.), epicatechin (10 mg/kg/day, i.p) or NAC (150 mg/kg/day, i.p.) did not show any effect on VEGF expression (*P<0.05, n=4 vehicle treated hyperoxia compared to normal oxygen).

Fig. 2.4.

A.

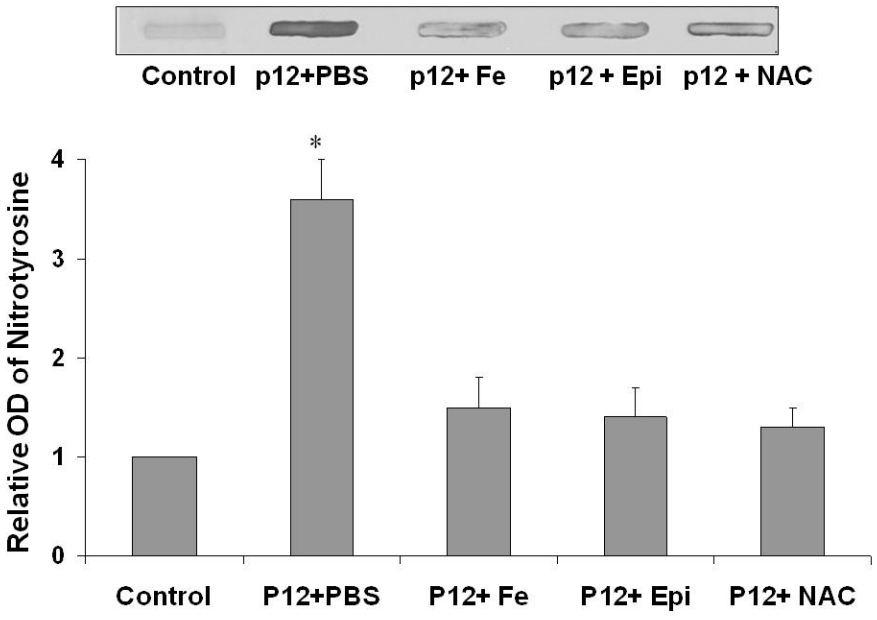
Control
p12+PBS
p12+ Fe
p12 + Epi
p12 + NAC
Relative OD of Nitrotyrosine
0
1
2
3
4
*
Control
P12+PBS
P12+ Fe
P12+ Epi
P12+ NAC

B.

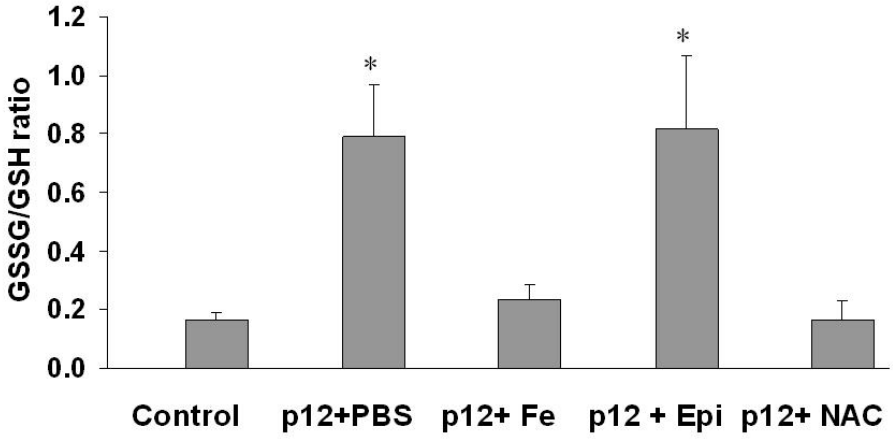
GSSG/GSH ratio
0.0
0.2
0.4
0.6
0.8
1.0
1.2
*
*
Control
p12+PBS
p12+ Fe
p12 + Epi
p12+ NAC

Fig. 2.4. Blocking tyrosine nitration selectively decreases nitrative stress but not antioxidant defense

(A) A representative image for slot blot analysis of retinal lysates (30 μg) shows that exposing retina to hyperoxia (p7-p12) resulted in significant increases in retinal nitrotyrosine formations. Treatment with FeTPPs (1 mg/kg/day, i.p.), epicatechin (10 mg/kg/day, i.p) or NAC (150 mg/kg/day, i.p.) significantly decreased tyrosine nitration (50%). (**P*<0.05, *n*=4 inhibitors compared to vehicle).

(B) Statistical analysis of the ratio of oxidized to reduced glutathione in different retinal lysate. Hyperoxia (p7-p12) decreased the retinal antioxidant defense with 4 fold. Treatment with FeTPPs (1 mg/kg/day, i.p.) or NAC (150 mg/kg/day, i.p.) restored the retinal antioxidant defense back to normal. Epicatechin (10 mg/kg/day, i.p) did not show any antioxidant properties. (**P*<0.05, *n*=4 FeTPPs and NAC compared to vehicle).

Fig. 2.5.

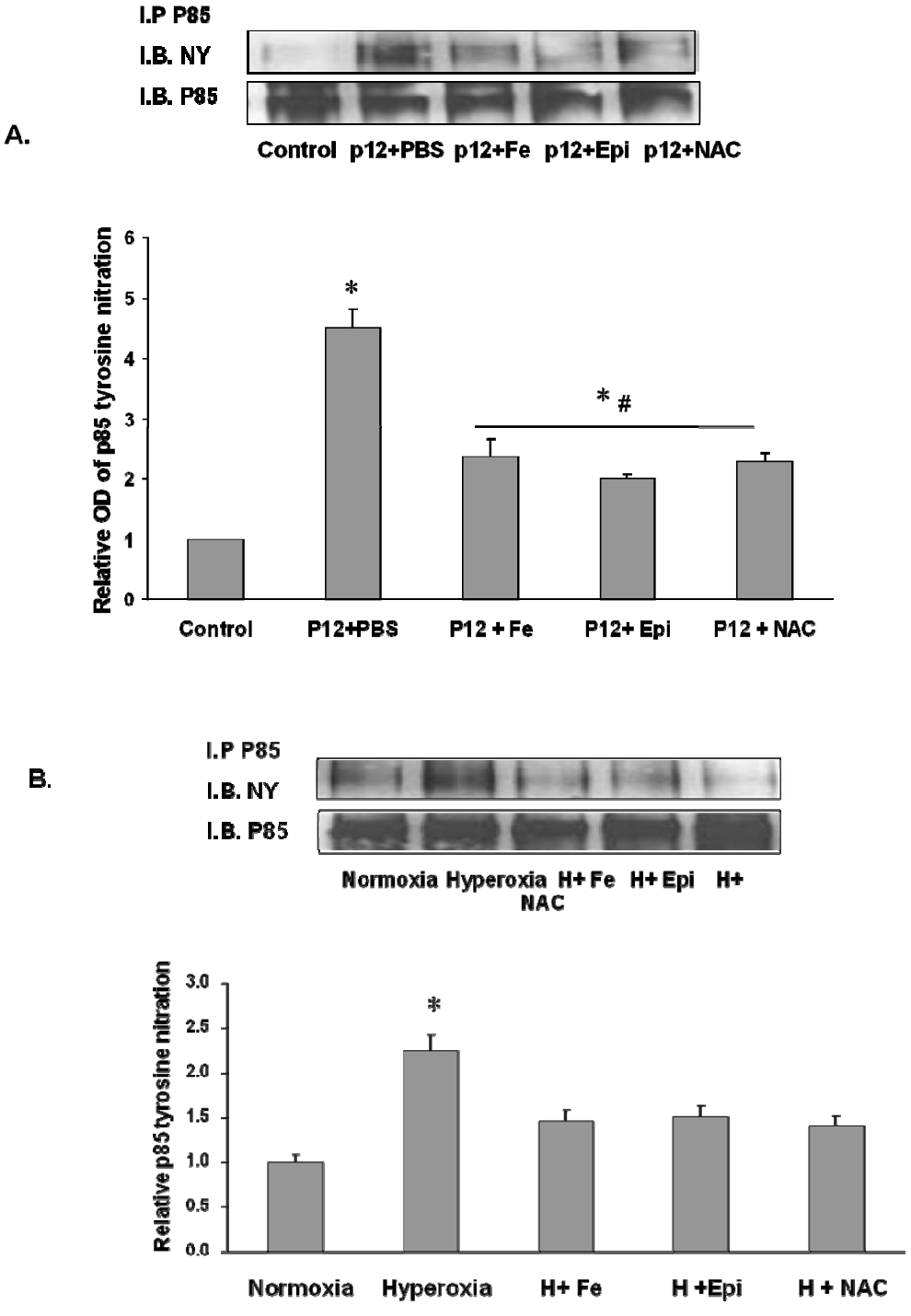
A.
I.P P85
I.B. NY
I.B. P85
Control p12+PBS p12+Fe p12+Epi p12+NAC
Relative OD of p85 tyrosine nitration
0
1
2
3
4
5
6
*
* #
Control
P12+PBS
P12 + Fe
P12+ Epi
P12 + NAC
B.
I.P P85
I.B. NY
I.B. P85
Normoxia Hyperoxia H+ Fe H+ Epi H+ NAC
Relative p85 tyrosine nitration
0.0
0.5
1.0
1.5
2.0
2.5
3.0
*
Normoxia
Hyperoxia
H+ Fe
H +Epi
H + NAC

Fig. 2.5. Hyperoxia causes tyrosine nitration of p85 subunit of PI 3-kinase

(A) Immunoprecipetation with anti-p85 subunit of PI 3-kinase and western blot analysis using anti-nitrotyrosine antibody show that exposing the retina to hyperoxia (p7-p12) resulted in significant increases in nitration on the regulatory p85 subunit compared with normal retinas. (n=4.) This effect was blocked by treatment with FeTPPs (1 mg/kg/day, i.p.), epicatechin (10 mg/kg/day, i.p) or NAC (150 mg/kg/day, i.p.) (**P*<0.05 vehicle compared to normal oxygen, # *P*<0.05 inhibitors compared to p12 hyperoxia).

(B) Immunoprecipetation with anti-p85 subunit of PI 3-kinase and western blot analysis using anti-nitrotyrosine antibody showed that cells ,cultured in high oxygen conditions (40%), significantly increased nitration of the regulatory p85 subunit compared with cells cultured in normal oxygen. This effect was blocked by the specific peroxynitrite decomposition catalyst FeTPPs (2.5 μM) and the specific nitration inhibitor epicatechin (100 μM) and thiol donor NAC (1 mM). (* P<0.05 vehicle compared to normal oxygen and inhibitors)

Fig. 2.6.

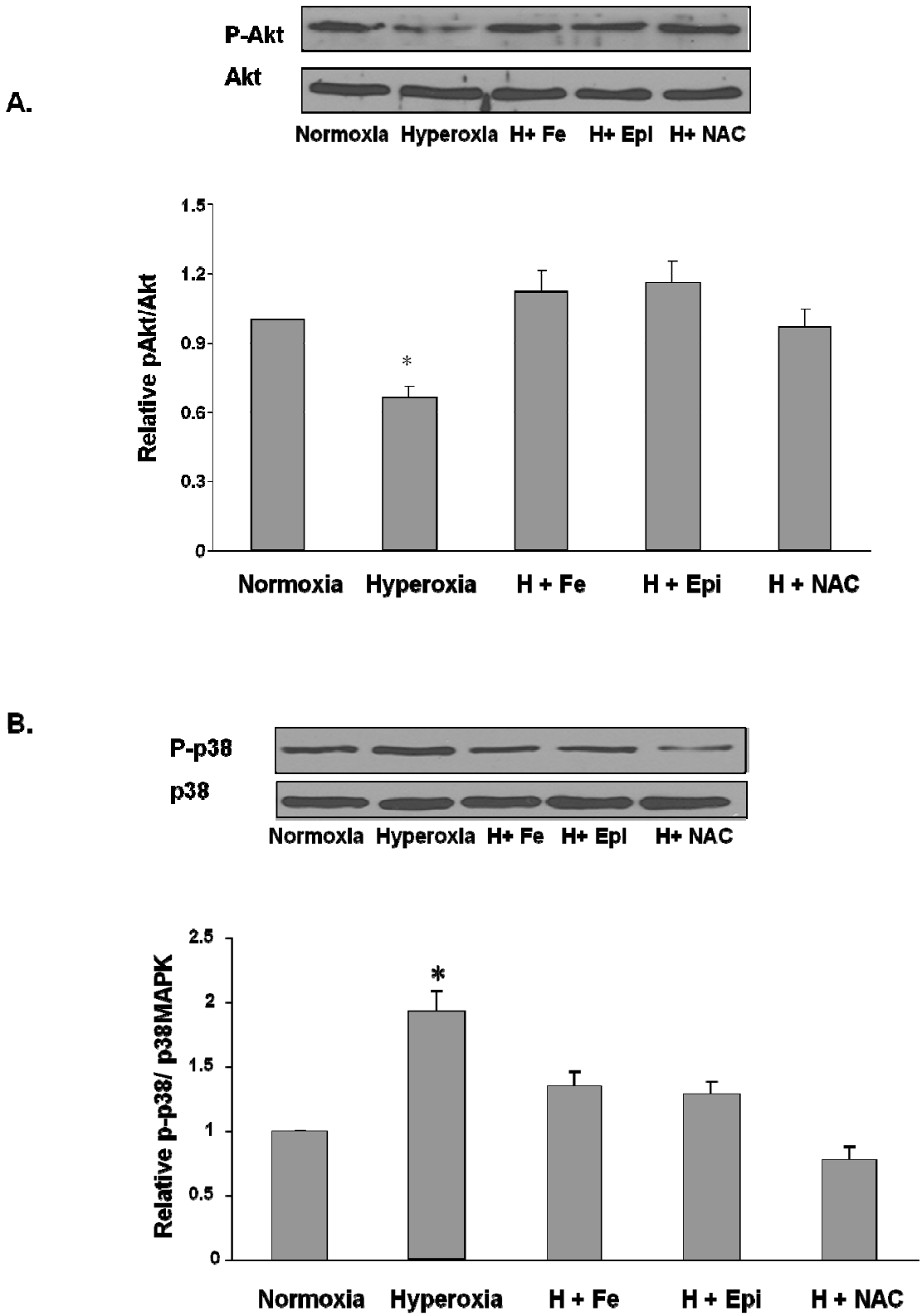
A.
P-Akt
Akt
Normoxia Hyperoxia H+ Fe H+ Epi H+ NAC
Relative pAkt/Akt
1.5
1.2
0.9
0.6
0.3
0
*
Normoxia Hyperoxia H + Fe H + Epi H + NAC
B.
P-p38
p38
Normoxia Hyperoxia H+ Fe H+ Epi H+ NAC
Relative p-p38/ p38MAPK
2.5
2
1.5
1
0.5
0
*
Normoxia Hyperoxia H + Fe H + Epi H + NAC

C.

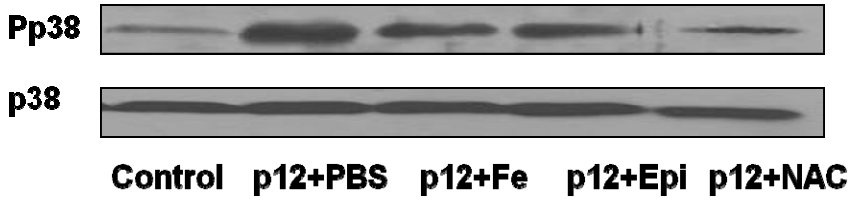
Pp38
p38
Control
p12+PBS
p12+Fe
p12+Epi
p12+NAC

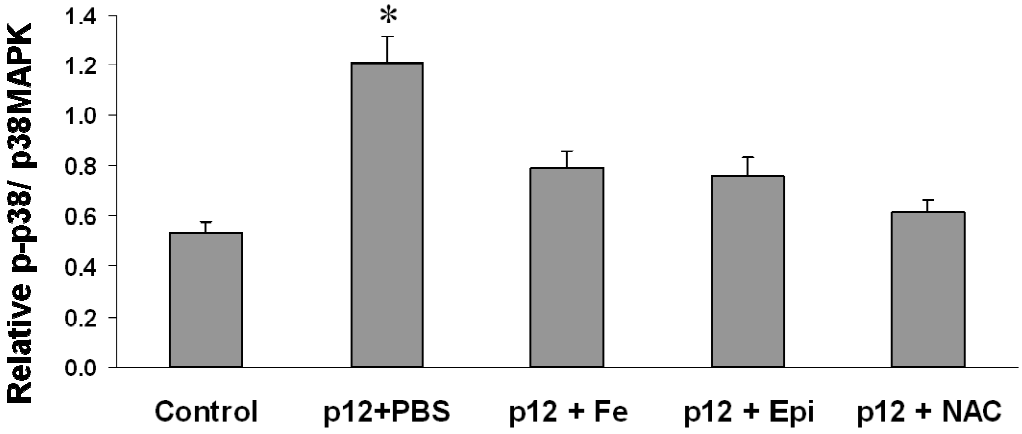
Relative p-p38/ p38MAPK
1.4
1.2
1.0
0.8
0.6
0.4
0.2
0.0
*
Control
p12+PBS
p12 + Fe
p12 + Epi
p12 + NAC

D.

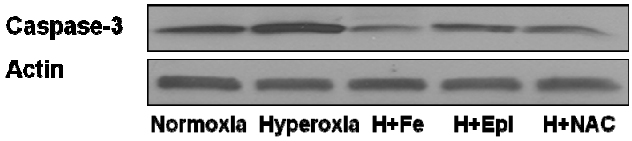
Caspase-3
Actin
Normoxia
Hyperoxia
H+Fe
H+Epi
H+NAC

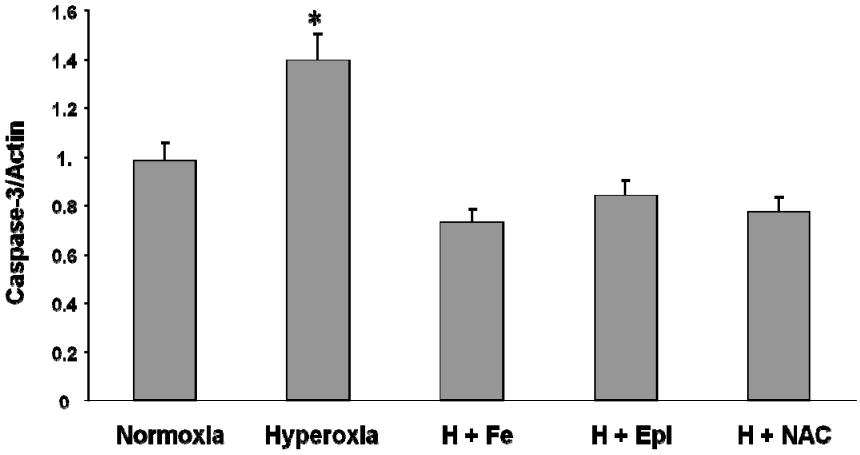
Caspase-3/Actin
1.6
1.4
1.2
1.
0.8
0.6
0.4
0.2
0
*
Normoxia
Hyperoxia
H + Fe
H + Epi
H + NAC

Fig. 2.6.Hyperoxia-induced nitration inhibits Akt survival and activates p38MAP kinase.

(A) Western Blot analysis of cell lysates (50 μg) cells were cultured in high oxygen conditions (40%) and compared to normoxia (20%). Hyperoxia decreased the Akt phosphorylation with 40% reduction. Treating cells with FeTPPs (2.5 μM), epicatechin (100 μM) or NAC (1 mM) for 48 hrs restored Akt activity. (* $P<0.05$ $n=4$, vehicle compared to normal oxygen and inhibitors)

(B) Western Blot analysis of cell lysates (50 μg) cells were cultured in high oxygen conditions (40%) and compared to normoxia (20%). Hyperoxia increased the p38 phosphorelation with 2 fold increase. Treating cells with FeTPPs (2.5 μM), epicatechin (100 μM) or NAC (1 mM) for 48 hrs decreased p38 phosphorelation. (* $P<0.05$, $n=4$ vehicle compared to normal oxygen and inhibitors).

(C) Western Blot analysis of retinal lysates (50 μg) show that exposing retina to hyperoxia (p7-p12) resulted in significant increases in p38 MAPK phosphorylation compared to normoxia. Retinas from PBS treated pups showed more than (2-fold) increase p38 MAPK phosphorylation compared to normoxia. Treatment with FeTPPs (1 mg/kg/day, i.p.), epicatechin (10 mg/kg/day, i.p) or NAC (150 mg/kg/day, i.p.) reduced p38 MAPK phosphorylation by 34.6%, 36.6% and 49.1% respectively. (*$P<0.05$, $n=4$ vehicle compared to normal oxygen and inhibitors).

(D) Blocking peroxynitrite formation or tyrosine nitration prevents apoptosis Western Blot analysis of cell lysates (50 μg), cell were cultured in high oxygen conditions (40%) and compared to normoxia (20%). Hyperoxia resulted in significant increases in apoptosis as indicated by 1.5 fold increase in cleaved Caspase-3 expression compared to normoxic control. Treatment with FeTPPs (2.5 μM), NAC (1 mM) or epicatechin (100 μM) for 48 hrs reduced cleaved caspase-3 expression to normal levels. (* $P<0.05$, n=4 vehicle compared to normal oxygen and inhibitors)

Fig. 2.7.

A.

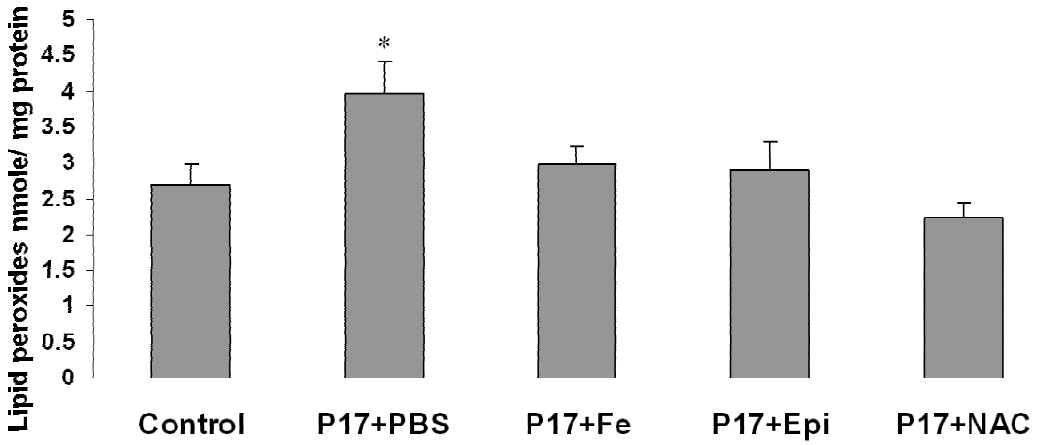
Lipid peroxides nmole/ mg protein
5
4.5
4
3.5
3
2.5
2
1.5
1
0.5
0
*
Control
P17+PBS
P17+Fe
P17+Epi
P17+NAC

B.

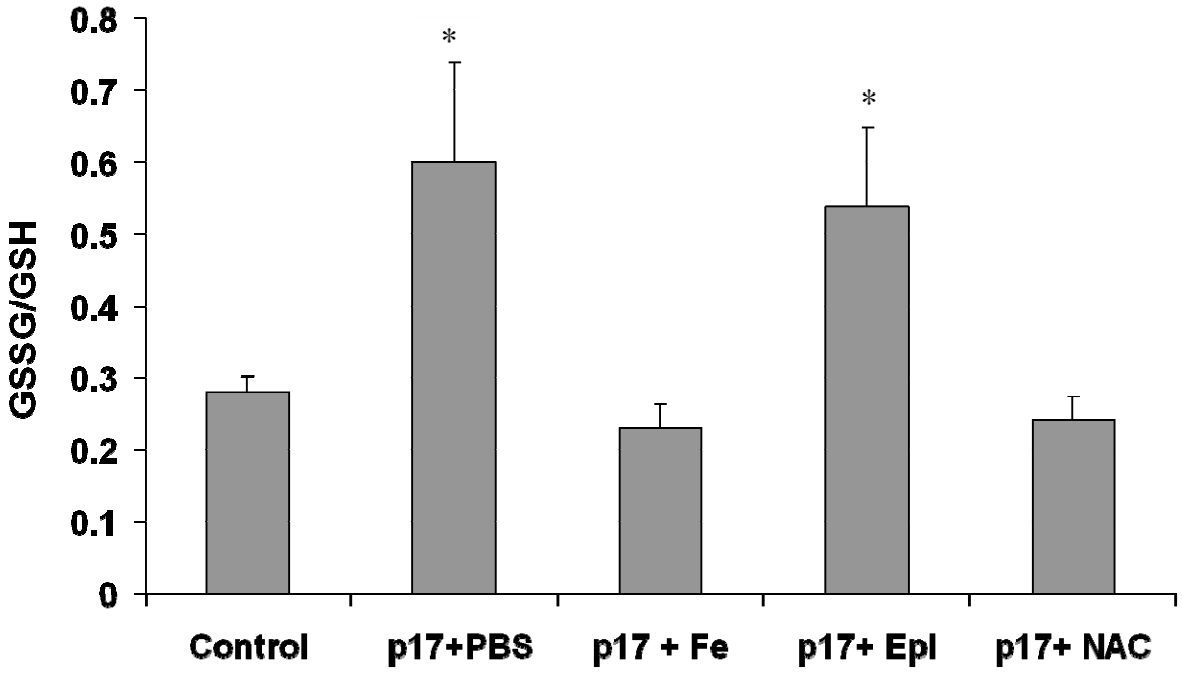
GSSG/GSH
0.8
0.7
0.6
0.5
0.4
0.3
0.2
0.1
0
*
*
Control
p17+PBS
p17 + Fe
p17+ Epl
p17+ NAC

Fig. 2.7. Early intervention of tyrosine nitration prevents retinal oxidative stress

(A) Statistical analysis of lipid peroxidation showing that hypoxia (p7-p17) increased retinal cellular injury indicated by increase in lipid peroxidation. Treatment with FeTPPs (1 mg/kg/day, i.p), epicatechin (10 mg/kg/day, i.p) or NAC (150 mg/kg/day, i.p.) decreased it. (* $P<0.05$, n=10-12 inhibitors compared to vehicle)

(B) Statistical analysis of the ratio of oxidized to reduced glutathione showing that hypoxia (p7-p17) decreased the retinal antioxidant defense with 4 fold. Treatment with FeTPPs (1 mg/kg/day, i.p.) or NAC (150 mg/kg/day, i.p.) restored the normal antioxidant defense. Epicatechin (10 mg/kg/day, i.p) did not show any antioxidant properties. (* $P<0.05$, n=10-12 FeTPPs and NAC compared to vehicle)

Fig. 2.8.

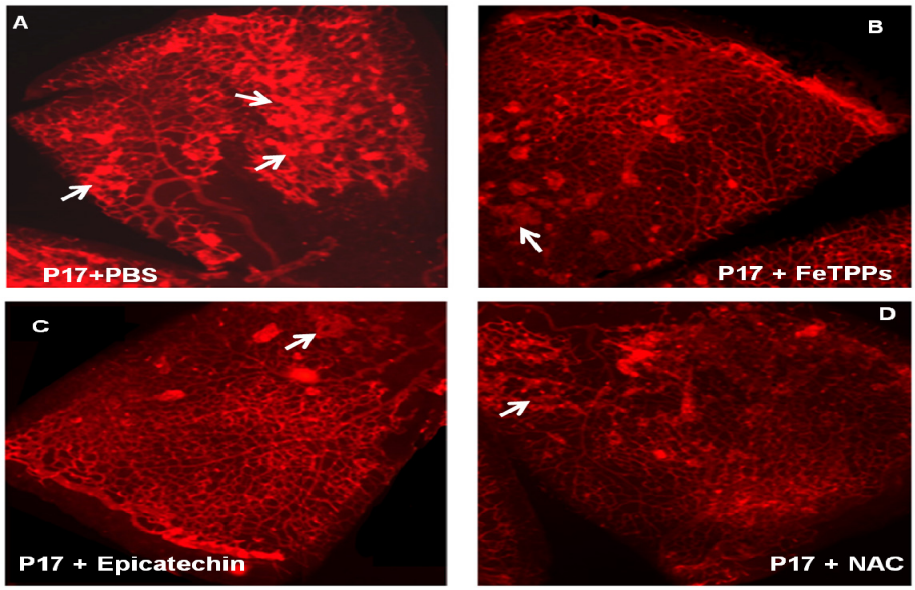
A
P17+PBS
B
P17 + FeTPPs
C
P17 + Epicatechin
D
P17 + NAC

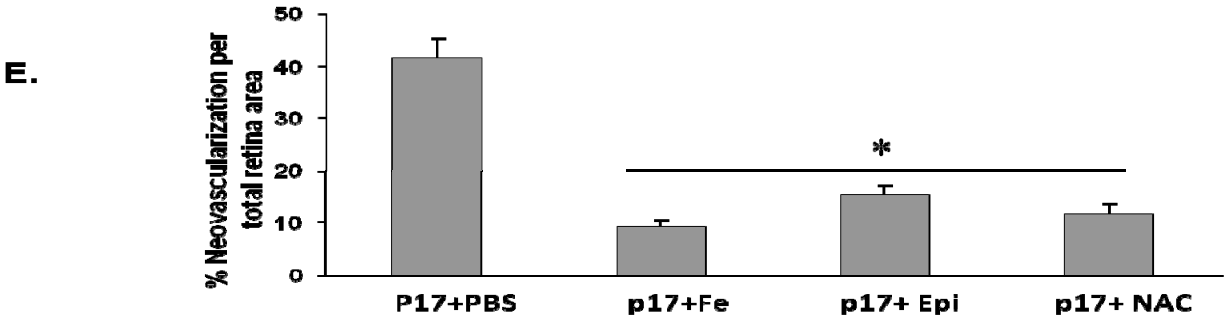
E.
% Neovascularization per total retina area
50
40
30
20
10
0
*
P17+PBS
p17+Fe
p17+ Epi
p17+ NAC

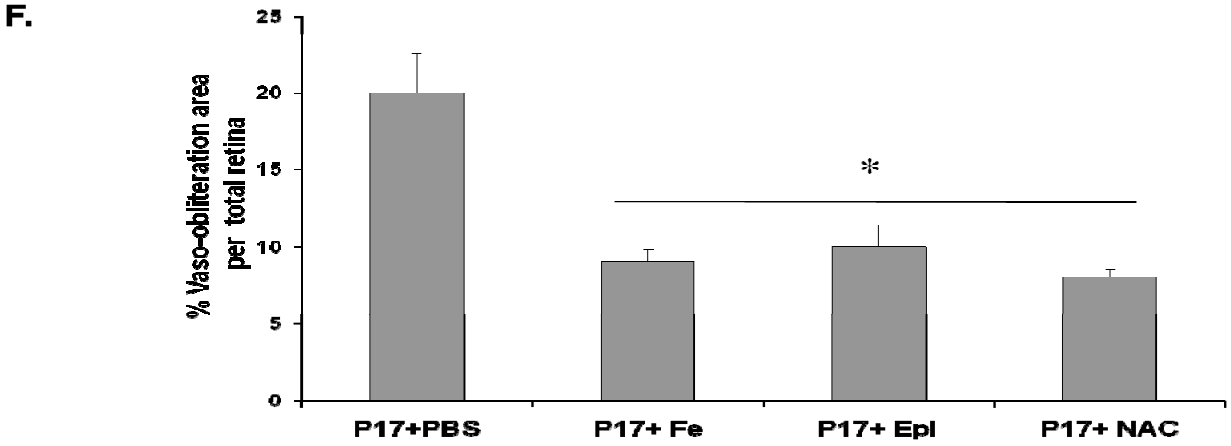
F.
% Vaso-obliteration area per total retina
25
20
15
10
5
0
*
P17+PBS
P17+ Fe
P17+ Epl
P17+ NAC

Fig. 2.8. Early intervention prevents retinal neovascularization

(A-D) Flat-mounted retinas reacted with GSI lectin to localize neovascularization. Mice pups were maintained in hyperoxia (p7-p17) and treated with FeTPPs (1 mg/kg/day, i.p.), epicatechin (10 mg/kg/day, i.p) or NAC (150 mg/kg/day, i.p.). Exposing the developing retina to high oxygen resulted in neovascularization indicated by tufts. Treatment with FeTPPs (1 mg/kg/day, i.p.), epicatechin (10 mg/kg/day, i.p) or NAC (150 mg/kg/day, i.p.) significantly reduced the neovascularization areas.

(E) Statistical analysis of the ratio of neovascularization areas to total retinal area showing the protective effects of blocking peroxynitrite formation and tyrosine nitration on retinal neovascularization. (* $P<0.05$, n=10-12 inhibitors compared to vehicle).

(F) Statistical analysis of the ratio of central capillary dropout areas to total retinal area in (p7-p17) treated retinas showing that treatment did not prevent physiological revascularization instead, FeTPPs, epicatechin and NAC helped in the vascular regrowth and reduced the retinal vaso-obliteration by 54%, 50%, 60% respectively. (* $P<0.05$, n=10-12 inhibitors compared to vehicle)

Fig. 2.9.

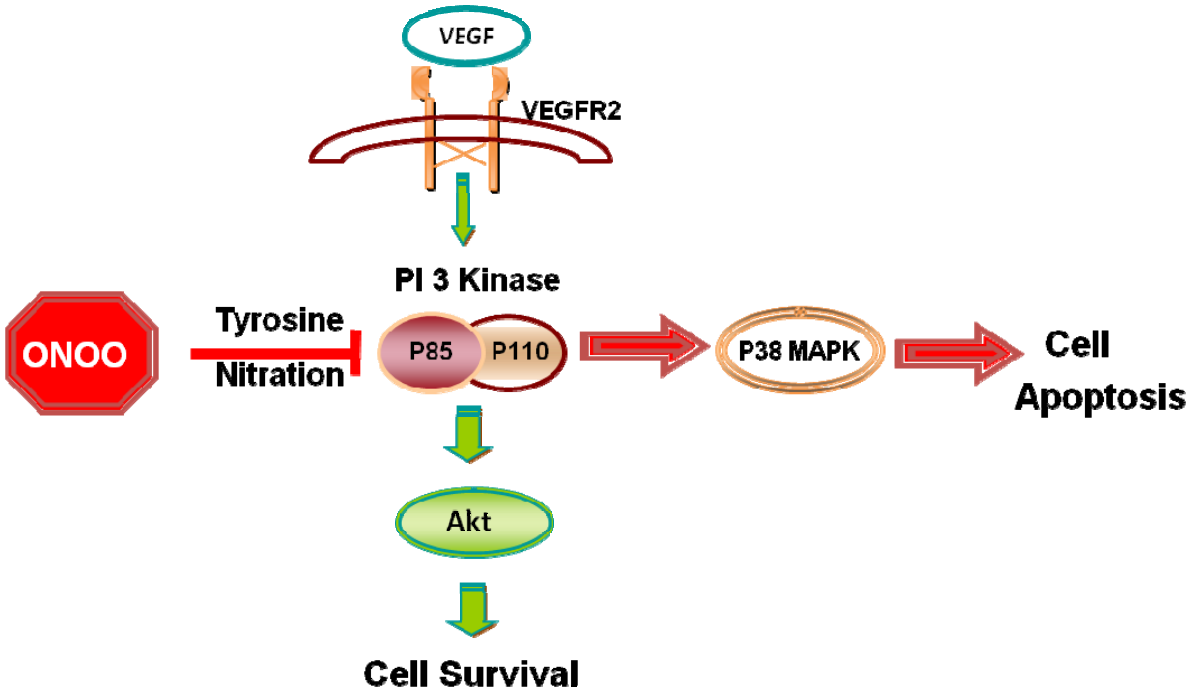

Fig. 2.9. A schematic representation of the proposed mechanism by which high oxygen via peroxynitrite inactivates VEGF/ PI 3-kinase/Akt-1 pro-survival pathway and stimulates cell death via activation of p38 MAP kinase pathway. Nitration of PI 3-Kinase is proposed as a mechanism by which peroxynitrite switches off the VEGF pro-survival and triggers the pro-apoptotic pathway.

CHAPTER 3

ROLE OF THIOREDOXIN INTERACTING PROTEIN IN VEGF ANGIOGENIC SIGNALING [1]

---

[1] Mohammed A. Abdelsaid and Azza B. El-Remessy
To be submitted to Journal of Angiogenesis, 1/15/2012.

Abstract

VEGF is a key player in the angiogenic process. Although the role of reactive oxygen species as signaling moieties in mediating the VEGF signal is well-documented, little is known about the role of the antioxidant defense system. The aim of this study is to determine the role of thioredoxin inhibiting protein (TXNIP), the endogenous inhibitor of thioredoxin, in regulating the VEGF angiogenic signal. TXNIP-deficient mice (TKO) were compared to wild type (Wt) or Wt treated with the GSH-precursor, N-acetyl cysteine (NAC, 500 mg/kg) using a hypoxia-induced neovascularization model. In response to hypoxia, retinas of TKO and NAC-treated mice experienced reductive stress indicated by significant increases in the thioredoxin reductase activity and GSH levels compared to Wt. These effects were associated with comparable levels of VEGF expression, impaired VEGFR2 activation and impaired physiological retinal revascularization and pathological neovascularization. In HME cells transduced with scrambled-siRNA, VEGF caused immediate activation of VEGFR2 that was associated with immediate and reversible oxidation of GSH levels. Immuno-precipitation studies revealed a strong association between VEGFR2 and low molecular weight protein tyrosine phosphatase (LMW-PTP). In scrambled-treated HME cells, VEGF caused reversible S-glutathionylation and inhibition of LMW-PTP. Silencing TXNIP expression using siRNA blunted VEGF-induced GSH oxidation, receptor phosphorylation and S-glutathionylation of LMW-PTP that culminated in inhibiting cell migration and tube formation in HME cells. VEGF induced vascular sprouting in aortic rings from Wt but not from TKO mice. In summary, our results elucidated the critical role of TXNIP expression for achieving a balanced redox-state to facilitate VEGF-mediated autoreceptor activation and angiogenic signal via s-glutathionylation of LMW-PTP.

Introduction

Although physiological angiogenesis is important for wound healing, recovery after stroke and myocardial infarction, pathological angiogenesis is of great clinical significance as in atherosclerosis, tumor growth, diabetic retinopathy and other chronic inflammatory disorders [1-5]. Vascular endothelial growth factor (VEGF) is one of the potent angiogenic growth factors that maintain endothelial cell survival and migration. VEGF-angiogenic signal occurs mainly via the activation of VEGFR-2 also known as Flk-1 [6-8]. Therefore, regulation of VEGFR-2 activation is critical for the VEGF mediated response. Over the past decade, evidence accumulated to emphasize the critical role of cellular redox homeostasis as a major modulator of angiogenesis. Extensive studies have shown that growth factor-induced reactive oxygen species (ROS) are critical signaling moieties for angiogenesis [9-11]. Also important, excessive ROS has a deleterious effect on angiogenesis, suggesting a need for a delicate redox balance [12, 13]. So far, vascular research has focused on identifying sources of ROS, yet the role of antioxidants remain to be fully understood.

Endothelial cells have two major antioxidant systems, the glutaredoxin system and the thioredoxin system. The cross talk between the two systems, reflected in oxidized to reduced glutathione (GSSG/GSH) ratio (cell antioxidant currency), determines cellular redox-state and other major cellular functions [14-20]. Recent studies have focused on the emerging critical role of the thioredoxin system in angiogenesis. The thioredoxin system is an ubiquitous thiol-reducing system that consists of thioredoxin (TRX), NADPH and homodimeric seleno-protein thioredoxin reductase [21]. Thioredoxin-interacting protein (TXNIP) regulates cellular redox-state by binding and inhibiting TRX [22]. TXNIP expression is known to be increased under

stress conditions, inflammation and hyperglycemia [23, 24]. Yet, the role of TXNIP in regulating cellular redox-state and VEGF-induced angiogenesis is unclear.

Herein, we studied the role of TXNIP protein in regulating VEGF-induced angiogenesis via modulating the cellular redox-state. Our results showed that knocking down TXNIP expression caused significant increases in cellular antioxidant defense that resulted in impaired VEGF angiogenic signal. Here, we tested the hypothesis that reductive stress scavenges VEGF-induced ROS, impairs VEGFR-2 phosphorylation and VEGF angiogenic signal by a mechanism involving the activation of phosphatases. The present study emphasizes the importance of TXNIP expression for endothelial redox homeostasis to facilitate VEGF-induced angiogenesis.

Materials and Methods

Animals.

Experiments were approved by the Institutional Committee for Animal Use in Research and Education at Charlie Norwood VA medical Center (ACORP # 09-11-020) and conformed to the ARVO Statement for the Use of Animals in Ophthalmic and Vision Research. All experiments were performed using age-matched wild type mice C57Bl/6 mice and TXNIP deficient mice (TKO). TKO mice were a kind gift from Dr. AJ Lusis and Dr. ST Hui at the BioSciences Center, San Diego State University, San Diego, CA [25, 26].

TKO breeding and genotyping.

Littermates of wild type and homozygous TKO were used. For genotyping, DNA was prepared by incubating ear tissue with proteinase K and digestion buffer for one hour at 95^0C. A mixture of Primer Sequence (5'-TGA-GGT-GGT-CTT-CAA-CGA-CC-3'. 5'GGA-AAG-ACA-ACG-CCA-GAA-GG-3' and 5'-CCT-TGA-GGA-AGC-TCG-AAG-CC-3'(IDT San Diego, CA)),

buffer and 2 mM $MgCl_2$ and polymerase enzyme (GoTAG Hot start polymerase, Promega, Madison, WI) were added to the DNA template. DNA segments were amplified using the Master plex-RealPlex2 (Eppendorf, Hauppauge, NY) and were detected with 1% agarose gel electrophoresis. Non-sense TXNIP allele was detected at 530 bp while wild type was detected at 699 bp.

TKO phenotyping.

TKO mice are similar in weight and activity to wild-type or heterozygous littermates, with no differences in food consumption or litter sizes. TXNIP deficient mice are characterized by a significant increase in the ratio of NADH to NAD and the hepatic ratios of reduced to oxidized glutathione. TXNIP deficient mice have fasting hyperinsulinemia, hypoglycemia, hypertriglyceridemia, and have higher than normal levels of ketone bodies [27, 28]. Our TKO phenotyping was in agreement with the TKO literature; in that the retinal lysate showed a 40 % reduction in TXNIP expression (Supp Fig. 1A). Retinas of TKO showed normal retinal vascular development patterns compared to wild type (Supp Fig. 1B).

Hypoxia-induced neovascularization.

Hypoxia-induced neovascularization was induced in newborn mice as described previously [13]. Briefly, on postnatal day 7 (p7), mice were placed along with their dam into a custom-built chamber in which the partial pressure of oxygen was maintained at 75% (Biospherix , Redfield, NY). Mice were maintained in 75% oxygen for up to 5 days (P12), after which they were transferred back to room air (relative hypoxia). Room temperature was maintained at 68°F, and rooms were illuminated with standard fluorescent lighting on a 12-hour light–dark cycle. Newborn mice were nursed by the dams that were given food (standard mouse chow) and water.

One set of wild type mice was treated during hypoxia by daily intraperitoneal injections (IP) with the general antioxidant, N-acetyl cysteine (500 mg/Kg, Sigma). Pups were deeply anesthetized by IP injection of Avertin 240 mg/Kg. One eye was enucleated and fixed in 2% PFA overnight to be flat- mounted. For the other eye, retinas were isolated and snap frozen for biochemical assays.

Analysis of revascularization and pathological neovascularization.

Retinal vascular distribution was analyzed using retinal flat mounts labeled with biotinylated *Griffonia simplicifolia* lectin B4 and Texas Red–conjugated Avidin D (Vector Laboratories, Burlingame, CA). Retinas were viewed and imaged with a fluorescence AxioObserver Zeiss Microscope (Germany). The areas of retinal neovascularization were assessed on p17 as described previously [13]. Briefly, retinal images were assessed for central revascularization areas, while neovascularization was quantified using AxioObserver Zeiss Microscope (Germany) software to detect areas of retinal tufts. Results were expressed as percentage of total retinal area.

Cell culture.

Primary cultures of human microvascular endothelial (HME) cells from retina and cell culture supplies were purchased from Cell Systems Corporation (Kirkland, WA). Experiments were performed using cells between passages (4-6). Cells were switched to serum free medium 6 hrs prior to stimulation with VEGF 20 ng/ml (R&D, Minneapolis, MN). The general antioxidant, N-acetyl cysteine (NAC, Sigma) was used at a concentration of 10 mM.

Silencing TXNIP expression.

Transfection of HME cells was performed using Amaxa nucleofector (Lonza, Germany) and electroporation and basic Nucleofector kit for cell line (Lonza, Germany) according to the manufacture protocol. First, optimization experiments were performed for the device program and the concentration of TXNIP siRNA (Dharmacon, USA) for maximum transfection efficacy

for HME cells, T005 program was selected as well as 300 ng of TXNIP siRNA (Dharmacon, USA), the same concentration was selected for scrambled siRNA for control. Cells were suspended in a nucleofection mixture with the siRNA, pmaxGFP and zapped. Cells were plated in complete medium to recover for 48 hrs. Transfection efficiency was assessed by calculating the percentage of GFP expressing cells to the total number of cells after imaging with fluorescence AxioObserver Zeiss Microscope (Germany) (Supl. Fig 2A) and Western blots for TXNIP expression (Fig 6A).

Cell migration assay.

Wound healing assay was performed as described before [9]. Briefly, HME cells were grown to confluence and switched to serum-free medium 6 hrs prior to experiment. The monolayer was wounded with a single sterile cell scraper of fixed diameter. Images of wounded areas were taken immediately and after 18 hours. Cell migration was calculated by measuring migration distance normalized to initial distance of wounding using AxioObserver Zeiss Microscope (Germany) software and expressed as the percentage of untreated control cells.

Tube formation assay.

Tube formation assay was performed as described previously [29]. Growth factor-reduced Matrigel (BD Biosciences) was used according to the manufacturer's protocol. HME were counted and plated at 2×10^4 cells/ml with Matrigel in a 96 well-plate. VEGF (20 ng/ml) was added for positive control. Eighteen hours later, images of the tube-like structures were captured using a Zeiss Axiovert microscope. Tube length was analyzed digitally using Zeiss Axiovert microscope software.

Aortic ring assay.

Eight week old adult males of Wt and TKO mice were euthanized and the aortas were removed and immediately transferred to iced serum-free media. The periaortic fibro-adipose tissue was carefully removed without damaging the aortic wall. The aorta was cut into one millimeter-long aortic segments. The aortic rings were then individually embedded in extracellular matrix proteins (Matrigel, BD Biosciences) for 10 days. Images of vascular sprouts were captured using a Zeiss Axiovert microscope. Tube length was analyzed digitally using Zeiss Axiovert microscope software**.** The greatest distance from the aortic ring body to the end of the vascular sprouts was measured in 3 rings per animal, 3-4 animals per group.

Oxidized and reduced Glutathione.

Reduced glutathione was measured as described before [13] using the Northwest Life Science kit (Vancouver, WA). Briefly, reduced-GSH was calculated by subtracting the oxidized-GSSG from the total glutathione. For total glutathione, cells were lysed in phosphate buffer (100 mM potassium phosphate and 1mM EDTA) and were mixed with an equal amount of DTNB (10 mM 5, 5'-dithiobis (2-nitrobenzoic acid) in the presence of glutathione reductase and NADPH producing a yellow color measured at 412 nm. To detect GSSG, samples were treated with 10 mM 2-vinylpyridine (Sigma) in ethanol to sequester all the reduced GSH then measured using the same protocol as the total glutathione.

Thioredoxin reductase activity.

Thioredoxin reductase activity was performed as described previously [30] using a colorimetric kit (Sigma). Briefly, retinal samples were homogenized in assay buffer followed by the addition of 5, 5¢-dithiobis (2-nitrobenzoic) acid (DTNB) with NADPH. Reduction of DTNP to 5-thio-2-

nitrobenzoic acid (TNB) produced a strong yellow color that is measured colorimetricaly at 412 nm. Thioredoxin reductase activity was expressed by unit/ug/min.

Immunoprecipitation and Western blot analysis.

Isolated retinas and HME cells were harvested after various treatments and lysed in modified RIPA buffer purchased from Millipore (Billerica, MA) for 30 min on ice. Insoluble material was removed by centrifugation at 14,000 *g* at 4°C for 30 min. Fifty μg of total protein was boiled in 6x Laemmli sample buffer, separated on a 10–12% SDS-polyacrylamide gel by electrophoresis, transferred to nitrocellulose, and reacted with the specific antibody. The primary antibodies were purchased as follow: Anti-VEGF (Calbiocam), phospho-Akt, or Akt (Cell Signaling), LMW-PTP (Exalpha, Maynard, MA), anti-GSH (Virogen, Boston) and TXNIP (Santa Cruz, Santa Cruz, CA). Primary antibodies were detected using a horseradish peroxidase-conjugated antibody and enhanced chemiluminescence (GE Healthcare, NJ).The films were scanned, and band intensity was quantified using densitometry software (Alpha Innotech).

For VEGF**,** retinal lysates were subjected to heparin beads (Sigma) as described before [31]. The beads were pelleted at 5000 x g for 1 min, washed in 400 mM NaCl and 20 mM Tris and loaded onto a 4-20% gradient Tris glycine pre-cast gel (BioRad). After blocking, the membrane was incubated with VEGF primary antibody (1:200) (Calbiocam). The band was visualized and quantified as described above.

For S-glutathionylation immunoprecipitation, cell lysate (200 μg) was immunoprecipitated with LMW-PTP primary antibody (5 μg) and A/G agarose beads (Santa Cruz, CA) overnight. The precipitated proteins were analyzed by SDS-PAGE and blotted with Anti-GSH and LMW-PTP antibody for equal loading.

Data Analysis.

The results were expressed as mean ± SE. Differences among experimental groups were evaluated by analysis of variance, and the significance of difference between groups was assessed by the post-hoc test (Fisher's PLSD) when indicated. Significance was defined as $P < 0.05$.

Results

Knocking down TXNIP expression shifts redox-state.

Thioredoxin-interacting protein (TXNIP) is an endogenous inhibitor for ROS scavenging protein, thioredoxin. TKO have a nonsense mutation in the TXNIP gene that results in expression of inactive TXNIP and an increase in cellular antioxidants. Our analysis showed that TKO retinas had significant increases (2-fold) in thioredoxin reductase activity and (3.5-fold) plasma reduced-glutathione when compared to age matched wild type under normoxic conditions (Fig. 1). Hypoxia caused significant reduction in antioxidant defense as indicated by a 20 percent reduction in retinal thioredoxin reductase activity and a 45 percent reduction in plasma reduced-glutathione levels in wild type animals. TKO pups exposed to hypoxia did also show a 40 percent reduction in thioredoxin reductase activity and a 42 percent decrease in reduced-glutathione compared to normoxic TKO pups. TKO exposed to hypoxia still had significant (1.5-fold) increased thioredoxin reductase activity and a 4-fold increase in reduced-glutathione compared to wild type exposed to hypoxia.

Knocking down TXNIP expression impairs VEGF-induced reparative and pathological neovascularization.

Hypoxia-induced neovascularization is a standard mouse model to study VEGF-mediated retinal angiogenesis [13, 32]. Exposing the developing mouse retinas to high-oxygen (from postnatal day 7- p7-p12) results in vaso-obliteration and hypoxia, which trigger the expression of VEGF and retinal neovascularization, peaking at post-natal day 17 (p17). VEGF induces both physiological revascularization of the central retina and the pathological neovascularization that appear as tufts emerging from the mid-peripheral retinal capillaries. As shown in Fig 2 A-E,

TXNIP deficiency impaired both physiological and pathological VEGF-induced neovascularization. TKO showed a 50 % reduction in physiological revascularization of central capillary drop out. TKO showed a 75% reduction in neovascularization when compared to wild type age matched animals.

Pharmacologically induced reductive stress impairs VEGF-induced reparative and pathological neovascularization.

We mimicked the acute shift in redox-state observed in TKO by treating mice with a high dose of the thiol donor and GSH-precursor N-acetyl cysteine (NAC, I.P 500 mg/kg). Plasma of the NAC-treated pups showed a 4-fold increase in reduced-GSH levels when compared to wild type PBS-treated age matched animals (Fig. 3F). Similar to TKO, treatment with NAC (500 mg/kg) impaired both VEGF-induced reparative vascularization (43%) of central retina and pathological neovascularization (70%) at periphery when compared to wild type PBS-treated age matched animals (Fig. 3A-E).

Knocking down TXNIP expression did not alter VEGF expression.

We next tested the effect of hypoxia on TXNIP expression. TKO showed 40 percent reduction of TXNIP expression compared to wild type mice under normoxic conditions. Hypoxia only doubled the TXNIP expression in wild type and wild type treated with NAC (Fig 4.A) but not in the TKO. We next examined the impact of increased cellular antioxidant defense on VEGF expression at p14, a known time point for maximum VEGF expression. Our results showed that wild type animals experienced a significant increase (1.7 fold) in VEGF expression after 2 days of relative hypoxia. In parallel, TXNIP deficient mice were not significantly different from wild type in VEGF expression. Hypoxia increased the VEGF expression in TKO mice 1.6 fold when compared to control (Fig. 4B). Acute reductive stress induced by I.P injection of NAC 500

mg/Kg did not show a significant difference from wild type either. As shown in Fig. 4C, hypoxia increased the VEGF expression 1.6 fold when compared to control (Fig. 4C).

Knocking down TXNIP expression decreases VEGFR2 phosphorylation in vivo.

We next examined the downstream VEGF signal and tested the VEGFR-2 phosphorylation. Tyrosine 996 (Y996), auto-phosphorylation site is required for the kinase activity. Our results showed that only wild-type pups showed increases (1.4 fold) in Y-996 phosphorylation. Alternatively, TKO mice showed a significant reduction of VEGF receptor phosphorylation (35 % reduction). To confirm our results we examined Akt, a downstream kinase from VEGFR2. In parallel, hypoxia increased Akt activation in wild type by 30% while TKO mice showed a significant decrease in Akt activation (28%) when compared to normoxic TKO animal but 60 % less when compared to wild type hypoxic animal(Fig. 5A-B) . Acute reductive stress induced by I.P injection of NAC 500 mg/Kg resulted in a significant reduction of VEGF receptor phosphorylation (21 % reduction) in wild type pups (Fig. 5C).

Silencing TXNIP expression increases cellular antioxidant defense and impairs VEGFR2 phosphorylation.

To examine the molecular mechanism of the impairment of VEGFR2 activation, we used an in vitro model. We silenced TXNIP expression in human microvascular endothelial (HME) cells using siRNA. As shown in Fig. 6A, silencing TXNIP expression in HME cells caused a significant reduction of TXNIP mRNA levels (20 percent, data not shown) and a reduction in TXNIP expression (48 percent) when compared to HME cells treated with scrambled siRNA (Fig. 6A). Silencing TXNIP expression caused a 1.6 fold increase in cellular antioxidant redox-state as indicated by increased cellular levels of reduced-glutathione (Fig. 6B). We have previously shown that VEGF causes a transient reduction in cellular redox-state that was restored

after 15 minutes [33]. As shown in Fig 6C, VEGF caused a transient reduction in reduced GSH levels that was restored back in 15 min for HME treated with scrambled siRNA. Silencing TXNIP with TXNIP siRNA increased the cellular antioxidant buffer capacity that blunted the VEGF redox effect.

We next examined the VEGF signal. VEGF stimulation caused a 1.6 fold increase in VEGFR-2 activation that was sustained over 5 minutes of treatment. Silencing TXNIP expression impaired VEGFR-2 activation in response to VEGF (Fig. 6D).

VEGF stimulates association of VEGFR-2 with LMW-PTP.

Low molecular weight protein tyrosine phosphatase (LMW-PTP) is a redox-regulated phosphatase that plays an important role in the angiogenic process via deactivation of growth factor tyrosine kinases [34, 35]. We examined the effects of VEGF on the interaction between LMW-PTP with VEGFR2. Here, we showed that LMW-PTP interacted with VEGFR2 after 15 minutes of VEGF stimulation to HME cells (Fig. 7A).

Silencing TXNIP expression blocks VEGF-induced S-glutathionylation of LMW-PTP.

S-glutathionylation is a reversible protective mechanism for cysteine modification in response to oxidative stress. We have previously shown that VEGF causes S-glutathionylation and inactivation of LMW-PTP that is reversible after 15-30 minutes [33]. We tested the effect of silencing TXNIP expression on VEGF-induced LMW-PTP S-glutathiolation. VEGF caused S-glutathionylation of LMW-PTP that peaked at 5-15 minutes and was restored after 15 min in HME treated with scrambled siRNA. Silencing TXNIP expression using TXNIP siRNA blunted the VEGF effect, we did not detect any change in LMW-PTP S-glutathiolation over 30 minute of

VEGF treatment (Fig. 7B). The specificity of detecting S-glutathionylation was confirmed by a complete blunting of the signal when samples were pretreated with DTT (Data not shown).

Silencing TXNIP expression inhibits VEGF angiogenic response.

As shown in Fig. 8A, VEGF (20 ng/ml) caused a 1.9 fold increase in the mean length of tube formation of HME treated with scrambled siRNA, and silencing TXNIP expression using siRNA impaired VEGF's ability to induce alignment of endothelial cells into tubes. In parallel, VEGF (20 ng/ml) caused a 1.6 fold increase in cell migration of HME treated with scrambled siRNA. Silencing TXNIP did not show any significant difference in cell migration from control even when stimulated with VEGF (Fig 8B). Inducing acute reductive stress using a high dose of NAC (10 mM) blunted the VEGF-induced cell migration (Fig 8C). Ex vivo studies using aortic rings of adult TKO mice showed an 80 percent reduction in tubes formed in Matrigel in response to VEGF when compared to wild type (Fig 8D).

Discussion

In the present study, we demonstrated the role of thioredoxin interacting protein (TXNIP), an endogenous inhibitor for the potent antioxidant thioredoxin system, in VEGF-induced angiogenic response. The findings can be summarized as: 1- TXNIP deficiency caused a positive shift in the cellular antioxidant defense but did not affect VEGF expression; 2- Reductive stress can impair VEGF angiogenic signal via blunting VEGF-mediated VEGFR-2 phosphorylation; 3- Our results identified LMW-PTP as interacting with VEGFR2. The present study emphasizes the importance of TXNIP expression for endothelial redox homeostasis to facilitate VEGF-induced angiogenesis.

Endothelial cells have two major antioxidant systems, the glutaredoxin system and the thioredoxin system. Previous studies showed crosstalk between the glutathione and thioredoxin systems to modulate cellular redox-state through changing the GSSG/GSH ratio [36]. Studies have shown that changes in the intracellular GSSG/GSH ratio is not only a measure of redox-state but can alter vital protein function, regulate HIF-1 induction during hypoxia, cell proliferation and VEGF angiogenic response [18-20, 37, 38]. Recent studies focused on the emerging critical role of the thioredoxin system in angiogenesis. Thioredoxin has two isoforms, TRX1 in the cytosol and TRX 2 in the mitochondria [14, 21]. TRX modulates cell growth and angiogenesis via NF-κB transcriptional pathways and increases VEGF and nitric oxide production [14-17, 39]. Thioredoxin-interacting protein (TXNIP) regulates the cellular redox-state by binding to and inhibiting TRX [22]. TXNIP expression is known to be increased under stress conditions, inflammation and hyperglycemia [23, 24], yet the role of TXNIP in redox regulation of VEGF-induced angiogenesis is unclear.

In the present study, we explored the role of TXNIP in VEGF-induced angiogenesis using TXNIP-deficient mice (TKO). These mice have a nonsense mutation in TXNIP resulting in reduced expression [25, 26]. Our TKO phenotyping was in agreement with the TKO literature and we found that TKO had significant increases in thioredoxin reductase activity and plasma reduced-glutathione [27, 28]. TKO are characterized with significant increases in the reduced to oxidized glutathione ratio, fasting hypoglycemia and hypertriglyceridemia. All our endpoints were assessed at postnatal day 14 and 17 and were done on non fasting pups. Hypoxia-induced neovascularization is a well-established mouse model for VEGF-induced angiogenesis [32]. VEGF causes physiological central revascularization, a measure of reparative angiogenesis and peripheral neovascularization, a measure of pathological angiogenesis. TKO mice showed a significant increase in antioxidant defense and a decrease in VEGF-induced revascularization and neovascularization. Recent studies showed important role of TXNIP to promote inflammation in endothelial cell as well as non-endothelial cells [23, 30, 40]. To explore the mechanism of impairment of VEGF angiogenic signal in retinal endothelial cells we examined VEGF levels and signals. Although TKO showed no significant difference in VEGF levels when compared to matched wild type, TKO showed a significant decrease in VEGFR2 phosphorylation. These results suggest a novel pathway in which TXNIP can modulate VEGF signal. We simulated the increase in cellular antioxidants by injecting high doses of N-acetyl cysteine, an antioxidant and thiol donor. Our previous study showed that NAC (150 mg/kg) restored GSSG/GSH ratio and VEGF survival signal in response to oxidative stress and here our results revealed that NAC (500 mg/kg) increased plasma glutathione ratio and impaired VEGF-induced angiogenesis via decreasing VEGFR-2 phosphorylation with no effect on VEGF levels. NAC treated pups showed high levels of TXNIP expression in response to hypoxia indicating

that the effect observed of VEGF signal impairment is related to reductive stress rather than TXNIP deficiency.

Since TXNIP lacks pharmacological inhibitors and to further explore the molecular mechanism, we silenced TXNIP expression in human microvascular endothelial cells using siRNA. Silencing TXNIP increased the cellular antioxidant defense as indicated by an increase in cellular reduced-glutathione, which blunted the VEGF-induced negative shift in the cellular redox-state and that was accompanied with reduction in the phosphorylation of VEGFR-2. The increase of the antioxidant defense silencing TXNIP or with high doses of NAC also resulted in loss of VEGF-mediated angiogenic response. We also confirmed our results with an ex-vivo assay. TKO aortic rings showed a significant reduction in vascular sprouting in response to VEGF. Our results were in agreement with others who showed that reductive stress can impair coronary collateral growth [41]. Recent clinical evidence showed a novel interaction of up-regulated thioredoxin system and down-regulated angiogenesis pathways in obese non-diabetic subjects [42].

The low molecular weight protein tyrosine phosphatase (LMW-PTP) is one of the non-receptor tyrosine phosphatase families that regulate cell growth and migration via dephosphorylation of growth factor receptor tyrosine kinases and focal adhesion kinase [34, 45, 46]. LMW-PTP is one of the redox regulated phosphatases [35, 47-50]. We examined the association between LMW-PTP and VEGFR-2. Our results showed that LMW-PTP is associated with VEGFR-2 after 15 minutes of VEGF stimulation, the time point where LMW-PTP activity is restored after a transient inactivation. Our recent work showed that VEGF-induced peroxynitrite caused the transient oxidation and inactivation of LMW-PTP via S-glutathionylation [33], herein we tested the effect of silencing TXNIP on VEGF-induced LMW-

PTP S-glutathionylation. Our results showed that increasing in the reduced-glutathione by knocking down TXNIP expression blunted VEGF-induced LMW-PTP S-glutathionylation and inhibition. Our results were in agreement with previous studies that related the LMW-PTP activity to the glutathione reducing system and cellular redox-state [51]. These results did not exclude the contribution of other phosphatases such as SHP-1, SHP-2, PTP 1B and PTEN.

In a summary, our study is the first to address the critical role of TXNIP in the VEGF angiogenic signal and also explored the molecular mechanism for reductive stress-induced impairments of VEGF angiogenic signal. We also elucidated the role of TXNIP in modulating the delicate cellular redox state, LMW-PTP S-glutathionylation and VEGF angiogenic signal.

Acknowledgment: Authors are grateful for technical expertise of Suraporn Matragoon and Bindu A Pillai.

Source of research support: American Heart Association pre-doctoral fellowship award#10PRE3660004 To MAA, AHA Scientist Development Grant to ABE and Career Development Award from Juvenile Diabetes Research Foundation (4-2008-149) to ABE.

Author Disclosure Statement

We do not have any commercial associations that might create a conflict of interest in connection with our manuscripts.

References

1. Carmeliet, P., *Angiogenesis in health and disease.* Nat Med, 2003. **9**(6): 653-60.
2. Munoz-Chapuli, R., A.R. Quesada, and M. Angel Medina, *Angiogenesis and signal transduction in endothelial cells.* Cell Mol Life Sci, 2004. **61**(17): 2224-43.
3. Abo-Auda, W. and R.L. Benza, *Therapeutic angiogenesis: review of current concepts and future directions.* J Heart Lung Transplant, 2003. **22**(4): 370-82.
4. Folkman, J., *Angiogenesis.* Annu Rev Med, 2006. **57**: 1-18.
5. Caldwell, R.B., et al., *Vascular endothelial growth factor and diabetic retinopathy: role of oxidative stress.* Curr Drug Targets, 2005. **6**(4): 511-24.
6. Testa, U., G. Pannitteri, and G.L. Condorelli, *Vascular endothelial growth factors in cardiovascular medicine.* J Cardiovasc Med (Hagerstown), 2008. **9**(12): 1190-221.
7. Ferrara, N., *Vascular endothelial growth factor.* Arterioscler Thromb Vasc Biol, 2009. **29**(6):789-91.
8. Uchida, C. and T.L. Haas, *Evolving strategies in manipulating VEGF/VEGFR signaling for the promotion of angiogenesis in ischemic muscle.* Curr Pharm Des, 2009. **15**(4): 411-21.
9. El-Remessy, A.B., et al., *Peroxynitrite mediates VEGF's angiogenic signal and function via a nitration-independent mechanism in endothelial cells.* Faseb J, 2007. **21**(10): 2528-39.
10. Colavitti, R., et al., *Reactive oxygen species as downstream mediators of angiogenic signaling by vascular endothelial growth factor receptor-2/KDR.* J Biol Chem, 2002. **277**(5): 3101-8.

11. Ushio-Fukai, M., *Redox signaling in angiogenesis: role of NADPH oxidase.* Cardiovasc Res, 2006. **71**(2): 226-35.

12. el-Remessy, A.B., et al., *Oxidative stress inactivates VEGF survival signaling in retinal endothelial cells via PI 3-kinase tyrosine nitration.* J Cell Sci, 2005. **118**(Pt 1): 243-52.

13. Abdelsaid, M.A., et al., *Early intervention of tyrosine nitration prevents vaso-obliteration and neovascularization in ischemic retinopathy.* J Pharmacol Exp Ther. **332**(1): 125-34.

14. Dunn, L.L., et al., *The emerging role of the thioredoxin system in angiogenesis.* Arterioscler Thromb Vasc Biol. **30**(11): 2089-98.

15. Dai, S., et al., *Endothelial-specific expression of mitochondrial thioredoxin promotes ischemia-mediated arteriogenesis and angiogenesis.* Arterioscler Thromb Vasc Biol, 2009. **29**(4): 495-502.

16. Kim, W.J., et al., *Antisense-thioredoxin inhibits angiogenesis via pVHL-mediated hypoxia-inducible factor-1alpha degradation.* Int J Oncol, 2005. **26**(4): 1049-52.

17. Welsh, S.J., et al., *The redox protein thioredoxin-1 (Trx-1) increases hypoxia-inducible factor 1alpha protein expression: Trx-1 overexpression results in increased vascular endothelial growth factor production and enhanced tumor angiogenesis.* Cancer Res, 2002. **62**(17): 5089-95.

18. Langston, W., et al., *Regulation of endothelial glutathione by ICAM-1 governs VEGF-A-mediated eNOS activity and angiogenesis.* Free Radic Biol Med, 2007. **42**(5): 720-9.

19. Okamoto, T., et al., *Activation of matrix metalloproteinases by peroxynitrite-induced protein S-glutathiolation via disulfide S-oxide formation.* J Biol Chem, 2001. **276**(31): 29596-602.

20. Rahman, I. and W. MacNee, *Oxidative stress and regulation of glutathione in lung inflammation.* Eur Respir J, 2000. **16**(3): 534-54.

21. Meyer, Y., et al., *Thioredoxins and glutaredoxins: unifying elements in redox biology.* Annu Rev Genet, 2009. **43**: 335-67.

22. Patwari, P., et al., *The interaction of thioredoxin with Txnip. Evidence for formation of a mixed disulfide by disulfide exchange.* J Biol Chem, 2006. **281**(31): 21884-91.

23. Perrone, L., et al., *Thioredoxin interacting protein (TXNIP) induces inflammation through chromatin modification in retinal capillary endothelial cells under diabetic conditions.* J Cell Physiol, 2009. **221**(1): 262-72.

24. Cha-Molstad, H., et al., *Glucose-stimulated expression of Txnip is mediated by carbohydrate response element-binding protein, p300, and histone H4 acetylation in pancreatic beta cells.* J Biol Chem, 2009. **284**(25): 16898-905.

25. Chen, J., et al., *Thioredoxin-interacting protein deficiency induces Akt/Bcl-xL signaling and pancreatic beta-cell mass and protects against diabetes.* Faseb J, 2008. **22**(10): 3581-94.

26. Hui, S.T., et al., *Txnip balances metabolic and growth signaling via PTEN disulfide reduction.* Proc Natl Acad Sci U S A, 2008. **105**(10): 3921-6.

27. Hui, T.Y., et al., *Mice lacking thioredoxin-interacting protein provide evidence linking cellular redox state to appropriate response to nutritional signals.* J Biol Chem, 2004. **279**(23): 24387-93.

28. Sheth, S.S., et al., *Thioredoxin-interacting protein deficiency disrupts the fasting-feeding metabolic transition.* J Lipid Res, 2005. **46**(1):123-34.

29. Kozak, A., et al., *Candesartan augments ischemia-induced proangiogenic state and results in sustained improvement after stroke.* Stroke, 2009. **40**(5): p. 1870-6.

30. Al-Gayyar, M.M., et al., *Thioredoxin interacting protein is a novel mediator of retinal inflammation and neurotoxicity.* Br J Pharmacol, 2011. **164**(1): p. 170-80.

31. Ferrara, N., et al., *Heterozygous embryonic lethality induced by targeted inactivation of the VEGF gene.* Nature, 1996. **380**(6573): p. 439-42.

32. Smith, L.E., et al., *Oxygen-induced retinopathy in the mouse.* Invest Ophthalmol Vis Sci, 1994. **35**(1): p. 101-11.

33. Abdelsaid, M.A. and A.B. El-Remessy, *VEGF induces S-glutathionylation of LMW-PTP to mediate its angiogenic signal.* **submitted** to Journal of Cell Science, 2011.

34. Huang, L., et al., *HCPTPA, a protein tyrosine phosphatase that regulates vascular endothelial growth factor receptor-mediated signal transduction and biological activity.* J Biol Chem, 1999. **274**(53): 38183-8.

35. Chiarugi, P., *PTPs versus PTKs: the redox side of the coin.* Free Radic Res, 2005. **39**(4): 353-64.

36. Casagrande, S., et al., *Glutathionylation of human thioredoxin: a possible crosstalk between the glutathione and thioredoxin systems.* Proc Natl Acad Sci U S A, 2002. **99**(15): 9745-9.

37. Tajima, M., et al., *The redox state of glutathione regulates the hypoxic induction of HIF-1.* Eur J Pharmacol, 2009. **606**(1-3): 45-9.

38. Hill, B.G. and A. Bhatnagar, *Protein S-glutathiolation: Redox-sensitive regulation of protein function.* J Mol Cell Cardiol. Mol Cell Cardiol. 2011 Jul 20.

39. Hirota, K., et al., *Distinct roles of thioredoxin in the cytoplasm and in the nucleus. A two-step mechanism of redox regulation of transcription factor NF-kappaB.* J Biol Chem, 1999. **274**(39): 27891-7.

40. Farrell, M.R., et al., *Thioredoxin-interacting protein inhibits hypoxia-inducible factor transcriptional activity.* Free Radic Biol Med. **49**(9): 1361-7.

41. Yun, J., et al., *Redox-dependent mechanisms in coronary collateral growth: the "redox window" hypothesis.* Antioxid Redox Signal, 2009. **11**(8): 1961-74.

42. Das, S.K., et al., *An integrative genomics approach identifies activation of thioredoxin/thioredoxin reductase-1-mediated oxidative stress defense pathway and inhibition of angiogenesis in obese nondiabetic human subjects.* J Clin Endocrinol Metab. **96**(8): E1308-13.

43. Dunn LL, B.A., Simpson P, Sieveking DP, Chow RW, Lim P, Ng and MKC., *Rescue of diabetes-related impairment of angiogenesis by gene silencing of thioredoxin-interacting protein.* Circulation. 2010;120:S1142., 2010.

44. Xiang, G., et al., *Catalytic degradation of vitamin D up-regulated protein 1 mRNA enhances cardiomyocyte survival and prevents left ventricular remodeling after myocardial ischemia.* J Biol Chem, 2005. **280**(47): 39394-402.

45. Buricchi, F., et al., *Redox regulation of ephrin/integrin cross-talk.* Cell Adh Migr, 2007. **1**(1): 33-42.

46. Giannoni, E., et al., *Lymphocyte function-associated antigen-1-mediated T cell adhesion is impaired by low molecular weight phosphotyrosine phosphatase-dependent inhibition of FAK activity.* J Biol Chem, 2003. **278**(38): 36763-76.

47. den Hertog, J., A. Groen, and T. van der Wijk, *Redox regulation of protein-tyrosine phosphatases.* Arch Biochem Biophys, 2005. **434**(1): 11-5.

48. Kanda, M., et al., *Glutaredoxin modulates platelet-derived growth factor-dependent cell signaling by regulating the redox status of low molecular weight protein-tyrosine phosphatase.* J Biol Chem, 2006. **281**(39): 28518-28.

49. Chiarugi, P. and T. Fiaschi, *Redox signalling in anchorage-dependent cell growth.* Cell Signal, 2007. **19**(4): 672-82.

50. Juarez, J.C., et al., *Superoxide dismutase 1 (SOD1) is essential for H2O2-mediated oxidation and inactivation of phosphatases in growth factor signaling.* Proc Natl Acad Sci U S A, 2008. **105**(20): 7147-52.

51. Xing, K., et al., *Low molecular weight protein tyrosine phosphatase (LMW-PTP) and its possible physiological functions of redox signaling in the eye lens.* Biochim Biophys Acta, 2007. **1774**(5): 545-55.

Fig. 3.1.

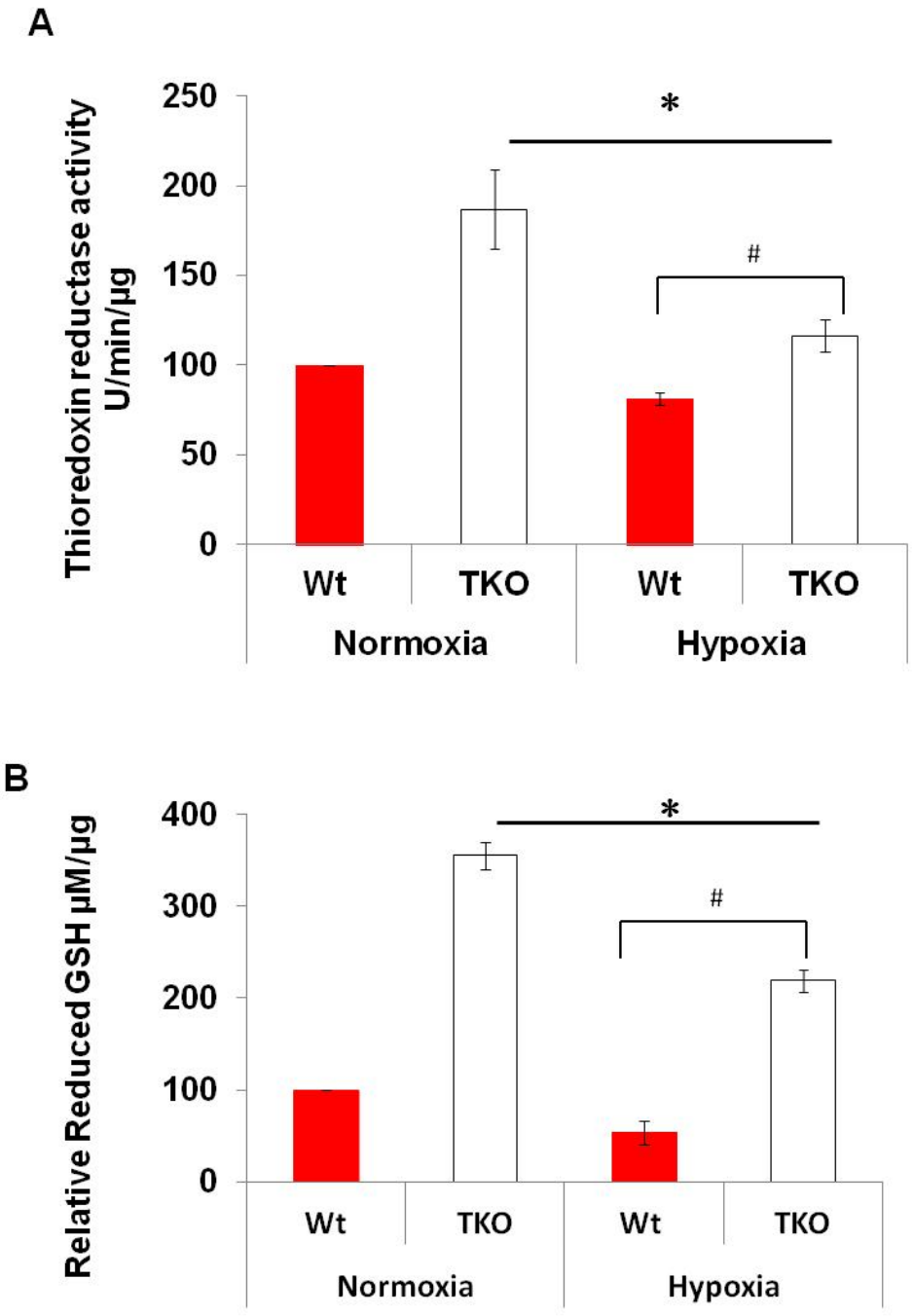
A
Thioredoxin reductase activity U/min/µg
250
200
150
100
50
0
*
#
Wt
TKO
Wt
TKO
Normoxia
Hypoxia
B
Relative Reduced GSH µM/µg
400
300
200
100
0
*
#
Wt
TKO
Wt
TKO
Normoxia
Hypoxia

Fig 3.1 Knocking down TXNIP expression alters cellular redox-state.

Using the hypoxia-induced mouse model, p17 Wt and TKO mice were exposed to relative hypoxia (from p12-p17). Retinas were examined for thioredoxin reductase activity while plasma was tested for reduced GSH levels. **A)** TKO mice showed significant increases (2-fold) in retinal thioredoxin reductase activity when compared to age matched wild type under normoxic conditions. Hypoxia caused significant reduction in thioredoxin reductase activity both in Wt (20%) and TKO (25%) when they compared to the same genotype at normoxic condition. The Thioredoxin reductase activity of TKO hypoxic retinas were significantly higher than the WT exposed to hypoxia. B) TKO showed increases (3.5-fold) plasma reduced-glutathione when compared to age matched wild type under normoxic conditions. Hypoxia caused significant reduction in plasma GSH levels in both Wt (45%) and TKO (42%) when they compared to the same genotype at normoxic condition. The reduced GSH levels of TKO hypoxic retinas were significantly higher than the WT exposed to hypoxia. (n=6-8, #,* $P< 0.05$ vs control)

Fig 3.2.

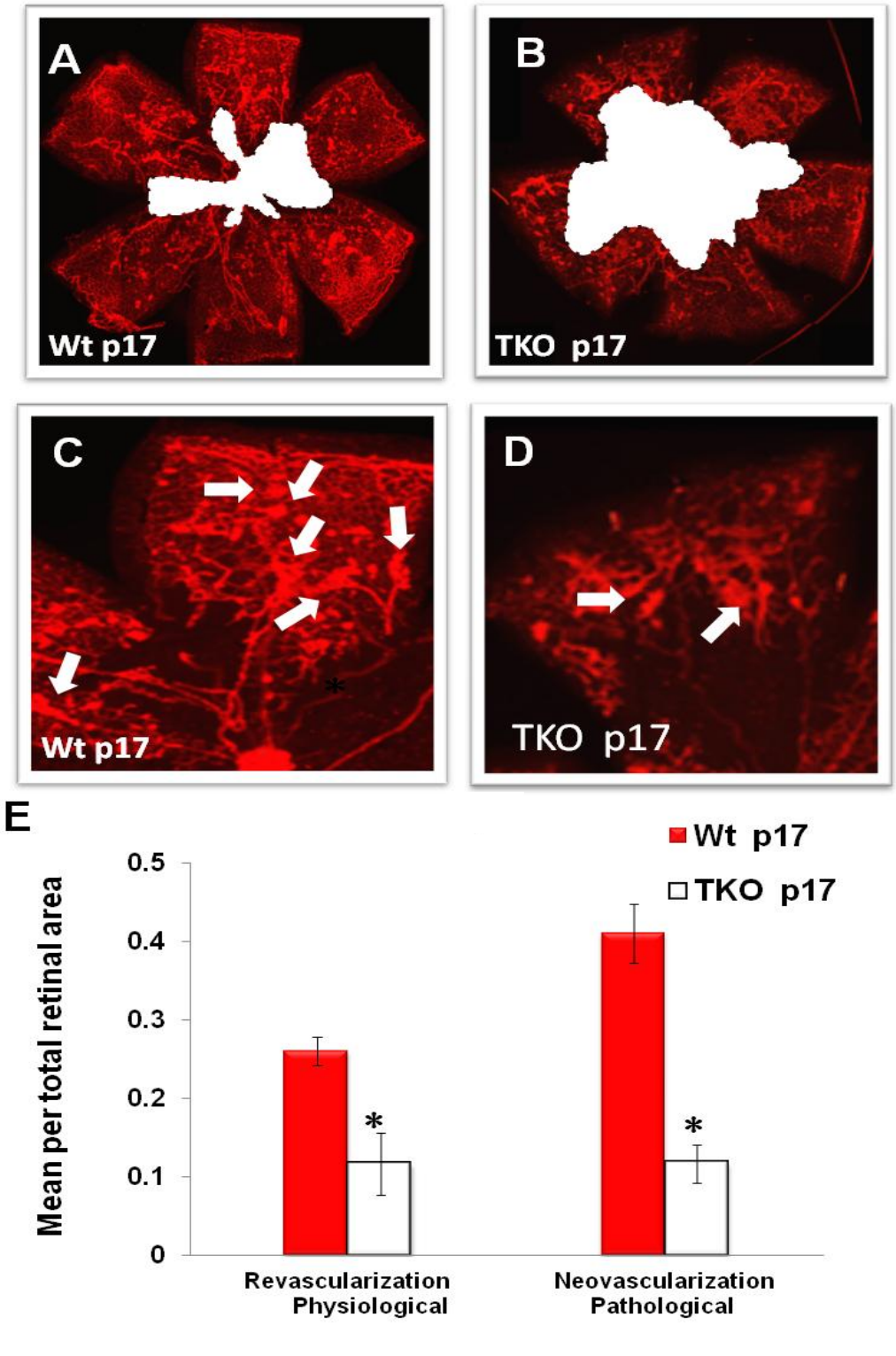
A
Wt p17
B
TKO p17
C
Wt p17
*
D
TKO p17
E
Wt p17
TKO p17
Mean per total retinal area
0.5
0.4
0.3
0.2
0.1
0
*
*
Revascularization
Physiological
Neovascularization
Pathological

3.2 Knocking down TXNIP expression impairs VEGF-induced reparative and pathological neovascularization.

Exposing the postnatal day 12 mice to relative hypoxia (from p12-p17) results in VEGF-induced revascularizations of the central capillary drop-out areas as well as the pathological mid-peripheral neovascularization. Knocking down TXNIP impaired both physiological and pathological VEGF-induced neovascularization. **A-E)** TKO showed 50 % reduction in physiological revascularization of central capillary drop out and 75% reduction in neovascularization when compared to wild type age matched animals. (n=6-8, * $P < 0.05$ vs control)

Fig 3.3.

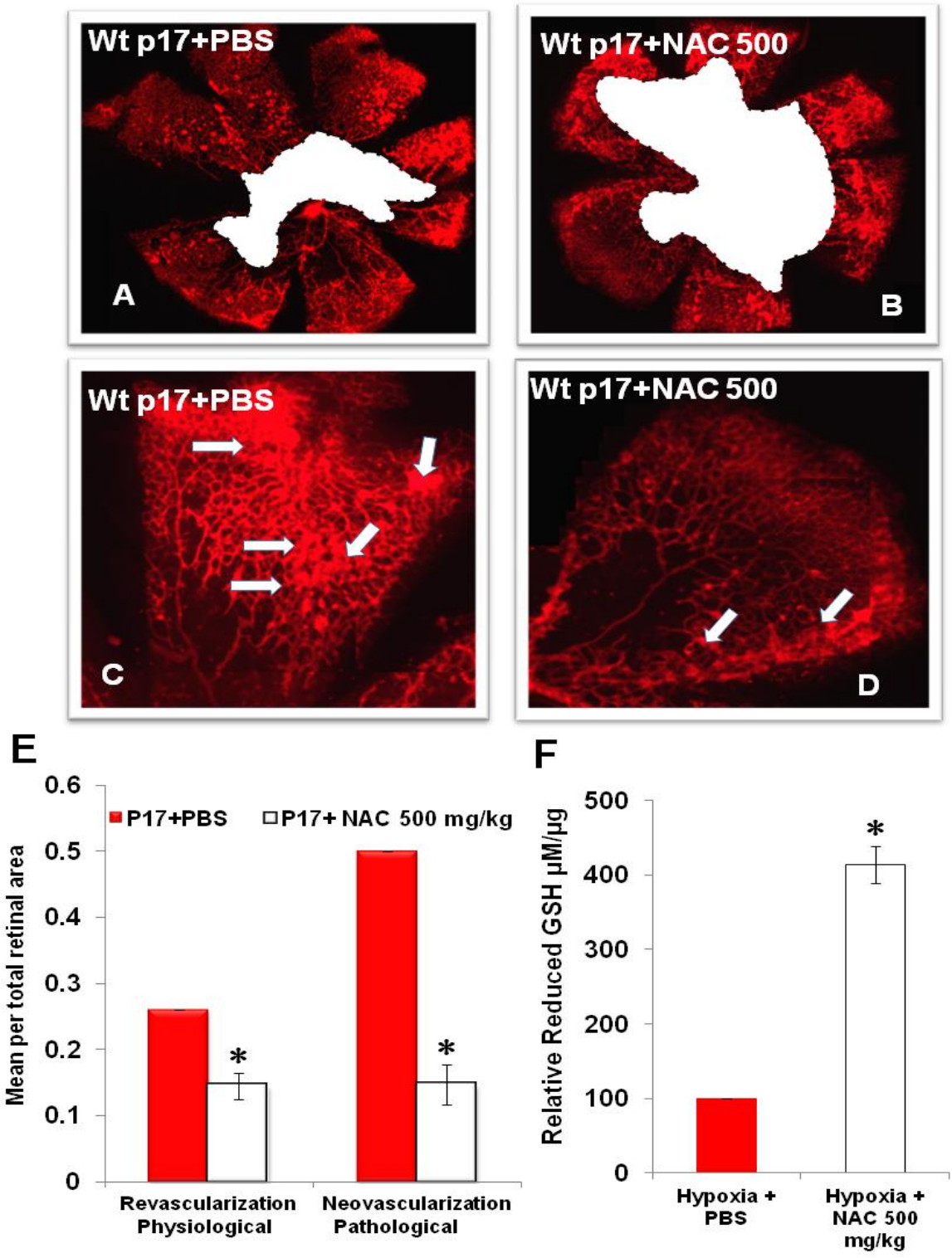
Wt p17+PBS
A
Wt p17+NAC 500
B
Wt p17+PBS
C
Wt p17+NAC 500
D
E
Mean per total retinal area
0.6
0.5
0.4
0.3
0.2
0.1
0
P17+PBS
P17+ NAC 500 mg/kg
*
*
Revascularization Physiological
Neovascularization Pathological
F
Relative Reduced GSH µM/µg
500
400
300
200
100
0
*
Hypoxia + PBS
Hypoxia + NAC 500 mg/kg

Fig. 3.3. Acute reductive stress impairs VEGF-induced reparative and pathological neovascularization.

Wild type mice and wild type-treated mice with a high dose of the thiol donor and general antioxidant N-acetyl cysteine (NAC, I.P 500 mg/kg) were subjected to relative hypoxia p12-p17. Plasma of the NAC-treated pups showed 4-fold increases in reduced-GSH levels when compared to wild type PBS-treated age matched animals. NAC (500 mg/kg) impaired both VEGF-induced reparative (43%) and pathological neovascularization (70%) when compared to wild type PBS-treated age matched animals. (n=6-8, * $P < 0.05$ vs control)

Fig. 3.4.

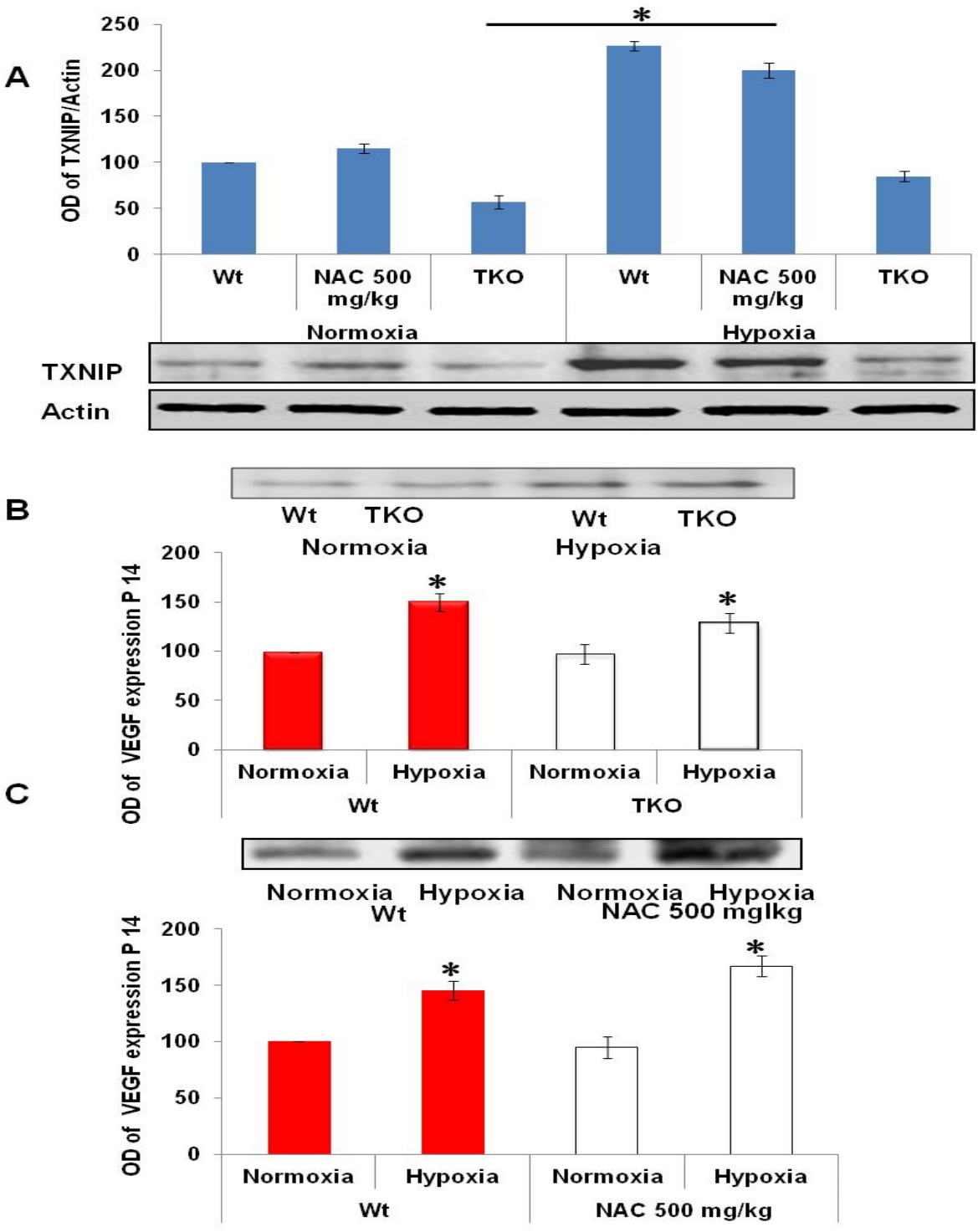
A
OD of TXNIP/Actin
250
200
150
100
50
0
*
Wt
NAC 500 mg/kg
TKO
Wt
NAC 500 mg/kg
TKO
Normoxia
Hypoxia
TXNIP
Actin
B
Wt
TKO
Wt
TKO
Normoxia
Hypoxia
C
OD of VEGF expression P 14
200
150
100
50
0
*
*
Normoxia
Hypoxia
Normoxia
Hypoxia
Wt
TKO
Normoxia
Hypoxia
Normoxia
Hypoxia
Wt
NAC 500 mglkg
OD of VEGF expression P 14
200
150
100
50
0
*
*
Normoxia
Hypoxia
Normoxia
Hypoxia
Wt
NAC 500 mg/kg

Fig. 3.4 Knocking down TXNIP expression did not alter VEGF expression.

Wild type mice, TKO and wild type-treating mice with a high dose of the thiol donor and general antioxidant N-acetyl cystiene (NAC, I.P 500 mg/kg) were subjected to relative hypoxia p12-p17. **A)** Retinas were assessed for TXNIP expression. Hypoxia only doubled the TXNIP expression in wild type and wild type treated with NAC (Fig 4.A).

B-C) P14 pups were assessed for VEGF expression. Hypoxia increased the VEGF expression in all groups 1.7, 1.8, 1.45 fold increase in wild type, wild type treated with NAC and TKO respectively. (n=6-8, * $P< 0.05$ vs control)

Fig. 3.5.

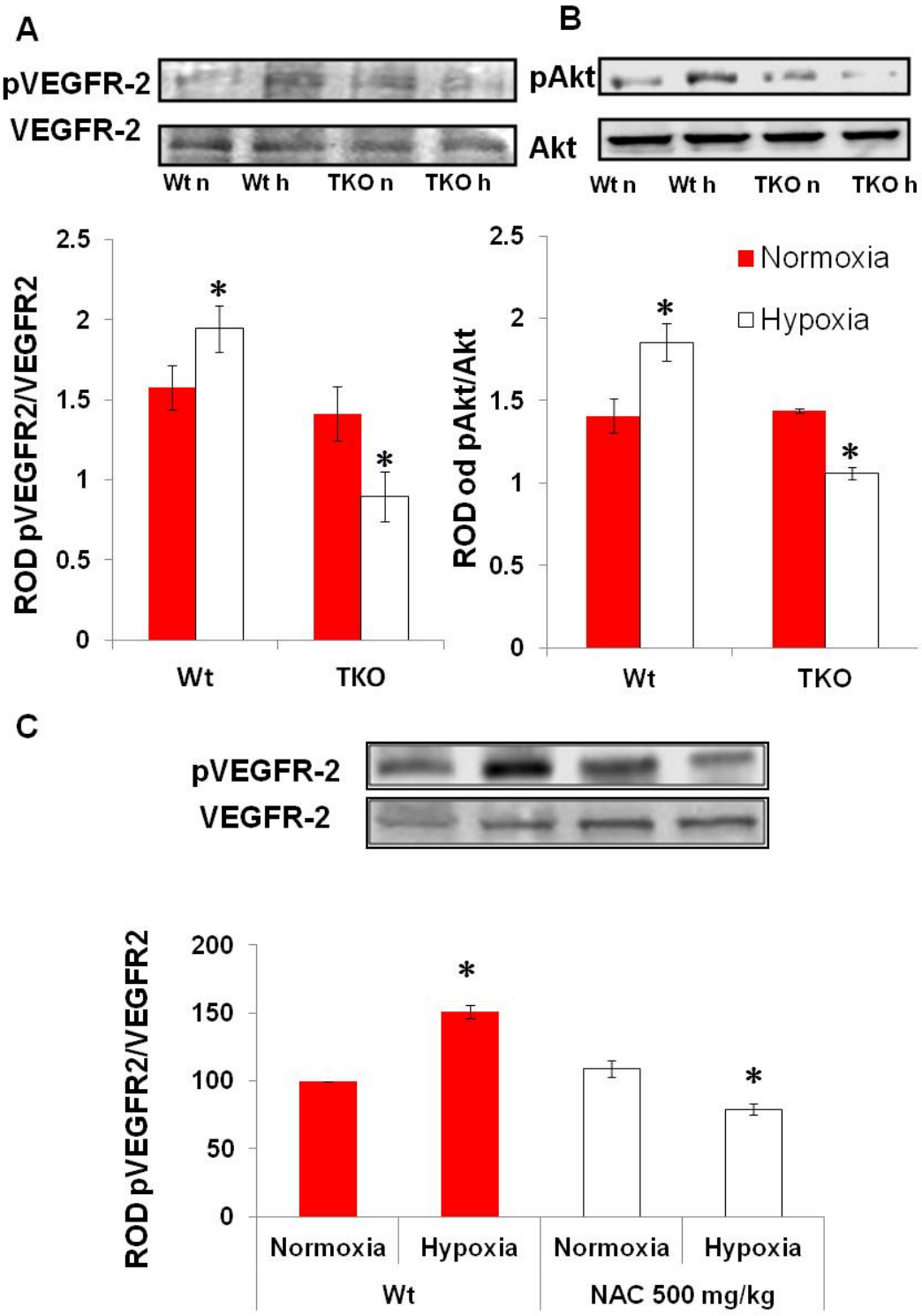
A
pVEGFR-2
VEGFR-2
Wt n
Wt h
TKO n
TKO h
B
pAkt
Akt
Wt n
Wt h
TKO n
TKO h
ROD pVEGFR2/VEGFR2
2.5
2
1.5
1
0.5
0
*
*
Wt
TKO
ROD od pAkt/Akt
2.5
2
1.5
1
0.5
0
Normoxia
Hypoxia
*
*
Wt
TKO
C
pVEGFR-2
VEGFR-2
ROD pVEGFR2/VEGFR2
200
150
100
50
0
*
*
Normoxia
Hypoxia
Normoxia
Hypoxia
Wt
NAC 500 mg/kg

Fig. 3.5. Knocking down TXNIP expression decreases VEGFR2 phosphorylation in vivo.

Wild type, TKO and wild type-NAC treated (NAC, I.P 500 mg/kg) were subjected to relative hypoxia p12-p14. VEGFR-2 phosphorylation was assessed in pup's retinas. A) Retinas of wild type pups showed increases (1.4 fold) in Y-996 phosphorylation while TKO and NAC treated wild type showed a significant reduction of VEGF receptor phosphorylation 35%, 21 % reduction respectively when compared to Wt normoxia animals and almost 55% and 50% when compared to Wt exposed to hypoxia. Hypoxia increased Akt activation in wild type by 30% while TKO mice showed a significant decrease in AKT activation 28% compared to normoxic Wt animals and 50% to Wt exposed to hypoxia. (n=6-8, * $P < 0.05$ vs control)

Fig. 3.6.

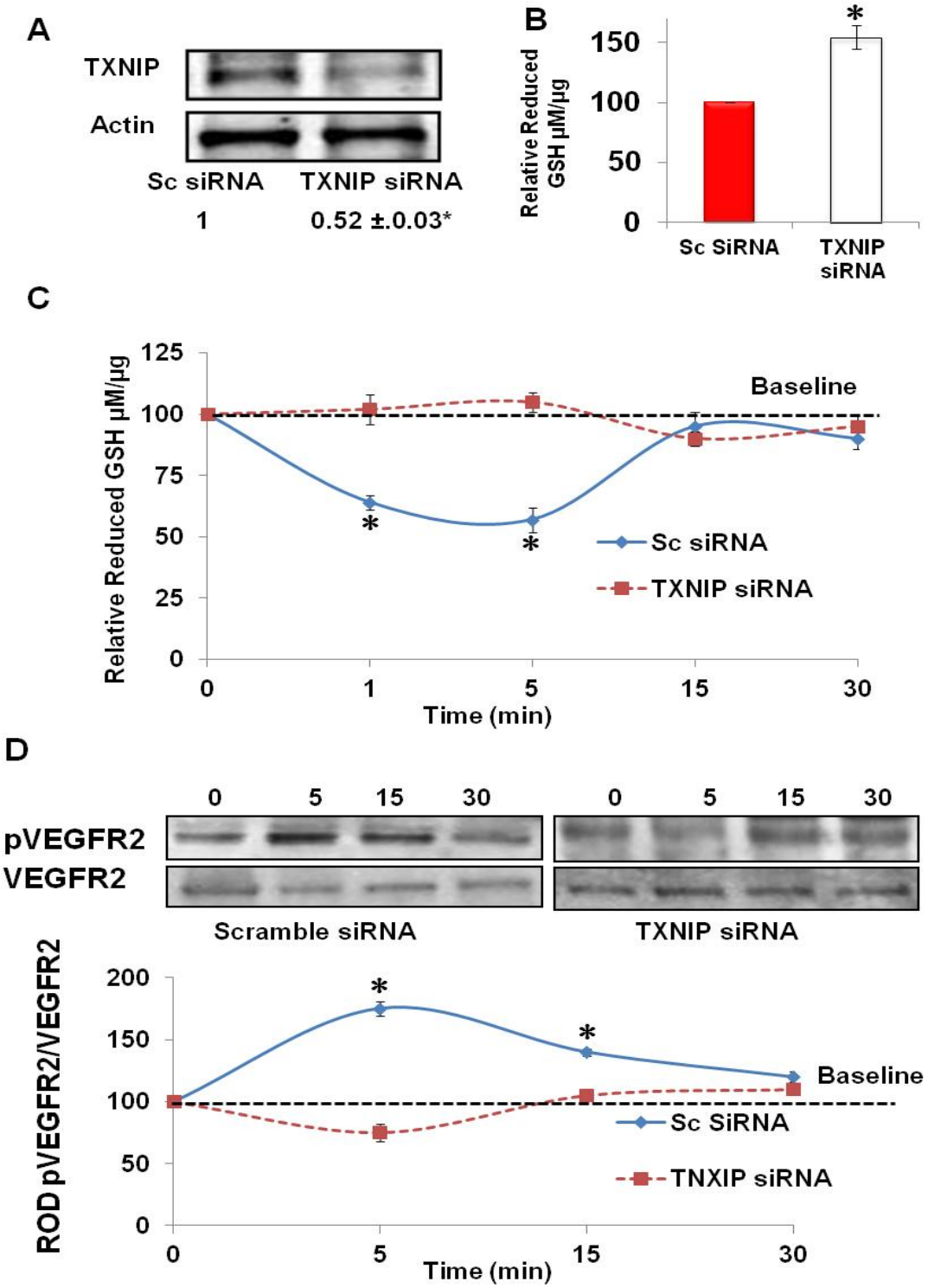
A
TXNIP
Actin
Sc siRNA
TXNIP siRNA
1
0.52 ±.0.03*
B
Relative Reduced GSH µM/µg
150
100
50
0
*
Sc SiRNA
TXNIP siRNA
C
Relative Reduced GSH µM/µg
125
100
75
50
25
0
Baseline
*
*
Sc siRNA
TXNIP siRNA
0
1
5
15
30
Time (min)
D
0
5
15
30
0
5
15
30
pVEGFR2
VEGFR2
Scramble siRNA
TXNIP siRNA
ROD pVEGFR2/VEGFR2
200
150
100
50
0
*
*
Baseline
Sc SiRNA
TNXIP siRNA
0
5
15
30
Time (min)

Fig. 3.6. **Silencing TXNIP expression increases cellular antioxidant defense and impairs VEGFR2 phosphorylation.**

TXNIP expression was silenced in human microvascular endothelial (HME) cells using siRNA. **A-B)** Silencing TXNIP expression in HME cells caused 48% reduction in TXNIP expression and 1.6 fold increases cellular levels of reduced- glutathione. **C)** Cells were treated with VEGF (20 ng/ml). VEGF caused transient reduction in reduced GSH levels that was restored back at 15 min for HME treated with scrambled siRNA. **D)** Silencing TXNIP blunted VEGF redox effect. Silencing TXNIP expression impaired VEGFR-2. (n=4-6, * $P < 0.05$ vs zero time)

Fig. 3.7.

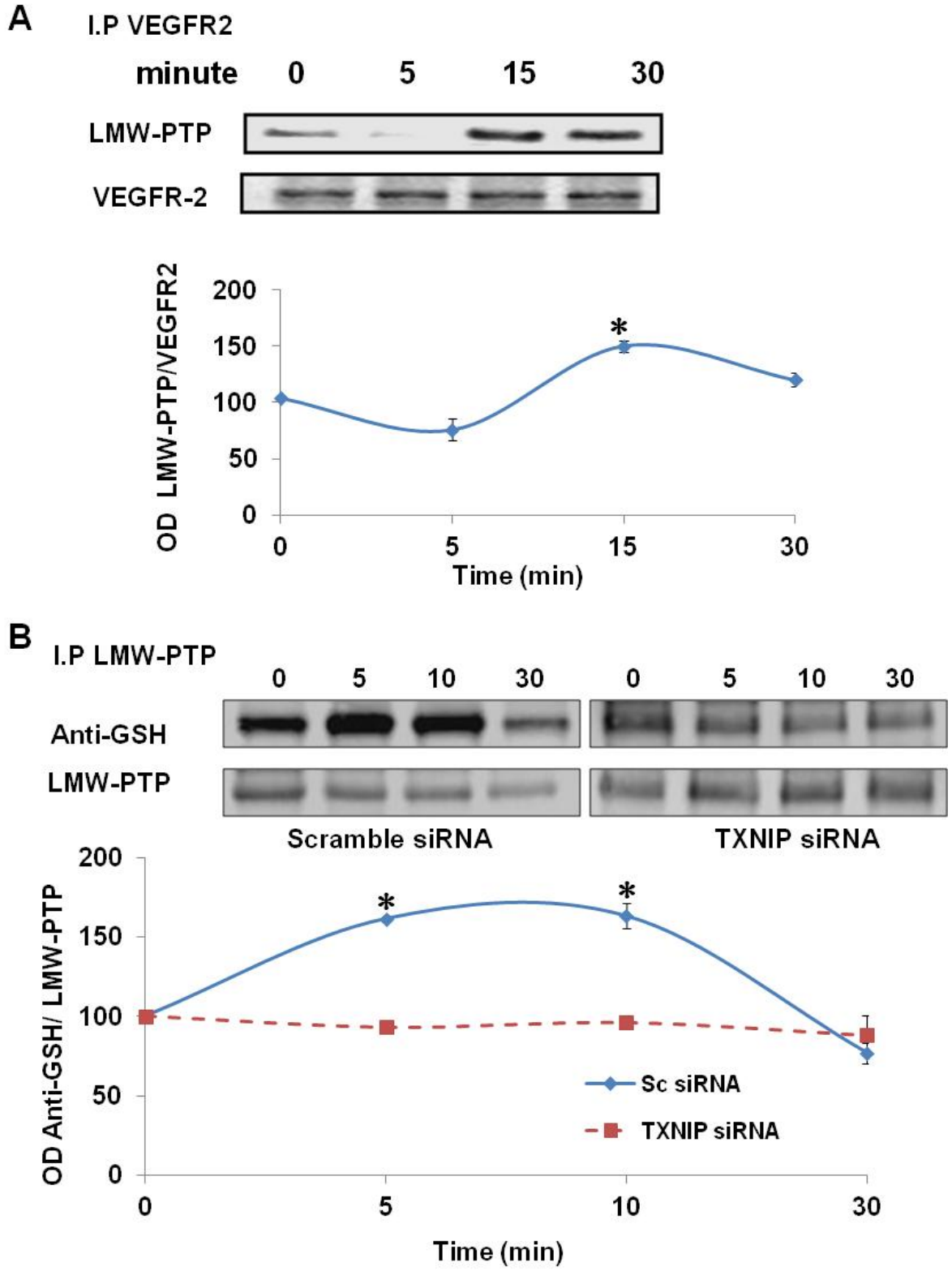
A
I.P VEGFR2
minute 0 5 15 30
LMW-PTP
VEGFR-2
OD LMW-PTP/VEGFR2
200
150
100
50
0
*
0 5 15 30
Time (min)
B
I.P LMW-PTP
0 5 10 30 0 5 10 30
Anti-GSH
LMW-PTP
Scramble siRNA
TXNIP siRNA
OD Anti-GSH/ LMW-PTP
200
150
100
50
0
* *
Sc siRNA
TXNIP siRNA
0 5 10 30
Time (min)

Fig. 3.7. VEGF stimulates association of VEGFR-2 with LMW-PTP.

A) HME Cells were treated with VEGF (20 ng/ml). Maximum association between LMW-PTP with VEGFR2 was at 15 minutes of VEGF stimulation.

B) Silencing TXNIP expression in HME using siRNA blunted VEGF effect and we did not detect any change in LMW-PTP S-glutathiolation over 30 minute of VEGF treatment. (n=4-6, * $P< 0.05$ vs zero time)

Fig. 3.8.

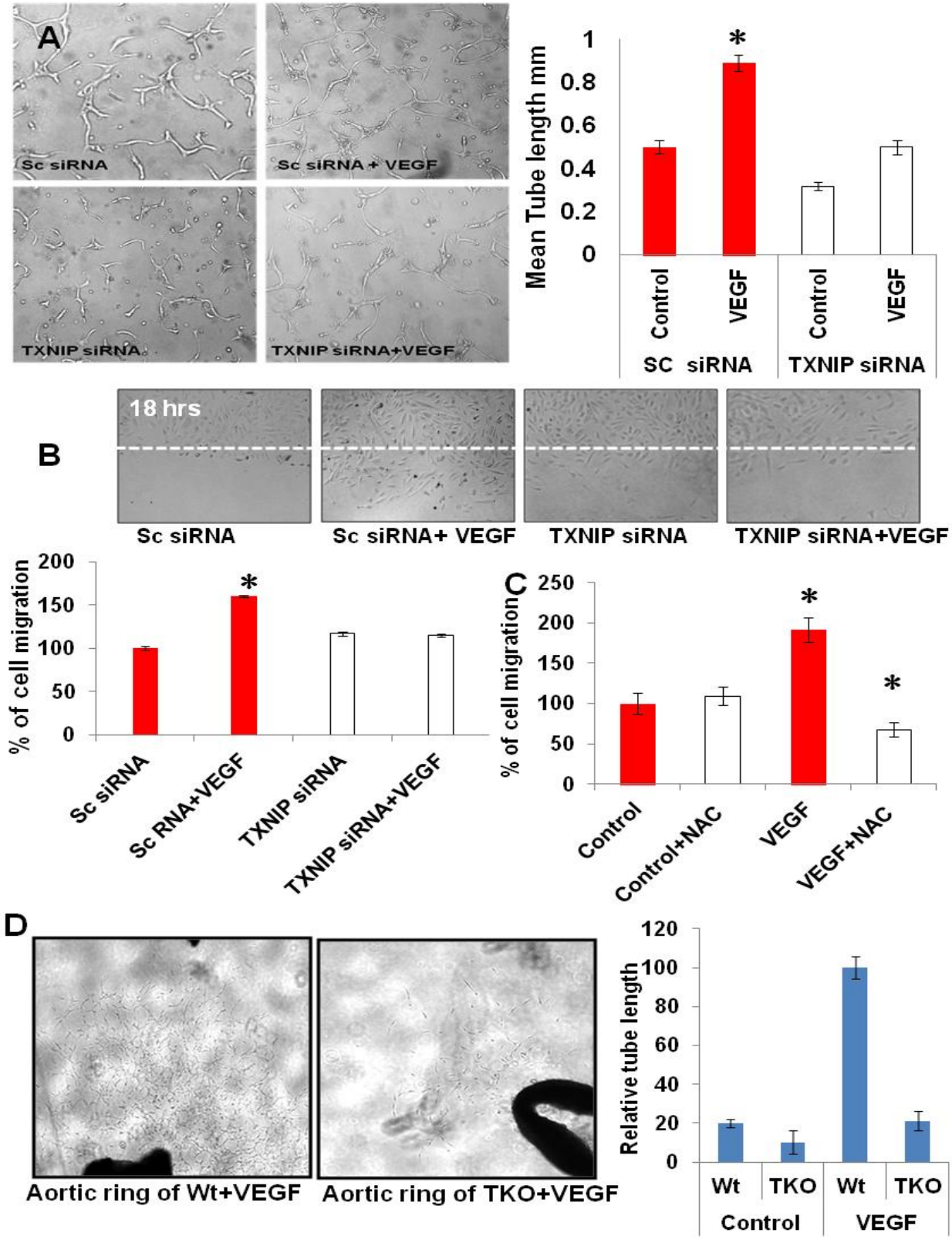
A
Sc siRNA
Sc siRNA + VEGF
TXNIP siRNA
TXNIP siRNA+VEGF
Mean Tube length mm
1
0.8
0.6
0.4
0.2
0
*
Control
VEGF
Control
VEGF
SC siRNA
TXNIP siRNA
B
18 hrs
Sc siRNA
Sc siRNA+ VEGF
TXNIP siRNA
TXNIP siRNA+VEGF
% of cell migration
200
150
100
50
0
*
Sc siRNA
Sc RNA+VEGF
TXNIP siRNA
TXNIP siRNA+VEGF
C
% of cell migration
250
200
150
100
50
0
*
*
Control
Control+NAC
VEGF
VEGF+NAC
D
Aortic ring of Wt+VEGF
Aortic ring of TKO+VEGF
Relative tube length
120
100
80
60
40
20
0
Wt
TKO
Wt
TKO
Control
VEGF

Fig. 3.8. Silencing TXNIP expression inhibits VEGF angiogenic response.

TXNIP expression was silenced in HME cells using siRNA. **A)** VEGF (20 ng/ml) caused 1.9 fold increases in mean length of tube formation of HME treated with scrambled siRNA, silencing TXNIP expression using siRNA impaired VEGF ability to induce alignment of endothelial cells into tubes. **B-C)** VEGF (20 ng/ml) caused 1.6 fold increases in cell migration of HME treated with scrambled siRNA. Silencing TXNIP or using high dose of NAC (10 mM) blunted the VEGF-induced cell migration. **D)** Aortic ring of TKO mice showed 80 percent reduction in vascular sprouts in Matrigel in response to VEGF when compared to wild type rings. (n=4-6, * $P < 0.05$ vs control)

Supplementary Fig. 3.1

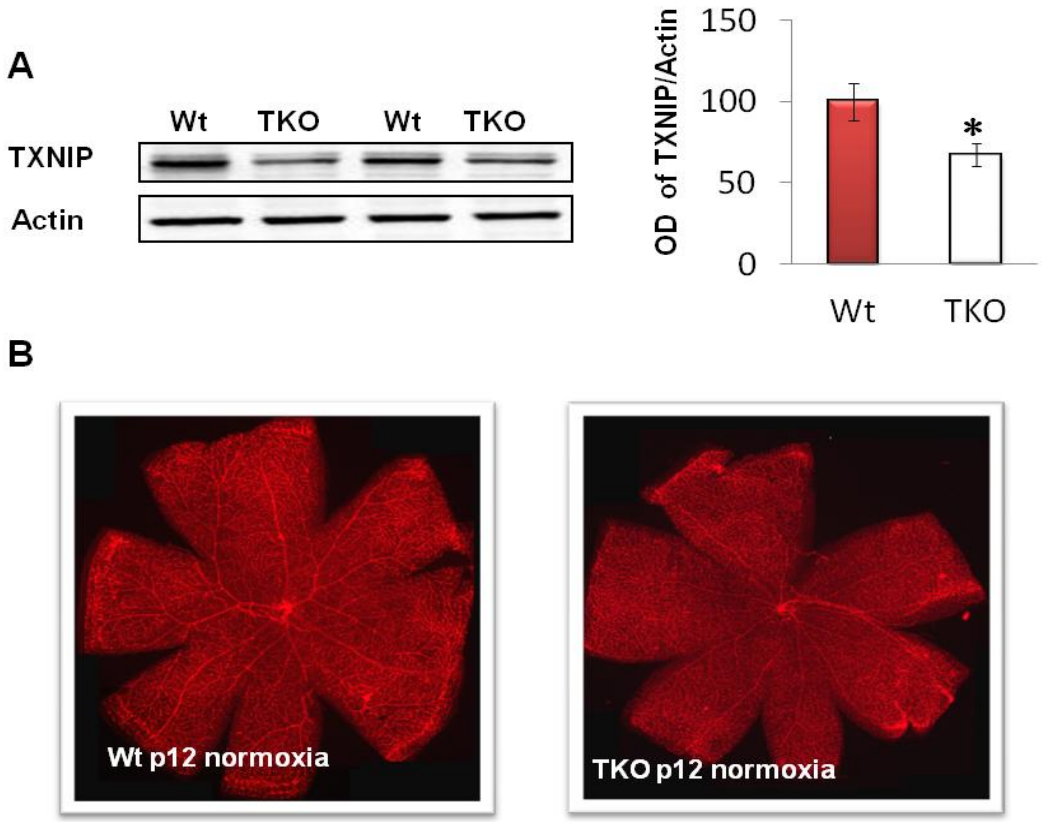

A) Western blot analysis of retinas of TKO vs Wt. Retinas of TKO Showed 40 percent less TXNIP expression compared to wild type.

B) Flat mount retinas stained with Isolectin B-4 special stain for retinal vasculature showing a normal development pattern of TKO mice retinas compared to control.

Supplementary Fig. 3.2

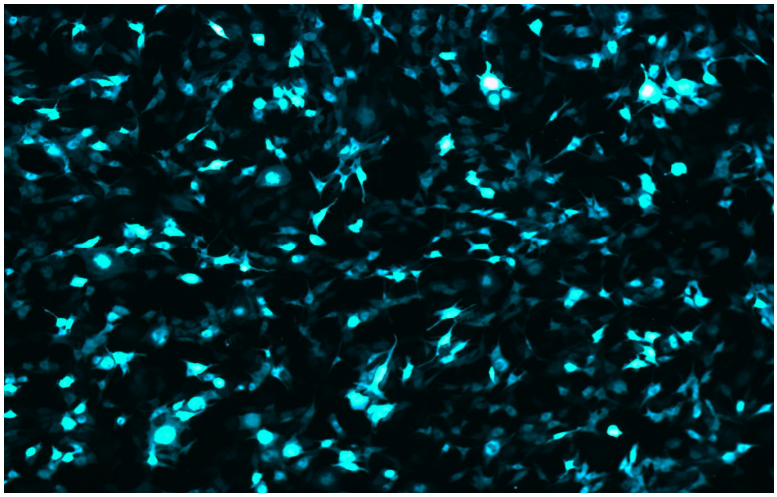

Transfection efficacy of TXNIP siRNA. Silencing TXNIP using siRNA was 85-90% efficient. Transfection efficiency was assessed by calculating percentage of GFP expressing cells to the total number of cells after imaging with fluorescence AxioObserver Zeiss Microscope (Germany).

CHAPTER 4

VEGF-INDUCED S-GLUTATHIONYLATION OF LMW-PTP REGULATES FAK ACTIVATION AND ENDOTHELIAL CELL MIGRATION [1]

---

[1] Mohammed A. Abdelsaid and Azza B. El-Remessy
Submitted to Journal of Cell Science, 10/15/2011.

Abstract

Angiogenesis plays both beneficial and detrimental roles in cardiovascular diseases. Although promising, the ability to regulate angiogenesis via delivery of VEGF remains an unrealized goal. We have previously shown that physiological levels of peroxynitrite (PN,1 μM) are required for the VEGF-mediated angiogenic response, yet the redox-regulated mechanisms governing the VEGF signal remain unexplored. We assessed the impact of VEGF and peroxynitrite on modifying redox-state, free glutathione (GSH) and S-glutathionylation on regulation of the low molecular weight protein tyrosine phosphatase (LMW-PTP) and focal adhesion kinase (FAK), key mediators of VEGF-mediated cell migration. Stimulation of human microvascular endothelial (HME) cells with VEGF (20 ng/ml) or PN (1 μM) caused an immediate and reversible negative-shift in the cellular redox-state and thiol oxidation of LMW-PTP that culminated in cell migration. VEGF caused a reversible S-glutathionylation of LMW-PTP, which coincided with reversible FAK activation, impaired phosphorylation and loss of activity of LMW-PTP. Modulating redox-state by decomposing peroxynitrite (FeTPPS, 2.5 μM) or GSH-precursor (NAC, 1 mM) caused a positive-shift of the redox-state, prevented VEGF-mediated S-glutathionylation and oxidative inhibition of LMW-PTP, FAK activation and cell migration. While mild oxidative stress achieved by combining VEGF with 0.1-0.2 mM PN augmented cell migration, acute shift to oxidative stress achieved by combining VEGF with 0.5 mM peroxynitrite induced and sustained FAK activation, LMW-PTP thiol oxidation and S-glutathionylation resulting in LMW-PTP inactivation and inhibited cell migration. In conclusion, our findings demonstrate that balanced redox-state is required for VEGF to facilitate reversible S-glutathionylation of LMW-PTP, FAK activation and endothelial cell migration. Shifting redox-state to reductive stress or oxidative stress blunted the VEGF-mediated angiogenic response.

Introduction

Angiogenesis plays both beneficial and detrimental roles in cardiovascular diseases. Promoting the angiogenic response has been demonstrated to be beneficial in treating ischemic conditions such as myocardial ischemia/infarction and delayed wound healing (Xiong et al.; van der Laan et al., 2009). In contrast, abnormally enhanced angiogenic responses are observed during diabetic retinopathy and atherosclerosis (Cao, 2010; Ali and El-Remessy, 2009; Chua and Arbiser, 2009). Although promising, the ability to regulate angiogenesis remains unrealized therapeutic goal. The role of reactive oxygen species (ROS) as a downstream messenger for vascular endothelial growth factor (VEGF) to promote angiogenesis has been established (reviewed in (Colavitti et al., 2002; Colavitti and Finkel, 2005; Ushio-Fukai, 2006; Ushio-Fukai, 2007)). Our group demonstrated a critical role of peroxynitrite, the reaction product of nitric oxide and superoxide anion, in modulating the VEGF signal. While physiologic low levels of peroxynitrite are required to mediate the VEGF angiogenic signal; pathological peroxynitrite levels impair VEGF's survival signal and can induce cell death (Gu et al., 2003; El-Remessy et al., 2005; El-Remessy et al., 2007; Abdelsaid et al., 2010). These studies suggest that there is an unidentified redox-regulated mechanism controlling VEGF angiogenic signal and function.

Glutathione (GSH), the most abundant intracellular thiol, not only regulates the redox-state but it functions as a signaling molecule to regulate cell proliferation and apoptosis (Rahman and MacNee, 2000; Okamoto et al., 2001). In response to peroxynitrite, protein thiols can undergo posttranslational modification by S-nitrosylation, oxidation, formation of disulfides, and S-glutathionylation (Wang et al., 2003; Clavreul et al., 2006; Dremina et al., 2007; Sethuraman et al., 2007; Liaudet et al., 2009; Chinta and Andersen, 2011). Under oxidative stress, S-glutathionylation, a reversible protein modification, occurs through formation of protein mixed

disulfides (protein–SSG) with GSH (Okamoto et al., 2001; Chen et al., 2010) and hence S-glutathionylation serves as a protective mechanism to protect regulatory thiols from irreversible oxidation (Shelton and Mieyal, 2008). De-glutathionylation is catalyzed generally by restoration of reductive GSH/GSSG ratio and more efficiently by the reducing systems, thioredoxin and glutaredoxin (Dalle-Donne et al., 2009). S-glutathionylation can result in transient activation or inactivation of the protein and its reversibility dictates its physiological relevance (Shelton and Mieyal, 2008).

Low molecular weight protein tyrosine phosphatase (LMW-PTP) regulates cytoskeleton rearrangement, endothelial cell growth and differentiation through its ability to bind and dephosphorylate focal adhesion kinase (FAK) and activated growth factor receptors (Huang et al., 1999; Raugei et al., 2002; Shimizu et al., 2005; Kanda et al., 2006). In particular, FAK plays a crucial role in VEGF-induced endothelial cell migration through regulation of focal adhesion assembly and disassembly (Chiarugi et al., 2003; Li and Hua, 2008; Tomar and Schlaepfer, 2009). LMW-PTP shares the CX_5R motive with other PTPs, which render them vulnerable targets for cellular redox-changes (Okamoto et al., 2001; Shackelford et al., 2005; Shelton and Mieyal, 2008). Furthermore, LMW-PTP has a unique property of having two cysteines located in the catalytic pocket; both cysteines must be reduced for enzyme phosphorylation and activity (Chiarugi, 2001; Chiarugi et al., 2001; Xing et al., 2007). Therefore, the activity of LMW-PTP is tightly linked to redox-changes and can be a molecular switch for regulation of the cell migration and the angiogenic process (Giannoni et al., 2006). Nevertheless, S-glutathionylation of LMW-PTP in response to VEGF and how it can regulate FAK migratory signal have not been elucidated.

Here, we demonstrate the molecular events by which VEGF differentially modulates GSH levels to facilitate S-glutathionylation of LMW-PTP, FAK activation and cell migration. We also demonstrate the impact of shifting the cellular redox-state to oxidative stress or reductive stress on VEGF-mediated S-glutathionylation of LMW-PTP and the angiogenic response.

Results

VEGF causes a reversible negative-shift in redox-state of endothelial cells.

We have previously showed that stimulation of endothelial cells with VEGF produces low levels of peroxynitrite (El-Remessy et al., 2007). To examine the effects of VEGF stimulation on the cellular redox-state, human microvascular endothelial (HME) cells were stimulated with VEGF (20 ng/ml). The cellular redox-state was assessed by reduced-glutathione (GSH) levels. Stimulation with VEGF caused oxidation of GSH that caused a negative shift in the endothelial redox-state as indicated by 34% and 38% reduction of GSH levels at 1 and 5 minutes, respectively. The cellular redox-state was restored to the basal level after 15-30 minutes (Fig 1A).

VEGF causes reversible thiol oxidation and inactivation of LMW-PTP in endothelial cells.

Since LMW-PTP is a redox-regulated phosphatase that plays an important role in the angiogenic process, we examined the effects of VEGF on the LMW-PTP redox-state. To quantify total free thiols, HME cells were labeled with fluorescein-tagged 5-iodo-acetamide (5-IAM). As shown in Fig. 1B, VEGF caused immediate thiol oxidation of LMW-PTP as indicated by reduction of free thiol by 40% and 35% at 1 and 5 min, respectively. In parallel to the cellular redox-state, LMW-PTP thiol oxidation was transient and free thiols were restored to normal levels at 15-30 minutes

(Fig. 1B). Since oxidation of LMW-PTP can inhibit its activation, we examined the phosphorylation of the LMW-PTP. Indeed, phosphorylation of LMW-PTP was blunted at 1 and 5 min, which coincided with its oxidation. VEGF treatment induced phosphorylation of LMW-PTP (1.7-fold) after 15 minutes, a time point where free thiols of LMW-PTP are reduced (see Fig. 1C).

VEGF causes reversible S-glutathionylation and inhibition of LMW-PTP activity.

S-glutathionylation is the final step for protective cysteine modification in response to oxidative stress. VEGF induced S-glutathionylation of LMW-PTP by 2.6 and 2.4 fold after 5 and 10 minutes, respectively. S-glutathionylation was reversible as the signal was blunted at 15-30 minutes (Fig 2A). The specificity of detecting S-glutathionylation was confirmed by complete blunting of the signal when samples were pretreated with DTT. Assessment of the phosphatase activity of LMW-PTP showed that oxidized-glutathione (GSSG 10 mM) significantly reduced the phosphatase activity to 29.7% of its basal levels. To further confirm the effect of S-glutathionylation on LMW-PTP enzymatic activity, reduced-glutathione (GSH 10 mM) increased LMW-PTP activity by 4 fold (Fig 2B).

VEGF-induced peroxynitrite stimulates FAK activation and association with LMW-PTP.

Because LMW-PTP is the specific phosphatase for FAK, we examined its tyrosine phosphorylation in response to VEGF. As shown in Fig. 3A, VEGF caused FAK activation that peaked at 15 minutes (2.5 fold), which was blocked with the peroxynitrite decomposition catalyst FeTPPS (2.5 μM), suggesting a key role of peroxynitrite (Fig. 3A, lower panel). In parallel, peroxynitrite (1 μM) induced FAK activation that peaked at 15 minutes (2.6 fold) compared to decomposed peroxynitrite (DPN) (Fig. 3B). We next tested the interaction between

the LMW-PTP and the FAK in response to VEGF treatment. As shown in Fig. 3C, our results showed that VEGF stimulated association between LMW-PTP and FAK that maxed at 15 minutes (1.9 fold), a time point that FAK is fully activated. The association resulted in blunting of the FAK activation (30 minutes).

Positive shift in redox-state inhibits S-glutathionylation of LMW-PTP and cell migration.

As shown in Fig. 4A, the ability of VEGF to oxidize GSH was blunted at 1-5 minutes with pretreatment with FeTPPS or NAC. Moreover, FeTPPS or NAC caused a positive shift in the cellular redox-state at 15-30 minutes by 1.9 fold. As shown in Fig 1.B, the maximum effect of VEGF on altering redox-state of LMW-PTP occurred between 1 and 5 minutes. We chose the 5 minute time point to examine the effect of the inhibitors. Treatment of HME cells with VEGF caused a 64% increase in LMW-PTP thiol oxidation that was blocked by FeTPPS or NAC (Fig. 4B). In parallel, physiological low levels of peroxynitrite (1 μM) caused a 65% increase in LMW-PTP thiol oxidation that was blocked by FeTPPS or NAC (Fig. 4C).

We next assessed the impact of reductive stress on VEGF-mediated S-glutathionylation of LMW-PTP and cell migration. As shown in Fig. 5A, pretreatment of HME cells with NAC or FeTPPS blunted VEGF induced S-glutathiolation of LMW-PTP that peaked at 5 min. The wound healing assay revealed a 1.8-fold increase in cell migration in response to VEGF when compared to control. Peroxynitrite (1 μM) mimicked VEGF action and caused a 1.5 fold increase in cell migration. Treatment of cells with FeTPPS (2.5 μM) or NAC (1 mM) significantly inhibited the VEGF-induced endothelial migration (Fig 5B-C).

Mild oxidative stress augments and acute oxidative stress inhibits VEGF-mediated cell migration

To elucidate the impact of oxidative stress milieu on the VEGF-mediated angiogenic response, HME cells were stimulated with VEGF (20 ng/ml) in combination with escalating levels of peroxynitrite (0.1 to 0.5 mM). As shown in Fig 7A, VEGF in combination with 0.1 or 0.2 mM peroxynitrite exerted comparable and reversible effects of oxidizing GSH to VEGF alone. In contrast, combining VEGF with peroxynitrite (0.3-0.5 mM) caused an immediate and dramatic oxidation (1-5 minutes) as indicated by oxidation of free GSH levels to 55 and 38% of its basal value that remained blunted to 60-45%, respectively over 30 minute (Fig. 6A). We next evaluated the action of these combinations on cell migration. As shown in (Fig. 6B), mild oxidative stress (0.1-0.2 mM) enhanced VEGF-mediated cell migration. Increasing levels (0.3-0.5 mM) peroxynitrite impaired VEGF's angiogenic action and halted cell migration. To confirm the effect of high level of peroxynitrite on LMW-PTP enzymatic activity, the phosphatase activity of LMW-PTP was assessed against different concentrations of peroxynitrite. Our results showed a concentration dependant inhibition of LMW-PTP activity that reached complete inhibition at 0.5 mM peroxynitrite (Fig 7C).

Acute oxidative stress sustains VEGF-mediated S-glutathionylation of LMW-PTP and FAK activation in HME cells.

To simulate pathological conditions, we evaluated the combination of VEGF with 0.5mM peroxynitrite on LMW-PTP protein modification. A significant and persistent thiol oxidation of LMW-PTP over 30 minutes time course was observed (Fig. 7A). In parallel, VEGF+0.5 mM peroxynitrite induced significant S-glutathionylation of LMW-PTP that persisted over 30 min (Fig. 7B). This effect was associated with complete loss of LMW-PTP phosphorylation for 30

minutes (Fig. 7C). Next, we examined activation of FAK^{Y397}, the auto-phosphorylation site of FAK. The combination of VEGF and peroxynitrite (0.5 mM) induced FAK activation (2.5 fold) at 15 minute that was sustained over 30-60 minutes (Fig 7D).

Discussion

The major findings of the present study can be summarized as follow: 1- VEGF-induced peroxynitrite transiently reduces the endothelial redox-state to facilitate reversible S-glutathionylation and inhibition of LMW-PTP and FAK activation and cell migration. 2- Reductive stress prevents S-glutathionylation of LMW-PTP, FAK activation, and cell migration. 3- While mild oxidative stress augments VEGF-mediated cell migration signal, acute oxidative stress sustains VEGF-mediated FAK activation, S-glutathiolation of LMW-PTP resulting in inhibiting its phosphorylation and cell migration.

We and others have demonstrated a critical role for ROS and peroxynitrite in mediating the VEGF angiogenic signal (Colavitti et al., 2002; Ushio-Fukai et al., 2002; El-Remessy et al., 2007). The potent inhibitory effect of decomposing peroxynitrite using FeTPPS or the thiol donor and GSH-precursor, NAC but not the nitration inhibitor suggested that VEGF can modulate GSH levels and induce cysteine modification to regulate the VEGF signal (Ushio-Fukai et al., 2002; El-Remessy et al., 2007). The mechanism of GSH antioxidant activity occurs via formation of reversible protein-glutathione disulfides, or S-glutathionylation (Shackelford et al., 2005). However, the impact of VEGF on modulating GSH and identifying a redox-sensitive molecular target to regulate angiogenesis remains unexplored. LMW-PTP is a redox-sensitive target that plays a pivotal role in VEGF-mediated cell migration and angiogenesis as it has been shown to regulate activation of VEGFR2 (Huang et al., 1999) as well as FAK (Chiarugi et al.,

2001). In the present study, we assessed the changes of total and reduced GSH as an indicator of the redox-state in response to VEGF in microvascular endothelial cells. Our results showed that VEGF caused an immediate oxidation of cellular free GSH, which is normally maintained at high levels (Okamoto et al., 2001). The oxidation was reversible as evidenced by restoration of reduced GSH within 15-30 minutes. In parallel, VEGF induced an immediate yet reversible thiol oxidation of LMW-PTP (1-5 minutes), which was restored to normal levels after 15 minutes. The activity of LMW-PTP is dually regulated where the two active cysteines (C13 and 18) located in the catalytic pocket must be reduced to allow enzyme phosphorylation and activity (Chiarugi, 2001; Chiarugi et al., 2001; Xing et al., 2007). In agreement, VEGF-induced phosphorylation of LMW-PTP was detected only after 15-30 minutes, a time frame where thiols of LMW-PTP are not oxidized. Our results lend further support to a recent report showing that VEGF increased thiol oxidation and formation of cysteine sulfenic acid (Cys-OH) of the scaffold protein (IQGAP1) to promote endothelial migration (Kaplan et al.).

There is growing evidence that active cysteine sites undergo posttranslational modification by disulphide bond, S-nitrosylation, oxidation to sulfenic acid (Cys-SOH) or S-glutathionylation. The later is perceived to represent a final step for cysteine modification to protect Cys-SOH from further irreversible oxidation to cysteine-sulfinic acid (Cys-SO_2H) and cysteine-sulfonic acid (Cys-SO_3H) (Barrett et al., 1999b). De-glutathionylation of a given protein dictates its physiological relevance (Shelton and Mieyal, 2008) and can be achieved by a reductive GSH/GSSG ratio and catalyzed specifically and efficiently by antioxidant systems-glutaredoxin and thioredoxin (Dalle-Donne et al., 2009). Here, we tested the hypothesis that VEGF-induced oxidation of GSH can stimulate S-glutathionylation of LMW-PTP and decrease its activity. Indeed, VEGF induced strong S-glutathionylation of LMW-PTP thiols (5-10

minutes) that coincided with blunted phosphorylation of LMW-PTP. S-Glutathionylation declined after 15-30 minutes, a time frame when the redox-state free GSH levels went back to base line and the phosphorylation of LMW-PTP was prominent (Fig.1). We next examined the effect of GSH or GSSG on recombinant LMW-PTP phosphatase activity. We used recombinant LMW-PTP for this assay to overcome the technical difficulty to dissect the activity of cellular LMW-PTP from other cellular phosphatases. Oxidized-glutathione GSSG inhibited the LMW-PTP phosphatase activity to one third of its basal value while the reduced-GSH increased LMW-PTP activity 4 fold. These results are in agreement with recent reports showing an inhibitory effect of S-glutathiolation and GSSG on VEGF-mediated eNOS activity (Langston et al., 2007; Chen et al., 2010).

Although S-glutathionylation is usually considered a protein modification in response to oxidative/nitrative stress, it can specifically modulate protein function and hence regulate cell signaling (Dalle-Donne et al., 2009). Reversible S-glutathionylation of PTP-1B and LMW-PTP has been demonstrated in response to superoxide anion and PDGF, respectively (Barrett et al., 1999a; Kanda et al., 2006). To further illustrate the impact of VEGF-induced S-glutathionylation of LMW-PTP, we examined activation of FAK and endothelial cell migration. VEGF or physiologic levels of peroxynitrite activated FAK peaked at 15 minutes. FAK activation was detected in endothelial cells treated with H_2O_2 (Vepa et al., 1999). The maximum association between LMW-PTP with FAK was observed in response to VEGF at 15 minutes, a time point where LMW-PTP was phosphorylated (its thiols are not oxidized or S-glutathionylated). While prior studies support the notion that thiols of LMW-PTP can be oxidized and that its activity is glutathione-dependent (Chiarugi et al., 2001; Kanda et al., 2006; Xing et al., 2007; de Souza

Malaspina et al., 2009), our results are the first to demonstrate S-glutathionylation of LMW-PTP as regulator of VEGF angiogenic signal.

The concept of the "redox window" where achieving a balanced redox-state is essential to allow reparative angiogenesis was recently introduced by W. Chilian group (Yun et al., 2009). Our results demonstrated that reductive stress or positive shifting of the redox-state by treating the cells with FeTPPS, the peroxynitrite decomposition catalyst or NAC, the GSH-precursor blunted VEGF-mediated thiol oxidation of LMW-PTP, S-glutathiolation of LMW-PTP, FAK activation and HME cell migration. These results lend further support to prior findings showing that shifting cellular redox-state by increasing the cellular antioxidant defense could impair the VEGF-mediated tube formation in vitro (Rocic et al., 2007), choroidal neovascularization (Hara et al., 2011) and tumor angiogenesis (Jo et al., 2011).

While oxidative stress can contribute to pathological neovascularization as in tumor angiogenesis and diabetic retinopathy (Ali and El-Remessy, 2009; Tertil et al., 2011), excessive oxidative stress can exert apoptotic effects (Gu et al., 2003; El-Remessy et al., 2005). To better understand the complex interplay of oxidative stress on the VEGF angiogenic signal, we examined its effect in combination with various levels of exogenous peroxynitrite. While combining VEGF with modest levels of peroxynitrite (0.1-0.2 mM) gradually shifted the redox-state to the negative side that was restored to the base line, its combination with peroxynitrite (0.3-0.5 mM) permanently remained negative. In parallel, modest increases of peroxynitrite (0.1-0.2 mM) augmented the VEGF angiogenic effect while excessive levels impaired VEGF angiogenic function. Although, generated using artificial system of oxidative stress, these results demonstrate the impact of local levels of ROS on modifying the outcome of growth factor signaling. In contrast to VEGF-mediated reversible S-glutathionylation, VEGF with 0.5 mM

peroxynitrite induced and sustained S-glutathionylation and thiol oxidation of LMW-PTP. These effects coincided with sustained FAK activation, blunted LMW-PTP phosphorylation. Moreover, peroxynitrite caused a concentration-dependent inhibition of LMW-PTP phosphatase activity that was completely impaired at 0.5 mM. The implication of irreversible S-glutathionylation on cell fate is not fully understood. Recent findings suggest an accumulation of misfolded or unfolded proteins and activation of apoptotic pathways (Uys et al., 2011).

In summary, this is the first report to demonstrate the molecular events by which VEGF-induced peroxynitrite modulates intracellular GSH levels and its downstream S-glutathionylation and phosphorylation of LMW-PTP to regulate angiogenic signal under physiological and pathological conditions. Our findings suggest that modulating the redox-state to achieve a balanced milieu is critical to facilitate the angiogenic signal of VEGF and achieve the therapeutic goal of delivery of pro-angiogenic growth factors to treat ischemic cardiovascular diseases.

Materials and Methods

Cell culture

Primary cultures of human microvascular endothelial cells (HME) from retina and cell culture supplies were purchased from Cell Systems Corporations (Kirkland, WA). Experiments were performed using cells between passages (4-6). Cells were switched to serum free medium 6 hrs prior to stimulation with VEGF 20 ng/ml (R&D, Minneapolis, MN) or peroxynitrite (Calbiochem, Darmstadt, Germany). Peroxynitrite was diluted in NaOH (0.01 N, Sigma, St. Louis, MO). The peroxynitrite decomposition catalyst 5,10,15,20 tetrakis(4 sulfonatophenyl) porphyrinato iron III chloride (FeTPPS, Calbiochem) was used at concentration of 2.5 μM while the general antioxidant, N-acetyl cysteine (NAC, Sigma) was used at concentration of 1 mM.

Oxidized and reduced Glutathione

Reduced glutathione was measured as described previously (Abdelsaid et al.) using the Northwest Life Science kit (Vancouver, WA). Briefly, reduced-GSH was calculated by subtracting the oxidized-GSSG from the total glutathione. For total glutathione, cells were lysed in phosphate buffer (100 mM potassium phosphate and 1 mM EDTA) and were mixed with an equal amount of DTNB (10 mM 5, 5'-dithiobis (2-nitrobenzoic acid) in the presence of glutathione reductase and NADPH producing a yellow color measured at 412 nm. To detect GSSG, samples were treated with 10 mM 2-vinylpyridine (Sigma) in ethanol to sequester all the reduced GSH then measured using the same protocol of the total glutathione.

LMW-PTP phosphatase activity

The activity was measured by a CycLex fluorometric kit from MBL (Woburn, MA). Briefly 3-o-methylfluorescein phosphate was used as a fluorescence substrate for the LMW-PTP. The reactions were incubated for 15 min at room temperature then the fluorescence intensity was

measured using a microtiter plate fluorometer with excitation at 482-502 nm and emission at 510-540 nm. Various concentrations of peroxynitrite (Calbiochem) were prepared by dilution in NaOH (0.01 N, Sigma). Oxidized-glutathione (GSSG, Fisher, Fair Lawn, NJ) and reduced-glutathione (GSH, sigma) were prepared in the assay buffer and used at a concentration of 10 mM.

Cell migration assay

The wound healing assay was performed as described previously (El-Remessy et al., 2007). Briefly, HME cells were grown to confluence and switched to serum-free medium 6 hrs prior to the experiment. The monolayer was wounded with a single sterile cell scraper of fixed diameter. Images of wounded areas were taken immediately and after 18 hours. Cell migration was calculated by measuring migration distance normalized to initial distance of wounding using an AxioObserver Zeiss Microscope (Germany) software and expressed as a percentage of untreated control cells.

Immunoprecipitation and Western Blot analysis

Isolated retinas and HME cells were harvested after various treatments and lysed in modified RIPA buffer purchased from Millipore (Billerica, MA) 30 min on ice. Insoluble material was removed by centrifugation at 14,000 *g* at 4°C for 30 min. Fifty μg of total protein was boiled in 6x Laemmli sample buffer, separated on a 10–12% SDS-polyacrylamide gel by electrophoresis, transferred to nitrocellulose, and reacted with a specific antibody. For immunoprecipitation, cell lysates (200 μg) were immunoprecipitated with FAK primary antibody (5 μg) and A/G agarose beads (Santa Cruz, CA) overnight. The precipitated proteins were analyzed by SDS-PAGE and blotted with anti-PY20 or FAK antibody for equal loading. The primary antibodies were purchased as follow: FAK (Millipore, Temecula, CA), pFAK (Thermo, Rockford, IL), LMW-

PTP (Exalpha, Maynard, MA), anti-fluorescein (Invitrogen, Carlsbad, CA), anti-GSH (Virogen, Boston) and phosphotyrosine PY-20 (Santa Cruz, Santa Cruz, CA). Primary antibodies were detected using a horseradish peroxidase-conjugated antibody and enhanced chemiluminescence (GE Healthcare, NJ).The films were scanned, and band intensity was quantified using densitometry software (Alpha Innotech).

Determination of LMW-PTP thiol oxidation and S-glutathionylation.

Oxidized thiols of LMW-PTP were determined using a previously described protocol (Chiarugi et al., 2003). Cellular or retinal lysates (200 μg) were labeled with fluorescein-tagged 5 iodo-acetamide (5-IAM, Sigma) followed by immunoprecipitation with LMW-PTP (5 μg) antibody and A/G agarose beads (Santa Cruz, CA) overnight. The beads were washed, analyzed by SDS-PAGE and blotted with anti-fluorescein or anti-LMW-PTP to check equal loading. S-glutathionylation was detected as described previously (Chen et al., 2007) with minor modification. Immunoprecipitated LMW-PTP were incubated with or without DTT (100 mM) at 70 °C for 10 minutes, and then immediately loaded onto a 4–20% Tris-glycine polyacrylamide gradient gel (BioRad, Hercules, CA) as described above. The membrane was blotted with anti-GSH or anti-LMW-PTP to check equal loading. For LMW-PTP phosphorylation, cell lysates were immunoprecipitated with LMW-PTP antibody as described above and the membrane was blotted with anti-PY20 or anti-LMW-PTP to check equal loading.

Data Analysis

The results were expressed as mean ± SE. Differences among experimental groups were evaluated by analysis of variance, and the significance of difference between groups was assessed by the post-hoc test (Fisher's PLSD) when indicated. Significance was defined as $P < 0.05$.

Acknowledgment: Authors are grateful for technical expertise of Ms. Suraporn Matragoon and Ms. Bindu A Pillai.

Source of research support: American Heart Association pre-doctoral fellowship award#10PRE3660004 To MAA, AHA Scientist Development Grant to ABE and Career Development Award from Juvenile Diabetes Research Foundation (4-2008-149) to ABE.

Author Disclosure Statement

We do not have any commercial associations that might create a conflict of interest in connection with our manuscripts.

References

Abdelsaid, M. A., Pillai, B. A., Matragoon, S., Prakash, R., Al-Shabrawey, M. and El-Remessy, A. B. (2010). Early intervention of tyrosine nitration prevents vaso-obliteration and neovascularization in ischemic retinopathy. *J Pharmacol Exp Ther* 332, 125-134.

Ali, T. K. and El-Remessy, A. B. (2009). Diabetic retinopathy: current management and experimental therapeutic targets. *Pharmacotherapy* 29, 182-192.

Barrett, W. C., DeGnore, J. P., Keng, Y. F., Zhang, Z. Y., Yim, M. B. and Chock, P. B. (1999a). Roles of superoxide radical anion in signal transduction mediated by reversible regulation of protein-tyrosine phosphatase 1B. *J Biol Chem* 274, 34543-34546.

Barrett, W. C., DeGnore, J. P., Konig, S., Fales, H. M., Keng, Y. F., Zhang, Z. Y., Yim, M. B. and Chock, P. B. (1999b). Regulation of PTP1B via glutathionylation of the active site cysteine 215. *Biochemistry* 38, 6699-6705.

Cao, Y. Angiogenesis: What can it offer for future medicine? (2010) *Exp Cell Res* 316, 1304-1308.

Chen, C. A., Wang, T. Y., Varadharaj, S., Reyes, L. A., Hemann, C., Talukder, M. A., Chen, Y. R., Druhan, L. J. and Zweier, J. L. (2010). S-glutathionylation uncouples eNOS and regulates its cellular and vascular function. *Nature* 468, 1115-1118.

Chen, C. L., Zhang, L., Yeh, A., Chen, C. A., Green-Church, K. B., Zweier, J. L. and Chen, Y. R. (2007). Site-specific S-glutathiolation of mitochondrial NADH ubiquinone reductase. *Biochemistry* 46, 5754-5765.

Chiarugi, P. (2001). The redox regulation of LMW-PTP during cell proliferation or growth inhibition. *IUBMB Life* 52, 55-59.

Chiarugi, P., Fiaschi, T., Taddei, M. L., Talini, D., Giannoni, E., Raugei, G. and Ramponi, G. (2001). Two vicinal cysteines confer a peculiar redox regulation to low molecular weight protein tyrosine phosphatase in response to platelet-derived growth factor receptor stimulation. *J Biol Chem* 276, 33478-33487.

Chiarugi, P., Pani, G., Giannoni, E., Taddei, L., Colavitti, R., Raugei, G., Symons, M., Borrello, S., Galeotti, T. and Ramponi, G. (2003). Reactive oxygen species as essential mediators of cell adhesion: the oxidative inhibition of a FAK tyrosine phosphatase is required for cell adhesion. *J Cell Biol* 161, 933-944.

Chinta, S. J. and Andersen, J. K. (2011). Nitrosylation and nitration of mitochondrial complex I in Parkinson's disease. *Free Radic Res* 45, 53-58.

Chua, R. A. and Arbiser, J. L. (2009). The role of angiogenesis in the pathogenesis of psoriasis. *Autoimmunity* 42, 574-579.

Clavreul, N., Adachi, T., Pimental, D. R., Ido, Y., Schoneich, C. and Cohen, R. A. (2006). S-glutathiolation by peroxynitrite of p21ras at cysteine-118 mediates its direct activation and downstream signaling in endothelial cells. *FASEB J* 20, 518-520.

Colavitti, R. and Finkel, T. (2005). Reactive oxygen species as mediators of cellular senescence. *IUBMB Life* 57, 277-281.

Colavitti, R., Pani, G., Bedogni, B., Anzevino, R., Borrello, S., Waltenberger, J. and Galeotti, T. (2002). Reactive oxygen species as downstream mediators of angiogenic signaling by vascular endothelial growth factor receptor-2/KDR. *J Biol Chem* 277, 3101-3108.

Dalle-Donne, I., Rossi, R., Colombo, G., Giustarini, D. and Milzani, A. (2009). Protein S-glutathionylation: a regulatory device from bacteria to humans. *Trends Biochem Sci* 34, 85-96.

de Souza Malaspina, T. S., Zambuzzi, W. F., dos Santos, C. X., Campanelli, A. P., Laurindo, F. R., Sogayar, M. C. and Granjeiro, J. M. (2009). A possible mechanism of low molecular weight protein tyrosine phosphatase (LMW-PTP) activity modulation by glutathione action during human osteoblast differentiation. *Arch Oral Biol* 54, 642-650.

Dremina, E. S., Sharov, V. S., Davies, M. J. and Schoneich, C. (2007). Oxidation and inactivation of SERCA by selective reaction of cysteine residues with amino acid peroxides. *Chem Res Toxicol* 20, 1462-1469.

El-Remessy, A. B., Bartoli, M., Platt, D. H., Fulton, D. and Caldwell, R. B. (2005). Oxidative stress inactivates VEGF survival signaling in retinal endothelial cells via PI 3-kinase tyrosine nitration. *J Cell Sci* 118, 243-252.

El-Remessy, A. B., Al-Shabrawey, M., Platt, D. H., Bartoli, M., Behzadian, M. A., Ghaly, N., Tsai, N., Motamed, K. and Caldwell, R. B. (2007). Peroxynitrite mediates VEGF's angiogenic signal and function via a nitration-independent mechanism in endothelial cells. *FASEB J* 21, 2528-2539.

Giannoni, E., Raugei, G., Chiarugi, P. and Ramponi, G. (2006). A novel redox-based switch: LMW-PTP oxidation enhances Grb2 binding and leads to ERK activation. *Biochem Biophys Res Commun* 348, 367-373.

Gu, X., El-Remessy, A. B., Brooks, S. E., Al-Shabrawey, M., Tsai, N. T. and Caldwell, R. B. (2003). Hyperoxia induces retinal vascular endothelial cell apoptosis through formation of peroxynitrite. *Am J Physiol Cell Physiol* 285, C546-554.

Hara, R., Inomata, Y., Kawaji, T., Sagara, N., Inatani, M., Fukushima, M. and Tanihara, H. (2011). Suppression of choroidal neovascularization by N-acetyl-cysteine in mice. *Curr Eye Res* 35, 1012-1020.

Huang, L., Sankar, S., Lin, C., Kontos, C. D., Schroff, A. D., Cha, E. H., Feng, S. M., Li, S. F., Yu, Z., Van Etten, R. L. et al. (1999). HCPTPA, a protein tyrosine phosphatase that regulates vascular endothelial growth factor receptor-mediated signal transduction and biological activity. *J Biol Chem* 274, 38183-38188.

Jo, M., Nishikawa, T., Nakajima, T., Okada, Y., Yamaguchi, K., Mitsuyoshi, H., Yasui, K., Minami, M., Iwai, M., Kagawa, K. et al. (2011). Oxidative stress is closely associated with tumor angiogenesis of hepatocellular carcinoma. *J Gastroenterol* 46, 809-821.

Kanda, M., Ihara, Y., Murata, H., Urata, Y., Kono, T., Yodoi, J., Seto, S., Yano, K. and Kondo, T. (2006). Glutaredoxin modulates platelet-derived growth factor-dependent cell signaling by regulating the redox status of low molecular weight protein-tyrosine phosphatase. *J Biol Chem* 281, 28518-28528.

Kaplan, N., Urao, N., Furuta, E., Kim, S. J., Razvi, M., Nakamura, Y., McKinney, R. D., Poole, L. B., Fukai, T. and Ushio-Fukai, M. Localized Cysteine Sulfenic Acid Formation by Vascular Endothelial Growth Factor: Role in Endothelial Cell Migration and Angiogenesis. *Free Radic Res*. 2011 Oct;45(10):1124-35.

Langston, W., Chidlow, J. H., Jr., Booth, B. A., Barlow, S. C., Lefer, D. J., Patel, R. P. and Kevil, C. G. (2007). Regulation of endothelial glutathione by ICAM-1 governs VEGF-A-mediated eNOS activity and angiogenesis. *Free Radic Biol Med* 42, 720-729.

Li, S. and Hua, Z. C. (2008). FAK expression regulation and therapeutic potential. *Adv Cancer Res* 101, 45-61.

Liaudet, L., Vassalli, G. and Pacher, P. (2009). Role of peroxynitrite in the redox regulation of cell signal transduction pathways. *Front Biosci* 14, 4809-4814.

Okamoto, T., Akaike, T., Sawa, T., Miyamoto, Y., van der Vliet, A. and Maeda, H. (2001). Activation of matrix metalloproteinases by peroxynitrite-induced protein S-glutathiolation via disulfide S-oxide formation. *J Biol Chem* 276, 29596-29602.

Rahman, I. and MacNee, W. (2000). Regulation of redox glutathione levels and gene transcription in lung inflammation: therapeutic approaches. *Free Radic Biol Med* 28, 1405-1420.

Raugei, G., Ramponi, G. and Chiarugi, P. (2002). Low molecular weight protein tyrosine phosphatases: small, but smart. *Cell Mol Life Sci* 59, 941-949.

Rocic, P., Kolz, C., Reed, R., Potter, B. and Chilian, W. M. (2007). Optimal reactive oxygen species concentration and p38 MAP kinase are required for coronary collateral growth. *Am J Physiol Heart Circ Physiol* 292, H2729-2736.

Sethuraman, M., Clavreul, N., Huang, H., McComb, M. E., Costello, C. E. and Cohen, R. A. (2007). Quantification of oxidative posttranslational modifications of cysteine thiols of p21ras associated with redox modulation of activity using isotope-coded affinity tags and mass spectrometry. *Free Radic Biol Med* 42, 823-829.

Shackelford, R. E., Heinloth, A. N., Heard, S. C. and Paules, R. S. (2005). Cellular and molecular targets of protein S-glutathiolation. *Antioxid Redox Signal* 7, 940-950.

Shelton, M. D. and Mieyal, J. J. (2008). Regulation by reversible S-glutathionylation: molecular targets implicated in inflammatory diseases. *Mol Cells* 25, 332-346.

Shimizu, H., Toyama, O., Shiota, M., Kim-Mitsuyama, S. and Miyazaki, H. (2005). Protein tyrosine phosphatase LMW-PTP exhibits distinct roles between vascular endothelial and smooth muscle cells. *J Recept Signal Transduct Res* 25, 19-33.

Tertil, M., Jozkowicz, A. and Dulak, J. (2011). Oxidative stress in tumor angiogenesis-therapeutic targets. *Curr Pharm Des* 16, 3877-3894.

Tomar, A. and Schlaepfer, D. D. (2009). Focal adhesion kinase: switching between GAPs and GEFs in the regulation of cell motility. *Curr Opin Cell Biol* 21, 676-683.

Ushio-Fukai, M. (2006). Redox signaling in angiogenesis: role of NADPH oxidase. *Cardiovasc Res* 71, 226-235.

Ushio-Fukai, M. (2007). VEGF signaling through NADPH oxidase-derived ROS. *Antioxid Redox Signal* 9, 731-739.

Ushio-Fukai, M., Tang, Y., Fukai, T., Dikalov, S. I., Ma, Y., Fujimoto, M., Quinn, M. T., Pagano, P. J., Johnson, C. and Alexander, R. W. (2002). Novel role of gp91(phox)-containing NAD(P)H oxidase in vascular endothelial growth factor-induced signaling and angiogenesis. *Circ Res* 91, 1160-1167.

Uys, J. D., Xiong, Y. and Townsend, D. M. (2011). Nitrosative stress-induced S-glutathionylation of protein disulfide isomerase. *Methods Enzymol* 490, 321-332.

van der Laan, A. M., Piek, J. J. and van Royen, N. (2009). Targeting angiogenesis to restore the microcirculation after reperfused MI. *Nat Rev Cardiol* 6, 515-523.

Vepa, S., Scribner, W. M., Parinandi, N. L., English, D., Garcia, J. G. and Natarajan, V. (1999). Hydrogen peroxide stimulates tyrosine phosphorylation of focal adhesion kinase in vascular endothelial cells. *Am J Physiol* 277, L150-158.

Wang, W. Q., Sun, J. P. and Zhang, Z. Y. (2003). An overview of the protein tyrosine phosphatase superfamily. *Curr Top Med Chem* 3, 739-748.

Xing, K., Raza, A., Lofgren, S., Fernando, M. R., Ho, Y. S. and Lou, M. F. (2007). Low molecular weight protein tyrosine phosphatase (LMW-PTP) and its possible physiological functions of redox signaling in the eye lens. *Biochim Biophys Acta* 1774, 545-555.

Xiong, Y., Mahmood, A. and Chopp, M. Angiogenesis, neurogenesis and brain recovery of function following injury. *Curr Opin Investig Drugs* 11, 298-308.

Yun, J., Rocic, P., Pung, Y. F., Belmadani, S., Carrao, A. C., Ohanyan, V. and Chilian, W. M. (2009). Redox-dependent mechanisms in coronary collateral growth: the "redox window" hypothesis. *Antioxid Redox Signal* 11, 1961-1974.

Fig. 4.1.

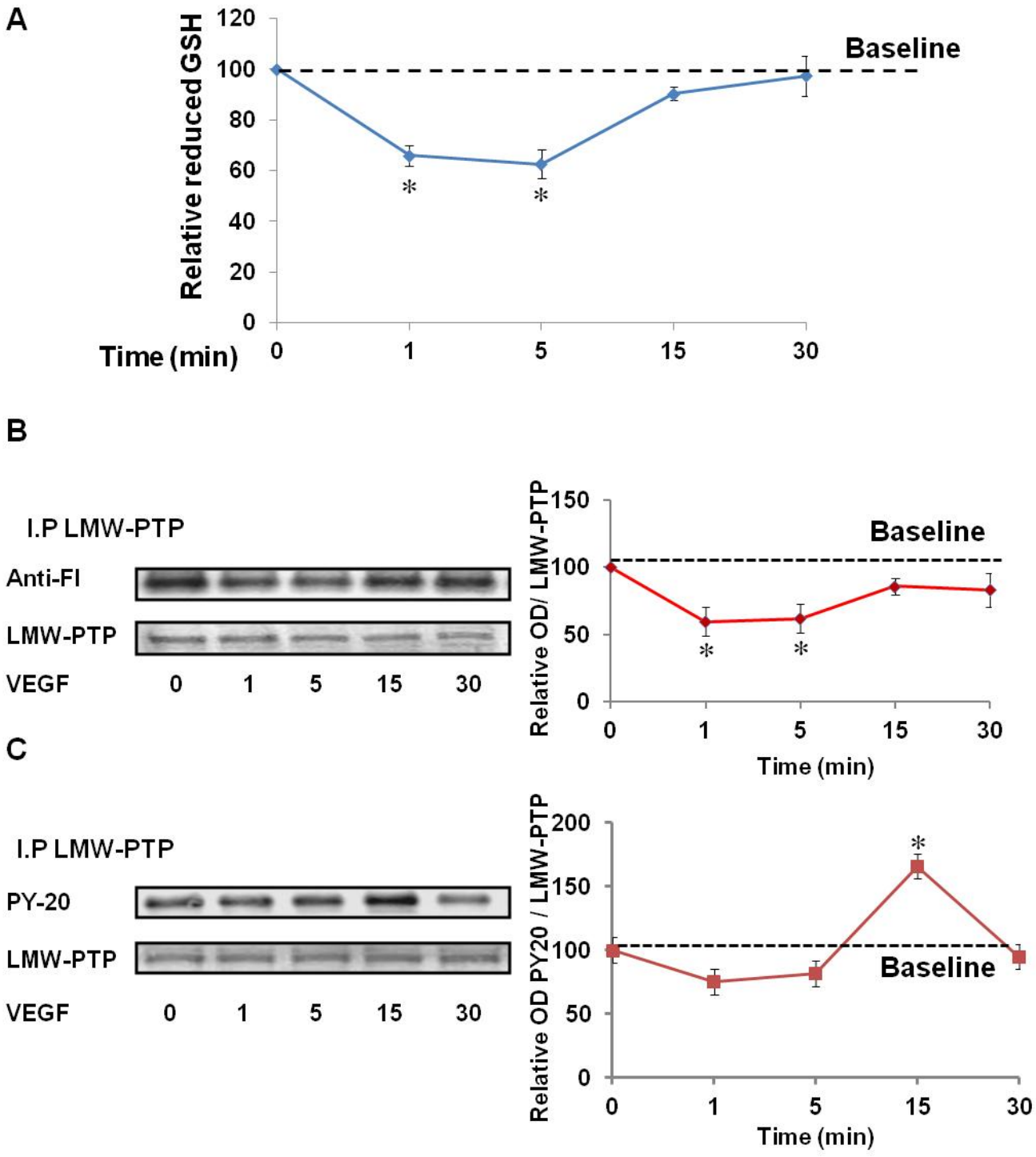
A
Relative reduced GSH
120
100
80
60
40
20
0
Baseline
*
*
Time (min)
0
1
5
15
30
B
I.P LMW-PTP
Anti-FI
LMW-PTP
VEGF
0
1
5
15
30
Relative OD/ LMW-PTP
150
100
50
0
Baseline
*
*
Time (min)
C
I.P LMW-PTP
PY-20
LMW-PTP
VEGF
0
1
5
15
30
Relative OD PY20 / LMW-PTP
200
150
100
50
0
*
Baseline
Time (min)

Fig 4.1 VEGF causes reversible negative-shift in cellular redox state and LMW-PTP in HME cells.

A. Relative levels of free GSH detected by DTNB. VEGF (20 ng/ml) caused transient decrease in GSH levels that was restored after 15 minutes. **B.** Thiol oxidation of LMW-PTP detected by immunoprecipitation of 5-IAM labeled lysate with anti-LMW-PTP and blotted with anti-fluorescein (anti-Fl). **C.** Phosphorylation of LMW-PTP was assessed by immunoprecipitation of LMW-PTP and blotted with anti-PY20. (n=4-6, *P<0.05 versus Zero time).

Fig. 4.2.

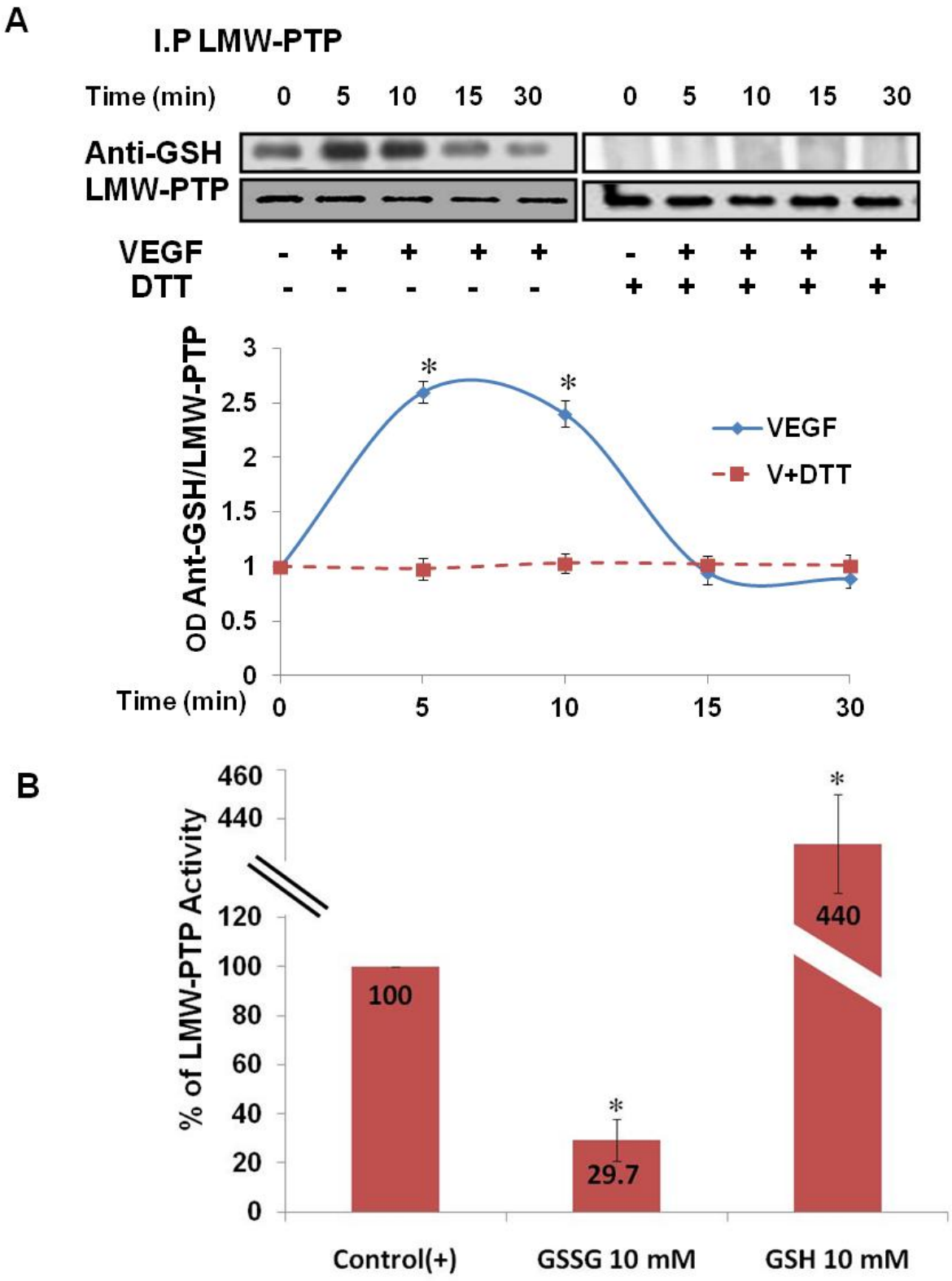
A
I.P LMW-PTP
Time (min) 0 5 10 15 30 0 5 10 15 30
Anti-GSH
LMW-PTP
VEGF - + + + + - + + + +
DTT - - - - - + + + + +
OD Ant-GSH/LMW-PTP
3
2.5
2
1.5
1
0.5
0
Time (min) 0 5 10 15 30
VEGF
V+DTT
B
% of LMW-PTP Activity
460
440
120
100
80
60
40
20
0
100
29.7
440
Control(+)
GSSG 10 mM
GSH 10 mM

Fig. 4.2. VEGF causes S-glutathionylation and inhibition of LMW-PTP activity in HME cells.

A. Cellular lysate was immunoprecipitated with LMW-PTP, incubated with or without DTT (100 mM) at 70^0C for 10 minutes then blotted with anti-GSH. VEGF induced significant and reversible S-glutathiolation of LMW-PTP at 5-10 min that was blunted after 15 min. (n=4, *P<0.05 versus Zero time). **B.** The LMW-PTP enzyme activity was tested against 10 mM of GSSG or GSH and compared to control. While GSSG caused significant decreases (70%) in the activity of LMW-PTP, GSH increased the enzyme activity to 4 times its basal value. (n=4, *P<0.05 versus control).

Fig. 4.3.

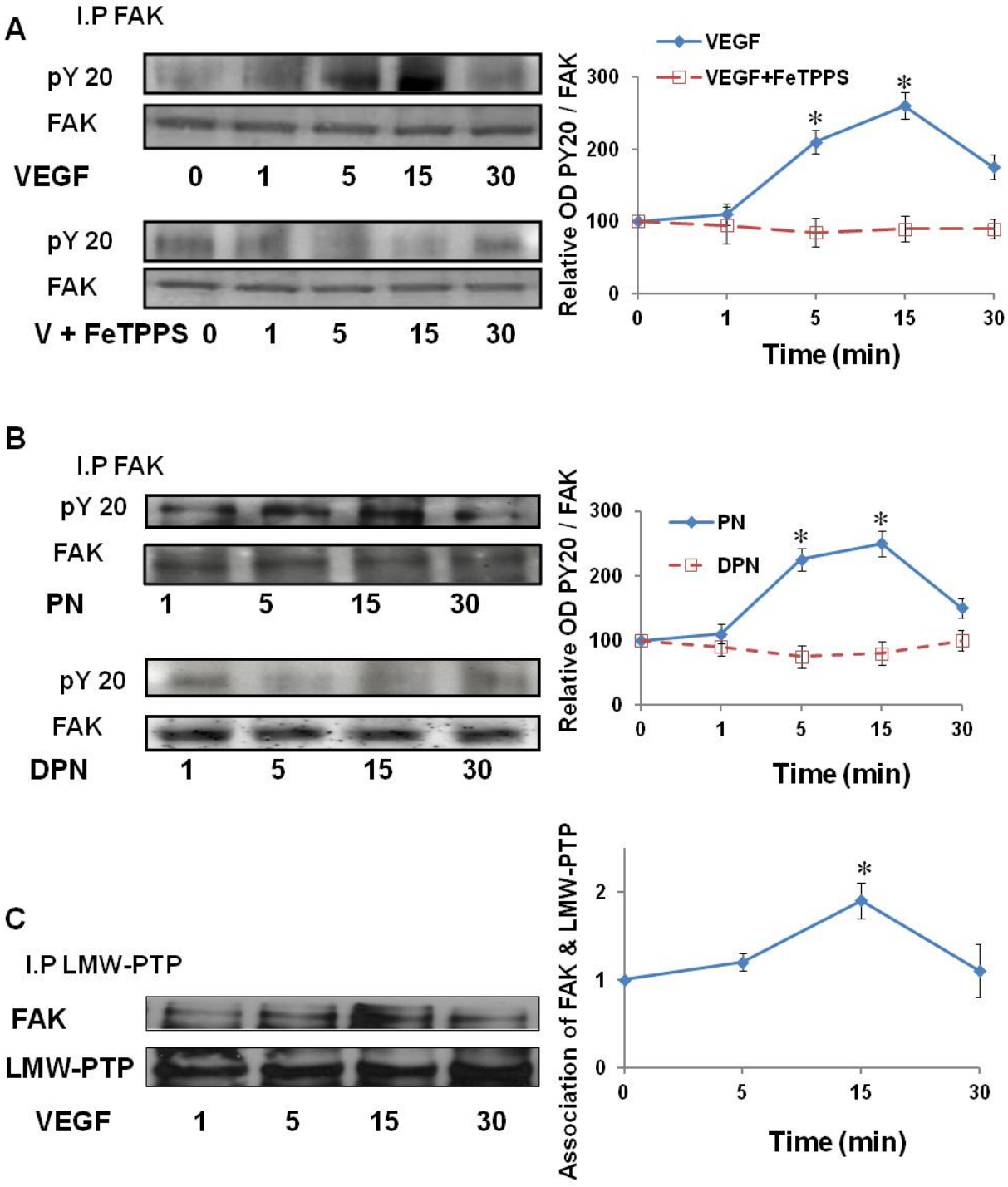
A
I.P FAK
pY 20
FAK
VEGF 0 1 5 15 30
pY 20
FAK
V + FeTPPS 0 1 5 15 30
VEGF
VEGF+FeTPPS
Relative OD PY20 / FAK
300
200
100
0
0 1 5 15 30
Time (min)
B
I.P FAK
pY 20
FAK
PN 1 5 15 30
pY 20
FAK
DPN 1 5 15 30
PN
DPN
Relative OD PY20 / FAK
300
200
100
0
0 1 5 15 30
Time (min)
C
I.P LMW-PTP
FAK
LMW-PTP
VEGF 1 5 15 30
Association of FAK & LMW-PTP
2
1
0
0 5 15 30
Time (min)

Fig. 4.3. VEGF-induced peroxynitrite stimulates FAK activation and association between LMW-PTP and FAK in HME cells.

A. Total FAK phosphorylation was assessed by immunoprecipitation of FAK and immunoblotting with anti-PY20. VEGF (20 ng/ml) caused a time-dependant FAK tyrosine phosphorylation that peaked at 15 min and was completely blocked with peroxynitrite decomposition catalyst FeTPPS (2.5 μM). **B.** Physiological levels of peroxynitrite (PN, 1 μM) but not the decomposed peroxynitrite (DPN), induced FAK phosphorylation that peaked at 15 min. **C.** VEGF stimulates association between LMW-PTP and FAK (1.9 fold) at 15 minutes. Cellular lysate was immunoprecipitated with anti-LMW-PTP and blotted with anti-FAK. (n=4, *$P<0.05$ versus Zero time).

Fig. 4.4.

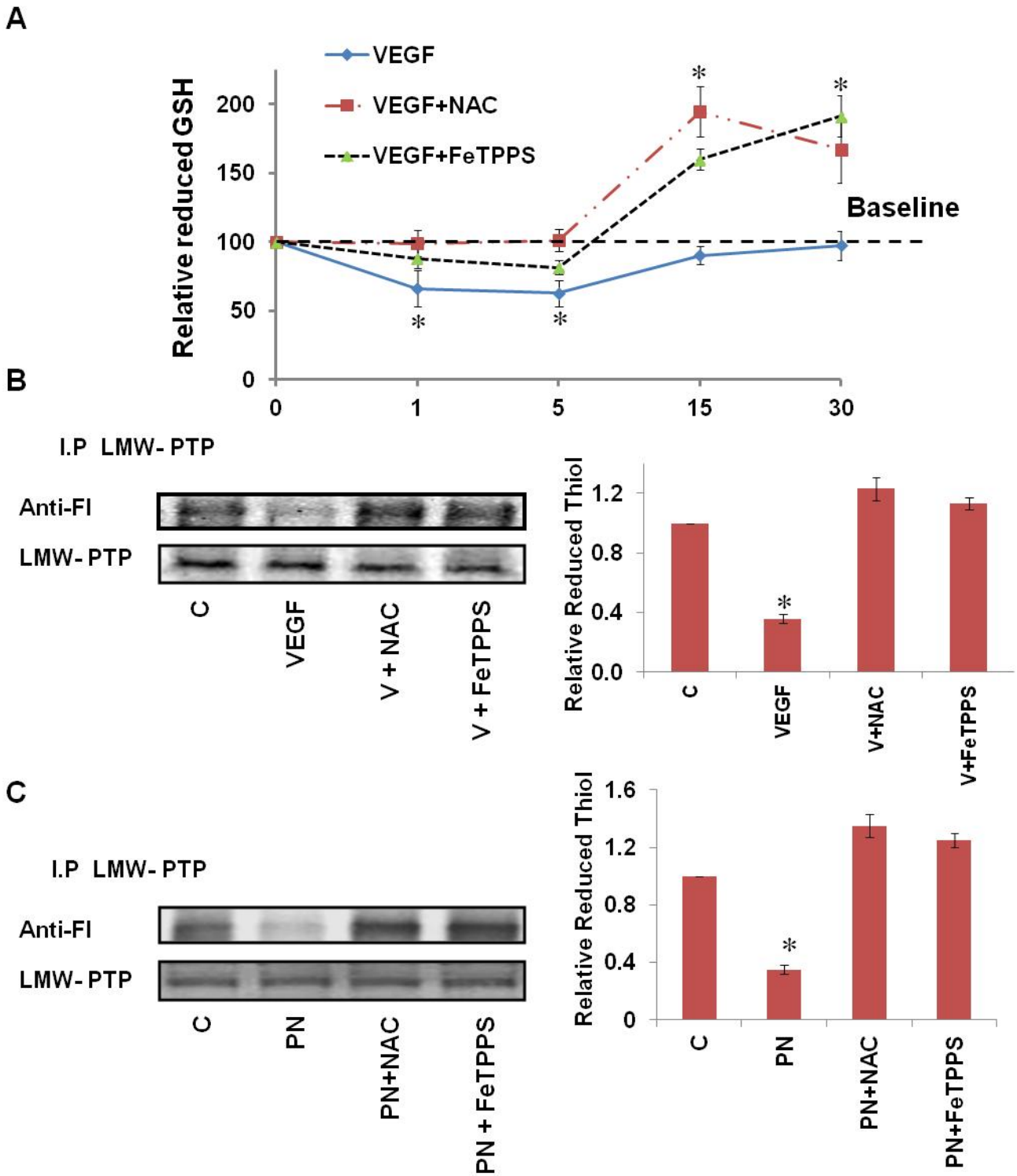
A
VEGF
VEGF+NAC
VEGF+FeTPPS
Relative reduced GSH
200
150
100
50
0
Baseline
0
1
5
15
30
*
B
I.P LMW- PTP
Anti-Fl
LMW- PTP
C
VEGF
V + NAC
V + FeTPPS
Relative Reduced Thiol
1.2
0.8
0.4
0.0
C
VEGF
V+NAC
V+FeTPPS
C
I.P LMW- PTP
Anti-Fl
LMW- PTP
C
PN
PN+NAC
PN + FeTPPS
Relative Reduced Thiol
1.6
1.2
0.8
0.4
0
C
PN
PN+NAC
PN+FeTPPS

Fig. 4.4. Reductive stress inhibits VEGF and PN-mediated LMW-PTP thiol oxidation.

A. Graph showing statistical analysis for the relative levels of free GSH detected by DTNB. VEGF (solid line) induced reversible oxidation of GSH that was restored back after 15-30 minutes. Treatment with the peroxynitrite decomposition catalyst FeTPPS (2.5 μM, dotted) or the GSH-precursor NAC (1mM, dash-dotted) blunted immediate VEGF effect and significantly shifted redox-state to the positive side within 15-30 minutes (n=4-6, *P<0.05 versus Zero time). **B-C**. Thiol oxidation of LMW-PTP was detected in 5-IAM labeled cell lysate by immunoprecipitation of LMW-PTP and blotting with anti-fluorescein (anti-Fl). NAC and FeTPPS prevented VEGF-mediated LMW-PTP thiol oxidation (B) as well as peroxynitrite (PN, 1 μM)-mediated LMW-PTP thiol oxidation. (n=4, *P<0.05 versus control).

Fig. 4.5.

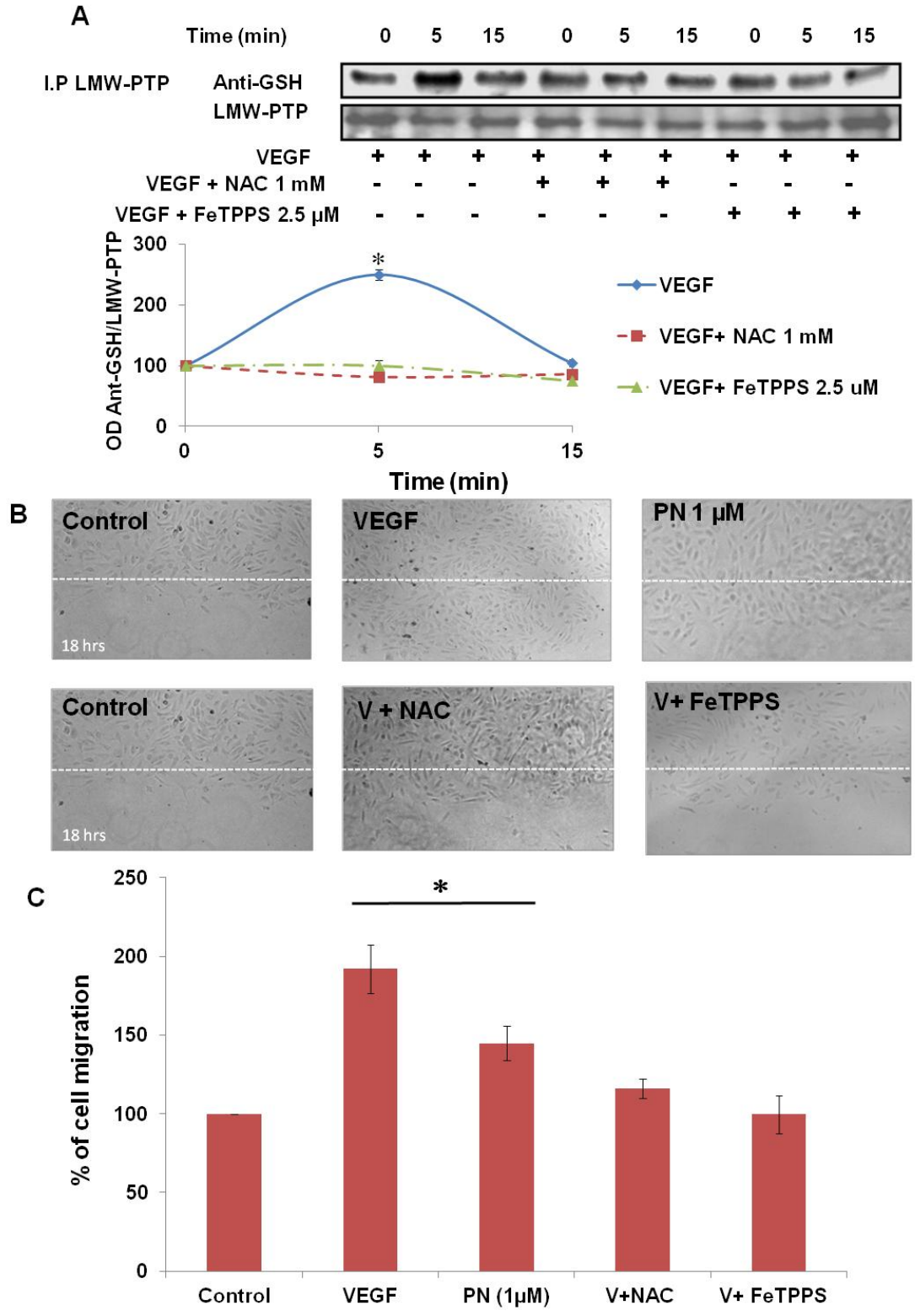
A
Time (min)
0 5 15 0 5 15 0 5 15
I.P LMW-PTP
Anti-GSH
LMW-PTP
VEGF + + + + + + + + +
VEGF + NAC 1 mM - - - + + + - - -
VEGF + FeTPPS 2.5 µM - - - - - - + + +
OD Ant-GSH/LMW-PTP
300
200
100
0
*
0
5
15
Time (min)
VEGF
VEGF+ NAC 1 mM
VEGF+ FeTPPS 2.5 uM
B
Control
18 hrs
VEGF
PN 1 µM
Control
18 hrs
V + NAC
V+ FeTPPS
C
250
200
150
100
50
0
% of cell migration
*
Control
VEGF
PN (1µM)
V+NAC
V+ FeTPPS

Fig. 4.5. Reductive stress inhibits VEGF-induced S-glutathionylation of LMW-PTP and HME cell migration. A.

Pretreatment of HME cells with NAC (1 mM) or FeTPPS blunted VEGF-mediated S-glutathionylation of LMW-PTP that peaked at 5 minutes. **B.** Representative micrographs for wounded HME cells after 18 hours of various treatments. **C.** Peroxynitrite (PN, 1 μM) mimicked VEGF in stimulating cell migration. The effects of VEGF were blunted by modulating redox-state using FeTPPS (2.5 μM) or NAC (1 mM). (n=4, *P<0.05 versus control).

Fig. 4.6.

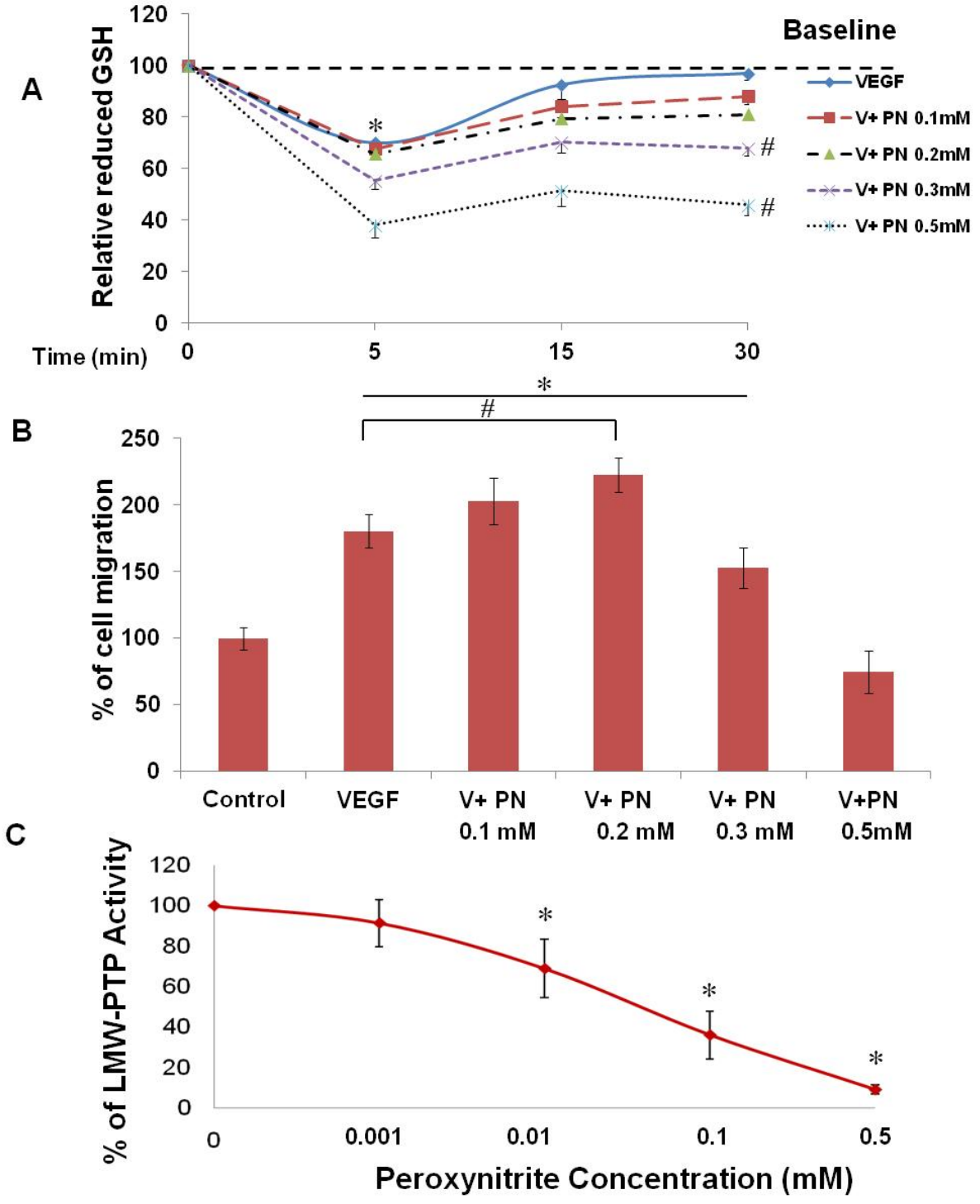
A
Relative reduced GSH
120
100
80
60
40
20
0
Time (min)
0
5
15
30
Baseline
VEGF
V+ PN 0.1mM
V+ PN 0.2mM
V+ PN 0.3mM
V+ PN 0.5mM
*
#
#
B
% of cell migration
250
200
150
100
50
0
Control
VEGF
V+ PN 0.1 mM
V+ PN 0.2 mM
V+ PN 0.3 mM
V+PN 0.5mM
*
#
C
% of LMW-PTP Activity
120
100
80
60
40
20
0
0
0.001
0.01
0.1
0.5
Peroxynitrite Concentration (mM)
*
*
*

Fig. 4.6. Mild oxidative stress augments and acute oxidative stress inhibits VEGF-mediated cell migration.

A. Graph showing the statistical analysis for the relative free GSH levels in response to VEGF (20 ng/ml) with escalating levels of peroxynitrite (0.1– 0.5 mM). Combination of VEGF and peroxynitrite (PN, 0.1-0.2mM) produced comparable pattern to VEGF alone. In contrast, combination of VEGF with peroxynitrite (PN, 0.3-0.5 mM) shifted redox-state to the negative side over 30 minutes. (n=4-6, *P<0.05 versus VEGF) B. Wound healing assay showing while combination of VEGF with mild oxidative stress (PN, 0.1-0.2 mM) enhanced VEGF-mediated cell migration, high oxidative stress (0.3-0.5 mM) impaired VEGF angiogenic action. (n=4, *P<0.05 versus Zero, # P<0.05 versus corresponding VEGF points). C. Peroxynitrite causes concentration-dependant reduction in recombinant LMW-PTP enzyme activity that reached maximum inhibition at 0.5 mM of peroxynitrite. (n=4-5, *P<0.05 versus control).

Fig. 4.7.

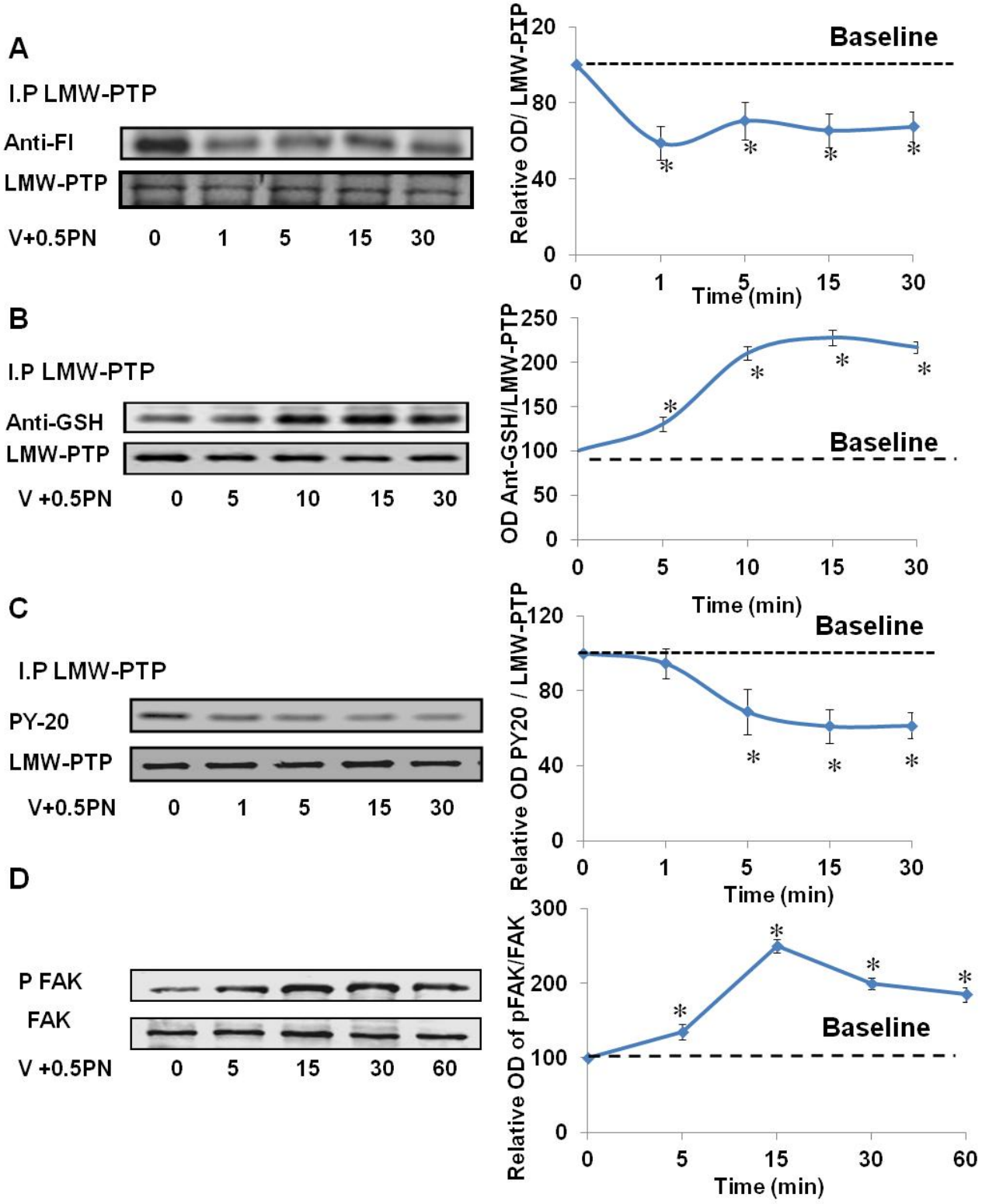
A
I.P LMW-PTP
Anti-Fl
LMW-PTP
V+0.5PN 0 1 5 15 30
Relative OD/ LMW-PTP
Baseline
Time (min)
B
I.P LMW-PTP
Anti-GSH
LMW-PTP
V +0.5PN 0 5 10 15 30
OD Ant-GSH/LMW-PTP
Baseline
Time (min)
C
I.P LMW-PTP
PY-20
LMW-PTP
V+0.5PN 0 1 5 15 30
Relative OD PY20 / LMW-PTP
Baseline
Time (min)
D
P FAK
FAK
V +0.5PN 0 5 15 30 60
Relative OD of pFAK/FAK
Baseline
Time (min)

Fig. 4.7. Acute oxidative stress sustains VEGF-mediated S-glutathionylation of LMW-PTP and FAK activation in HME cells.

Thiol oxidation and S-glutathionylation of LMW-PTP were assessed as described in method section. A. Combination of VEGF with 0.5 mM peroxynitrite induced immediate thiol oxidation of LMW-PTP (40%) that persisted over 30 minutes. B. Combination of VEGF with 0.5 mM peroxynitrite induced S-glutathionylation (2-fold) of LMW-PTP that persisted over 30 minutes. C. Combination of VEGF with 0.5mM peroxynitrite significantly blunted LMW-PTP phosphorylation to 50% of its basal levels over 30 minutes. D. A Combination of VEGF with 0.5 mM peroxynitrite induced FAK-Y397 activation that persisted over 60 minutes. (n=4, *P<0.05 versus Zero time).

Fig. 4.8.

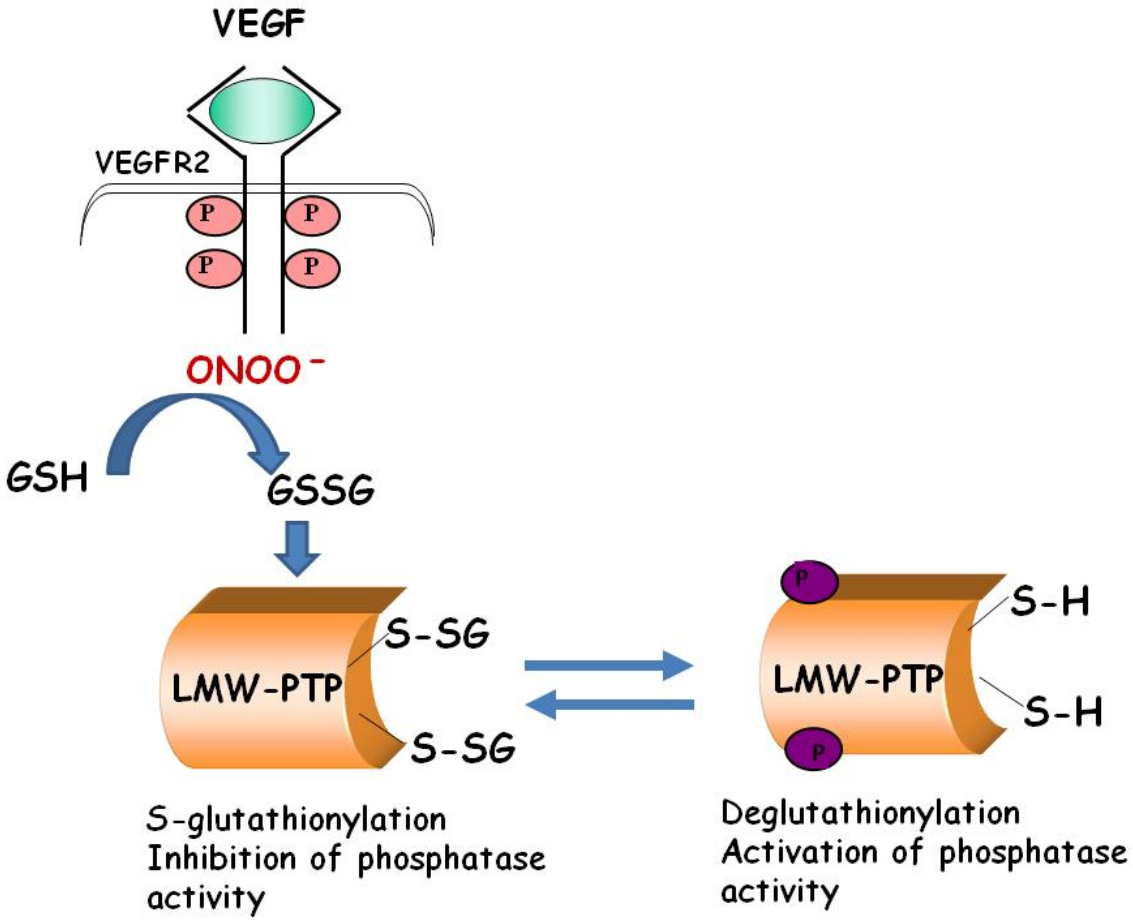

Fig. 4.8. Schematic representation of the proposed mechanism of VEGF-mediated s-glutathionylation of LMW-PTP and regulation of angiogenic response.

CHAPTER 5

DISCUSSION

The main findings of the project can be summarized as follows: 1) Shifting redox-state to an excessive oxidative stress impaired VEGF's downstream survival signal via tyrosine nitration. 2) Shifting the redox-state to a reductive state impaired the VEGF-mediated receptor activation and angiogenic signal. 3) VEGF requires a delicate balance of cellular redox-state to transduce its signal. Our studies identified a novel molecular switch, LMW-PTP to regulate the VEGF signal at the VEGFR2 receptor level and downstream at the FAK level suggesting that targeting LMW-PTP expression and activity can modulate angiogenesis.

Angiogenesis is the formation of new blood vessels from existing ones. Reparative angiogenesis plays a pivotal role in wound healing and as a body defense mechanism [1-5]. In contrast, pathological angiogenesis is detrimental in tumor growth, diabetic retinopathy and atherosclerosis (reviewed in [6-8]). Increases in the levels of vascular endothelial growth factor (VEGF) in ischemic conditions was pursued in angiogenesis [1-5]. VEGF showed promising results in promoting therapeutic angiogenesis in experimental studies only, initial phase I/II controlled clinical trials in patients with ischemic heart disease or peripheral arterial occlusive disease have subsequently failed to show significant therapeutic improvements [1, 9-11]. Alternatively, clinical evidence supported the use of anti-VEGF therapy in various cancer types [12-15] as well as the retinal proliferative diseases [16-18]. Although successful, anti-VEGF treatments are limited by depriving tissues of the intrinsic protective effects of VEGF as well as

they do not target the initial insult. All together, these results suggest the great need for new treatment options for modulating angiogenesis via a downstream signal from VEGF.

Accumulated clinical evidence, which supported the role of oxidative stress as a common player in a majority of ischemic cardiovascular diseases, underlined antioxidant therapy as an attractive treatment option. However, controlled clinical trials of antioxidants including the Cardiovascular Disease, Hypertension and Hyperlipidemia, Adult-Onset Diabetes, Obesity, and Stroke (CHAOS) study, the Heart Outcomes Prevention Evaluation (HOPE) trial, the Secondary Prevention with and the Heart Protection Study (HPS) presented contradictory and disappointing results [19-21]. Striking limitations, in most trials of antioxidants, included the absence of a biochemical or biomarker for patient inclusion, use of non-specific antioxidants, cell permeability and dose selection of the selected antioxidants. In addition, it was not investigated whether antioxidant therapy managed to reverse the oxidative stress-induced protein post-translational modifications in these patients. Therefore, these observations identified a gap in our knowledge about our understanding of oxidative stress-mediated protein modifications and how they can affect outcome in cardiovascular diseases. The current project explored the interplay between oxidative stress, VEGF and outcome retinal vasculature through three inter-related studies. Using cell permeable inhibitors, we determined its subsequent effects on specific protein changes. In the first study, we examined the molecular mechanism by which oxidative stress impairs VEGF signal. Next, we examined the effect of reductive stress on the VEGF signal. Finally, we identified a novel molecular switch of the VEGF angiogenic signal.

Peroxynitrite, the reaction product of nitric oxide and superoxide anion, can cause two main protein post-translational modifications either through nitration of the tyrosine moiety or oxidation of reduced thiol groups [22-24]. High levels of peroxynitrite causes the nitration of the

tyrosine moieties resulting in hindering tyrosine phosphorylation and hence loss of protein function [25, 26]. Alternatively, thiol oxidation can occur at both low physiologic and high pathological levels of peroxynitrite and as such, can either activate or inactivate protein function [27].

To examine the interplay between VEGF, peroxynitrite and angiogenesis, we used the hypoxia-induced neovascularization mouse model as it has two distinct stages: an initial stage of hyperoxia-induced excessive peroxynitrite formation and retinal vaso-obliteration followed by a later stage of relative hypoxia, mild oxidative insult and retinal neovascularization. We examined potentially safe selective inhibitors including the antioxidant and glutathione (GSH) precursor N-acetyl cysteine (NAC) and epicatechin, a flavenoid of the green tea extract that selectively blocks peroxynitrite-mediated tyrosine nitration. We compared these drugs to the specific peroxynitrite decomposition catalyst FeTPPS. The high content of iron in the specific peroxynitrite decomposition catalyst, FeTPPS, would prevent its use in humans on a chronic basis.

Clinical evidence has shown that patients with ischemic retinopathy and ischemic cardiovascular disease have less cellular antioxidant defenses [28, 29]. In agreement, our results using an experimental model of ischemic retinopathy demonestrated increased peroxynitrite formation and reduced cellular antioxidant defense as indicated by oxidized to reduced glutathione (GSSG/GSH) ratio. Our results identified nitration of tyrosine p85 kinase and inhibition of PI 3kinase/Akt survival pathway resulting in retinal cell death. Treatment with epicatechin prevented the nitration but did not alter the GSSG/GSH ratio confirming that nitration inhibition plays a vascular protective effect. We demonstrated that NAC at 150 mg/kg caused a recovery of cellular antioxidant defense as indicated by restoration of the oxidized to reduced glutathione (GSSG/GSH) ratio and prevented tyrosine nitration and restored the VEGF

survival signal (Chapter 2). To further elucidate the importance of using the proper dose of antioxidant, NAC at a high dose (500 mg/kg) caused reductive stress that impaired the VEGF-induced angiogenic response and aggravated retinal cell death (Chapter 3).

The concept of a redox window for promoting angiogenesis was first introduced by the Chilian group, where they showed that reductive stress can impair coronary collateral growth [30]. However, whether the concept can be validated in other vascular beds and the molecular mechanism remain unexplored.

In our study, we examined the change in the cellular redox-state using escalating levels of peroxynitrite from physiological, mild and acute oxidative and reductive stress to identify the molecular mechanism for VEGF signal impairment. We adopted a model of reductive stress via knocking down thioredoxin interacting protein (TXNIP), an endogenous inhibitor for the potent antioxidant thioredoxin system. Adult TXNIP deficient mice (TKO) are characterized by a significant increase in the ratio of reduced to oxidized glutathione, fasting hypoglycemia and hypertriglyceridemia. Our experiments were performed on pups and under non fasting condition, so the metabolic phenotype should not affect our results. Complementary *in vitro and ex-vivo* studies were conducted to examine the VEGF and its downstream angiogenesis signal after silencing TXNIP expression in human microvascular endothelial cells.

Low molecular weight protein tyrosine phosphatase (LMW-PTP) has a unique property of having two cysteines located in the catalytic pocket. Both cysteines must be reduced for enzyme phosphorylation and activity [31-33]. LMW-PTP plays a pivotal role in angiogenesis as it has been shown to regulate focal adhesion kinase (FAK) [31, 33]. Yet, whether the VEGF angiogenic signal involves regulating LMW-PTP phosphatase activity has not been explored. Our results showed that VEGF or peroxynitrite can induce transient oxidative inhibition of

LMW-PTP. In response to peroxynitrite, protein thiols can undergo post-translational modification by S-nitrosylation, oxidation, formation of disulfides, and S-glutathionylation [35-40]. S-glutathionylation, a reversible protein modification, occurs as a protective mechanism to protect regulatory thiols from irreversible oxidation and it is an essential ultimate step for reversible recovery for oxidized thiols [41, 42]. Our results showed that physiological levels of peroxynitrite caused transient S-glutathionylation of LMW-PTP while high levels sustained LMW-PTP S-glutathionylation. Our results showed that reductive stress blunted VEGF-mediated oxidative inhibition of the phosphatase activity leading to sustained activation and inhibition of VEGFR-2 phosphorylation.

In summary, the project illustrates the importance of a balanced cellular redox-state to facilitate the VEGF angiogenic signal. While mild oxidative stress augments the VEGF-mediated cell migration signal, acute oxidative stress as well as reductive stress impaired the VEGF angiogenic signal. We identified the LMW-PTP as a redox regulated target to modulate the VEGF angiogenic response. Our results offer pre-clinical evidence and support the critical role of achieving balanced cellular redox-state to develop therapeutics for diseases characterized with aberrant angiogenesis.

References

1. Testa, U., G. Pannitteri, and G.L. Condorelli, *Vascular endothelial growth factors in cardiovascular medicine.* J Cardiovasc Med (Hagerstown), 2008. **9**(12): 1190-221.
2. Kozak, A., et al., *Candesartan augments ischemia-induced proangiogenic state and results in sustained improvement after stroke.* Stroke, 2009. **40**(5): 1870-6.
3. Kalil, R.A., et al., *VEGF gene therapy for angiogenesis in refractory angina: phase I/II clinical trial.* Rev Bras Cir Cardiovasc. **25**(3): 311-21.
4. Yang, J.P., et al., *The dose-effectiveness of intranasal VEGF in treatment of experimental stroke.* Neurosci Lett, 2009. **461**(3):212-6.
5. Losordo, D.W., et al., *Gene therapy for myocardial angiogenesis: initial clinical results with direct myocardial injection of phVEGF165 as sole therapy for myocardial ischemia.* Circulation, 1998. **98**(25): 2800-4.
6. Brastianos, P.K. and T.T. Batchelor, *Vascular endothelial growth factor inhibitors in malignant gliomas.* Target Oncol. **5**(3): 167-74.
7. Ali, T.K. and A.B. El-Remessy, *Diabetic retinopathy: current management and experimental therapeutic targets.* Pharmacotherapy, 2009. **29**(2): 182-92.
8. Armstrong, A.W., et al., *Angiogenesis and oxidative stress: common mechanisms linking psoriasis with atherosclerosis.* J Dermatol Sci. **63**(1): 1-9.
9. Makinen, K., et al., *Increased vascularity detected by digital subtraction angiography after VEGF gene transfer to human lower limb artery: a randomized, placebo-controlled, double-blinded phase II study.* Mol Ther, 2002. **6**(1): 127-33.

10. Rajagopalan, S., et al., *Regional angiogenesis with vascular endothelial growth factor in peripheral arterial disease: a phase II randomized, double-blind, controlled study of adenoviral delivery of vascular endothelial growth factor 121 in patients with disabling intermittent claudication.* Circulation, 2003. **108**(16): 1933-8.

11. Kusumanto, Y.H., et al., *Treatment with intramuscular vascular endothelial growth factor gene compared with placebo for patients with diabetes mellitus and critical limb ischemia: a double-blind randomized trial.* Hum Gene Ther, 2006. **17**(6): 683-91.

12. Kindler, H.L., et al., *Phase II trial of bevacizumab plus gemcitabine in patients with advanced pancreatic cancer.* J Clin Oncol, 2005. **23**(31): 8033-40.

13. Emmanouilides, C., et al., *Anti-VEGF antibody bevacizumab (Avastin) with 5FU/LV as third line treatment for colorectal cancer.* Tech Coloproctol, 2004. **8 Suppl 1**: s50-2.

14. Burger, R.A., et al., *Phase II trial of bevacizumab in persistent or recurrent epithelial ovarian cancer or primary peritoneal cancer: a Gynecologic Oncology Group Study.* J Clin Oncol, 2007. **25**(33): 5165-71.

15. Dickler, M.N., et al., *A phase II trial of erlotinib in combination with bevacizumab in patients with metastatic breast cancer.* Clin Cancer Res, 2008. **14**(23): 7878-83.

16. Ouhadj, O., et al., *[Intravitreal ranibizumab injections for the treatment of choroidal neovascularization complicating high myopia]*. J Fr Ophtalmol. **33**(9): 649-54.

17. Jorge, R., et al., *Intravitreal bevacizumab (Avastin) for persistent new vessels in diabetic retinopathy (IBEPE study).* Retina, 2006. **26**(9): 1006-13.

18. Cunningham, E.T., Jr., et al., *A phase II randomized double-masked trial of pegaptanib, an anti-vascular endothelial growth factor aptamer, for diabetic macular edema.* Ophthalmology, 2005. **112**(10):1747-57.

19. Lonn, E., et al., *Effects of ramipril and vitamin E on atherosclerosis: the study to evaluate carotid ultrasound changes in patients treated with ramipril and vitamin E (SECURE).* Circulation, 2001. **103**(7): 919-25.

20. McQueen, M.J., et al., *The HOPE (Heart Outcomes Prevention Evaluation) Study and its consequences.* Scand J Clin Lab Invest Suppl, 2005. **240**: 143-56.

21. *Results of the low-dose (20 mg) pravastatin GISSI Prevenzione trial in 4271 patients with recent myocardial infarction: do stopped trials contribute to overall knowledge? GISSI Prevenzione Investigators (Gruppo Italiano per lo Studio della Sopravvivenza nell'Infarto Miocardico).* Ital Heart J, 2000. **1**(12): 810-20.

22. El-Remessy, A.B., et al., *Peroxynitrite mediates VEGF's angiogenic signal and function via a nitration-independent mechanism in endothelial cells.* Faseb J, 2007. **21**(10): 2528-39.

23. El-Remessy, A.B., et al., *Oxidative stress inactivates VEGF survival signaling in retinal endothelial cells via PI 3-kinase tyrosine nitration.* J Cell Sci, 2005. **118**(Pt 1): 243-52.

24. Gu, W., et al., *Reactive oxygen species are critical mediators of coronary collateral development in a canine model.* Am J Physiol Heart Circ Physiol, 2003. **285**(4):H1582-9.

25. Peluffo, G. and R. Radi, *Biochemistry of protein tyrosine nitration in cardiovascular pathology.* Cardiovasc Res, 2007. **75**(2): 291-302.

26. Zou, M.H., R. Cohen, and V. Ullrich, *Peroxynitrite and vascular endothelial dysfunction in diabetes mellitus.* Endothelium, 2004. **11**(2): 89-97.

27. Landino, L.M., *Protein thiol modification by peroxynitrite anion and nitric oxide donors.* Methods Enzymol, 2008. **440**: 95-109.

28. Papp, A., et al., *Glutathione status in retinopathy of prematurity.* Free Radic Biol Med, 1999. **27**(7-8): 738-43.

29. Koc, F., et al., *Antioxidant status and levels of antioxidant vitamins in coronary artery ectasia.* Coron Artery Dis. **22**(5): 306-10.

30. Yun, J., et al., *Redox-dependent mechanisms in coronary collateral growth: the "redox window" hypothesis.* Antioxid Redox Signal, 2009. **11**(8): 1961-74.

31. Chiarugi, P., *The redox regulation of LMW-PTP during cell proliferation or growth inhibition.* IUBMB Life, 2001. **52**(1-2): 55-9.

32. Xing, K., et al., *Low molecular weight protein tyrosine phosphatase (LMW-PTP) and its possible physiological functions of redox signaling in the eye lens.* Biochim Biophys Acta, 2007. **1774**(5): 545-55.

33. Chiarugi, P., et al., *Two vicinal cysteines confer a peculiar redox regulation to low molecular weight protein tyrosine phosphatase in response to platelet-derived growth factor receptor stimulation.* J Biol Chem, 2001. **276**(36): 33478-87.

34. Huang, L., et al., *HCPTPA, a protein tyrosine phosphatase that regulates vascular endothelial growth factor receptor-mediated signal transduction and biological activity.* J Biol Chem, 1999. **274**(53): 38183-8.

35. Wang, W.Q., J.P. Sun, and Z.Y. Zhang, *An overview of the protein tyrosine phosphatase superfamily.* Curr Top Med Chem, 2003. **3**(7): 739-48.

36. Clavreul, N., et al., *S-glutathiolation by peroxynitrite of p21ras at cysteine-118 mediates its direct activation and downstream signaling in endothelial cells.* FASEB J, 2006. **20**(3): 518-20.

37. Dremina, E.S., et al., *Oxidation and inactivation of SERCA by selective reaction of cysteine residues with amino acid peroxides.* Chem Res Toxicol, 2007. **20**(10):. 1462-9.

38. Sethuraman, M., et al., *Quantification of oxidative posttranslational modifications of cysteine thiols of p21ras associated with redox modulation of activity using isotope-coded affinity tags and mass spectrometry.* Free Radic Biol Med, 2007. **42**(6): 823-9.

39. Liaudet, L., G. Vassalli, and P. Pacher, *Role of peroxynitrite in the redox regulation of cell signal transduction pathways.* Front Biosci, 2009. **14**: 809-14.

40. Chinta, S.J. and J.K. Andersen, *Nitrosylation and nitration of mitochondrial complex I in Parkinson's disease.* Free Radic Res. **45**(1): 53-8.

41. Chen, J., et al., *Thioredoxin-interacting protein deficiency induces Akt/Bcl-xL signaling and pancreatic beta-cell mass and protects against diabetes.* Faseb J, 2008. **22**(10): 3581-94.

42. Okamoto, T., et al., *Activation of matrix metalloproteinases by peroxynitrite-induced protein S-glutathiolation via disulfide S-oxide formation.* J Biol Chem, 2001. **276**(31): 29596-602.